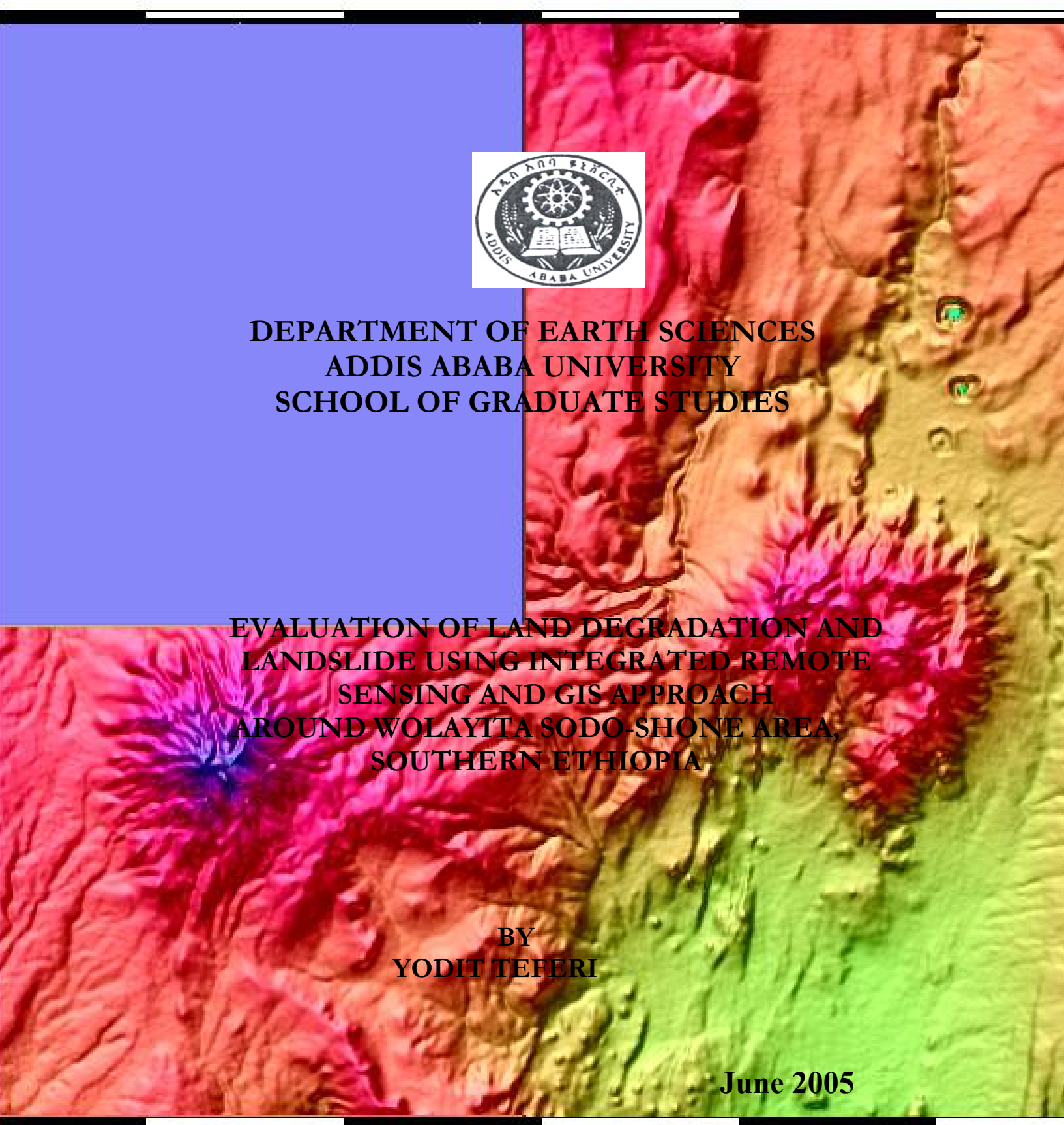

DEPARTMENT OF EARTH SCIENCES
ADDIS ABABA UNIVERSITY
SCHOOL OF GRADUATE STUDIES

EVALUATION OF LAND DEGRADATION AND LANDSLIDE USING INTEGRATED REMOTE SENSING AND GIS APPROACH AROUND WOLAYITA SODO-SHONE AREA, SOUTHERN ETHIOPIA

BY
YODIT TEFERI

June 2005

EVALUATION OF LAND DEGRADATION AND LANDSLIDE USING INTEGRATED REMOTE SENSING AND GIS APPROACH AROUND WOLAYITA SODO-SHONE AREA, SOUTHERN ETHIOPIA

A THESIS PRESENTED TO
THE SCHOOL OF GRADUATE STUDIES OF
ADDIS ABABA UNIVERSITY

In partial Fulfillment of the requirements for the Degree
Master of Science in Earth Sciences.

BY
YODIT TEFERI
JUNE 2005

ADDIS ABABA UNIVERSITY
SCHOOL OF GRADUATE STUDIES

EVALUATION OF LAND DEGRADATION AND LANDSLIDE USING INTEGRATED REMOTE SENSING AND GIS APPROACH AROUND WOLAYITA SODO-SHONE AREA, SOUTHERN ETHIOPIA

By
YODIT TEFERI
Faculty of Natural Science
Department of Earth Sciences.

Approval By Board of Examiners

Dr. Dereje Ayalew _____
Chairman, Department
Graduate Committee

Dr. Tesfaye Korme _____
Advisor

Dr. Asfawossen Asrat _____
Advisor

Dr. Bekele Abebe _____
Advisor

Dr. Gezahegn Yirgu _____
Examiner

Dr. Mohamed Umer _____
Examiner

Dr. K. S. R. Murthy _____
Examiner

Declaration

I, the under signed, declare that this thesis is my work and that all sources of material used for the thesis have been dully acknowledged.

Name : Yodit Teferi
Signature:_____
Place and date of submission,
July 2005, Addis Ababa.

Table of Content

List of Figures

List of Tables

Acknowledgment

The compilation of this thesis would have not been possible without the assistance of many people and various institutions. I would like to take this opportunity to express my appreciation to every one who assists me in one or another way.

I am very much indebted to Dr. Tesfaye Korme, my advisor and initiator of this work. His constructive comments and advises were the base of this study. I appreciate his courage for creating a pleasant working atmosphere and giving guidance. He is always enthusiastic to help his students. I am so grateful and I would like to thank him for sharing his office & office accommodation, for availing relevant reference materials and his determined assistance during the field trip. Above all that, I thank him for sharing his knowledge, for directing the paper in the right path and support through out the study period.

I would also like to express my deepest gratitude to my advisor, Dr. Asfawossen Asrat for his constructive criticism and valuable counsel. I really appreciate his generosity in sharing his tight schedule to comment on this work. His assistance and advice in various stages of the thesis and comments on most of the chapter were beneficial.

My warmest gratitude also goes to Zeleke Kibebew for his contributions and valuable suggestions during the challenging field survey and the progress of this work. Moreover, I am very grateful to him for sharing his time and knowledge without hesitations.

Many thanks extend to all of the staffs in the Earth Science Department, who helped me in one way or another during my stay in A.A.U. Without their dedicated assistance, success wouldn't have been possible.

I am also very grateful to National Metrological Agency, Central Statistics Authority, Soil Laboratory of Technological Faculty of AAU & Petrological Laboratory of the Earth Science Department, for allowing me to use their data and facility.

I am very much thankful to all administrative personnel of SNNPR for their cooperation during the preliminary field work. I am grateful to Officer Daniel Gezahegn who provided me all the valuable data concerning landslide of the area.

I deeply appreciate and respect my office of Oromia Mines and Energy Bureau and all my colleagues, for supporting me to take up the M.Sc. program and arranging a vehicle for the field work.

I am especially indebted to my fiancé, Dr. Berhanu Ayana, for his encouragements, wonderful advises, endless support and love. He is my source of strength in every aspect of life. My special thanks to my parents, Teferi Getaneh and Romanwork Mengistu, sister, Gifty and brothers, Behailu, Mati and Dan for being on my side all the time, when things workout or seem to be wrong, for their endless love, encouragement and support. I also extend my gratitude to all my uncles especially Wasse Berhanu, aunts, cousins and relatives.

Last but not least, I would like to express my warm appreciation to my colleagues and my life long friends, especially, Sewit Assefaw and Rahel Kifle for sharing our university lives together. My appreciation also goes to Asefa Kumsa for his continues support from abroad. I am also grateful for the joy, support and kindness offered to me by many fellow post graduate students, especially Zelalem Shiferaw, in Earth Science and various departments of Science Faculty.

Abstract

In this study two major environmental hazards, namely land degradation and landslide have been investigated. These hazards have clear dynamic relationships given that both are chaotic phenomena that can be triggered by unstable equilibrium situation occurring drastically and abruptly to the environment.

Southern Nation's National Peoples Region is one of the most populated regions in the country. The area is situated in the western margin of the Ethiopian Main Rift system and it is structurally controlled and tectonically active. Therefore, the study area is an excellent site where natural and human induced or anthropogenic factors work jointly to result in such a staggering environmental damage. Generally, it is a place where most favorable factors of land degradation and landslide coincide in space.

An integrated GIS and remote sensing approach was very helpful to study the intensity and extent of the two environmental hazards. The degradation rate that was calculated in areal base using cross classification of temporal data shows the degradation rate is becoming severe with time. The degradation rate that was 1.8 sq. km/year between 1984 and 1995 has increased in to 3.1 sq. km/year in recent times (till 2001). These figures show that the rate of degradation is increasing at an alarming rate.

The amount of soil lost from the study area is estimated using cut and fill technique applied on 5 representative sites. Profiling was done using GPS reading taken at every 5-10m interval and organized in a database. The volume loss calculated shows that 2,485,818 m^3 amount of soil is lost from 291,241 m^2 area; with the net lose per area being about 8.53 m^3.

Factors that are found to be significant in triggering the Land degradation in the study area include structure, lithology, landuse/ landcover, slope, soil, drainage, and climate. Similarly these factors with addition of slope aspect play an important roll in aggravating the frequently occurring landslide.

The presence of all the factors that are responsible for the staggering environmental hazard and their coincidence in space and time indicate that the area is highly prone to these hazards. Factors that are considered to be responsible for the two environmental hazards were weighted in hierarchical order using the MCE approach to produce susceptibility maps that express the likelihood occurrences of the hazards in the area on the bases of the local terrain condition.

PART- I

General introduction and Description of the study area

Chapter-1

1.1 Introduction

This Study deals with the study of two major environmental hazards, namely land degradation and landslide. Mass movements and land degradation are environmental hazards with clear dynamic relationships. There are interrelated bonds between degradation and mass movements, since small landslides often convert into gully heads, while gullies frequently develop laterally due to mass wasting. They work hand in hand to accomplish their destruction. Mass movements as well as land degradation are chaotic phenomena that can be triggered by unstable equilibrium situation occurring drastically and abruptly to the environment.

Landslide is land degradation in action. Landslide assists land degradation by removing the top fertile layer. The bare soil left behind is very vulnerable to erosion from raindrop impact, run-off and wind action; as a result it will expose the bedrock. One time event of landslide may not cause degradation, but its repetitive action will lead to a degradation action then pilot the area to a bad land.

Both land degradation and landslides can impose a negative impact on human life, but their cause, duration, frequency, speed and amount of damage may vary. For example, land degradation can be caused by natural, human induced (anthropogenic) and/or both factors. Some of the natural causes include due to geology of the area, topography, tectonic structure, soil structure, draught and major climatic change. Anthropogenic or human induced factors include, deforestation, over grazing, intensive farming, road construction, urbanization, and so on. Land degradation is not a one second event; it rather takes from a few years to hundreds of years depending on the controlling factors time and space coincidence. Its duration can also vary from some years to many hundreds of years based on how fast preventing actions are taken, what measures are taken and how effective they are. The damage caused due to land degradation may not be seen immediately since it takes years to happen. As land degradation happen sluggishly, it hardly ever give rise to instantaneous action. However, the manifestation of the damage can be seen gradually by its indicators, such as decreasing the amount of soil, soil nutrients, declining the amount of crop yield and also by loss of natural beauty of the land.

It is difficult to imagine that the rate of formation of the soil takes as many years as compared to its loss.

Landslide can also be caused by natural and manmade factors and/or both. Natural factors include gravity, geology (lithologic units and tectonic structures like faults, etc.), drainage pattern, topography (slope angle and aspect) and rainfall. Clearing of vegetation, cultivating sloppy parts, over grazing, construction of infrastructures and urbanization are some of the human induced factors. Land slide takes few seconds to occur if the important triggering factors are coinciding with the precise time and space. The major thing that makes landslide dangerous is its unexpected nature. Landslide may cause sever damage to human life and their property. On these bases, landslide damages can be seen immediately following its occurrence. The events duration may be short, but its memory of the damage on human life and property lasts long.

Land degradation has both on-site and off-site effects. Major on-site effects are the lowering of the productive capacity of the land, reduction of livestock yields and increasing the need to use more fertilizers. This leads the farmer especially of that of the third world to have additional expenses which may be an extra burden on them. The off-site effects of degradation include changing the direction of water course, decline in river water quality, and increasing sedimentation of river beds and reservoirs.

So due to all the above reasons, it is not questionable how much dangerous and alarming the two hazards are. In developing countries like Ethiopia, where it is difficult to feed people three times a day, the loss of resources and human life is extremely unaffordable. In Ethiopia where the economic policy is agricultural lead and where 85% of the population depends on farming activity, loss of a minute amount of fertile soil and other natural resources, has great influence on agriculture and economy of the country, which will in turn influence the socio economic standard of the farmer. Hence, it is prerequisite to pay utmost attention on the two hazards.

Remote sensing and GIS technology is proved to be excellent tools for the studies of land degradation and landslide hazard prone areas. Its purpose is not only limited to assist in environmental hazard investigations by deriving area-wide land use, geological and geomorphologic information in land degradation - landslide prone areas, but also for direct delineation of land

degradation and landslide surface boundaries, monitoring their activity, identifying and mapping potential environmental hazard prone areas.

In order to study these environmental hazards in an effective way, application of integrated Remote Sensing and GIS analysis is an appropriate technique. Integrated Remote Sensing and GIS application for mapping and monitoring of mass movements and degradation, using ancillary information in combination with remote sensing data, is rapidly developing. Moreover, satellite images of various multi-spectral, multi-temporal, spatial and radiometric resolutions have been successfully used to environmental studies to discriminate and delineate landslide and gully types.

This research work is conducted in Wolayita Sodo – Shone area that is situated in the Southern Nations, Nationalities and Peoples Region. The study area is chosen for the fact that it is severely affected by the two environmental hazards. The damage that is caused by these environmental hazards is increasing from time to time. So it needs researchers', government officials, NGO'S and other organizations attention.

1.2 Objectives of the study

The rate of land degradation in the area is exceptionally high and is a threat to the agriculture potential of this area and even to that of the country. The population is growing at the rate of about 2.66 percent in rural areas and 4 percent per annum in urban areas (Woody Biomass, 2001). The use of Marginal and steep lands for cultivation is increasing, leading to accelerated soil erosion, and to declining and more variable crop yields. Increasing population and expansion of small-scale agriculture are the most important factors in the declining of natural forests throughout the area and its vicinity. Due to these reasons a scarcity of wood for fuel and construction exists in many parts. The shortage of wood for fuel leads to the use of cow dung and crop residue as a source of fuel mostly in rural areas. To use these materials for a fuel has its own consequences. Animal dung can be helpful to the soil as a fertilizer and the crop residue can be a food to the cattle. So using them for a fuel will hinder the gain that the land should get. Areas of unrestricted grazing land are rapidly losing ground under the increase of cropland. As a result, cultivated lands are often used as temporary grazing areas after harvesting. As a consequence of the factors explained, the soil loss rate from cultivated parts is increasing.

Moreover natural impacts such as topography, local slopes controlled by tributaries of Bilate, tectonic structures, soil texture, drainage, lithology and erosive rains play significant role in aggravating the degradation in the study area. It is believed that the area is an excellent exhibit where natural and man made factors work hand in hand to precipitate such a staggering environmental damage. In addition to the intense land degradation, frequent landslide events are also common in the area due to the impact of several factors.

In relation to the above condition, this study has three main objectives:

- to apply integrated approach of GIS and Remote Sensing technique to evaluate the extent and cause of land degradation and land slide in the area;
- to use integrated techniques of GIS and Remote Sensing to zone landslide susceptible areas and
- to recommend conservation and prevention strategy and techniques,

The specific objectives of the study include to:

- investigate the causes of land degradation and landslide
- to quantify the amount of soil loss
- to identify the physical processes associated with initiation and development of land degradation and landslide
- to assess changes in the degraded areas through time (temporal analysis of degraded areas)
- to assess the knowledge and attitudes of the farming community
- to identify the possibilities for rehabilitation of degraded areas
- to do event mapping for the land slide
- to zone land slide susceptible areas
- to contribute a base line data for future research since the area is not much explored

1.3 Description of the study area

1.3.1 Location

The study area is found in the Southern Nations, Nationalities and Peoples Region at about 355km (Shone town) and 380 km (Sodo town), South of Addis Ababa. It is bounded by N 6º 50' to N7º20'

latitudes and E 37°45' to E 38°5' longitudes (Figure 1.1), and has a total area of about 1750 km^2. The altitudinal range in the area is between 1500 m.a.s.l (in Blate River Valley) and about 2900 m.a.s.l (at the pick of mount Damot). The topography is mainly rugged and structurally controlled.

1.3.2 Accessibility

The main asphalt road in Ethiopia extends radially from Addis Ababa to most capital or other economic and administrative centers. Addis Ababa is connected to Awassa, the administrative capital of the region, by an asphalt road. The study area (Sodo-Shone) is linked to the administrative capital through an asphalted all weather road. The zonal towns are mostly connected to the study area by gravel surfaced road. Lots of woredas and market places are linked to the administrative capital of the region and to the Zone by all weather and dry weather tracks. However, most areas still necessitate an all-weather link to the capital or other economic and administrative centers.

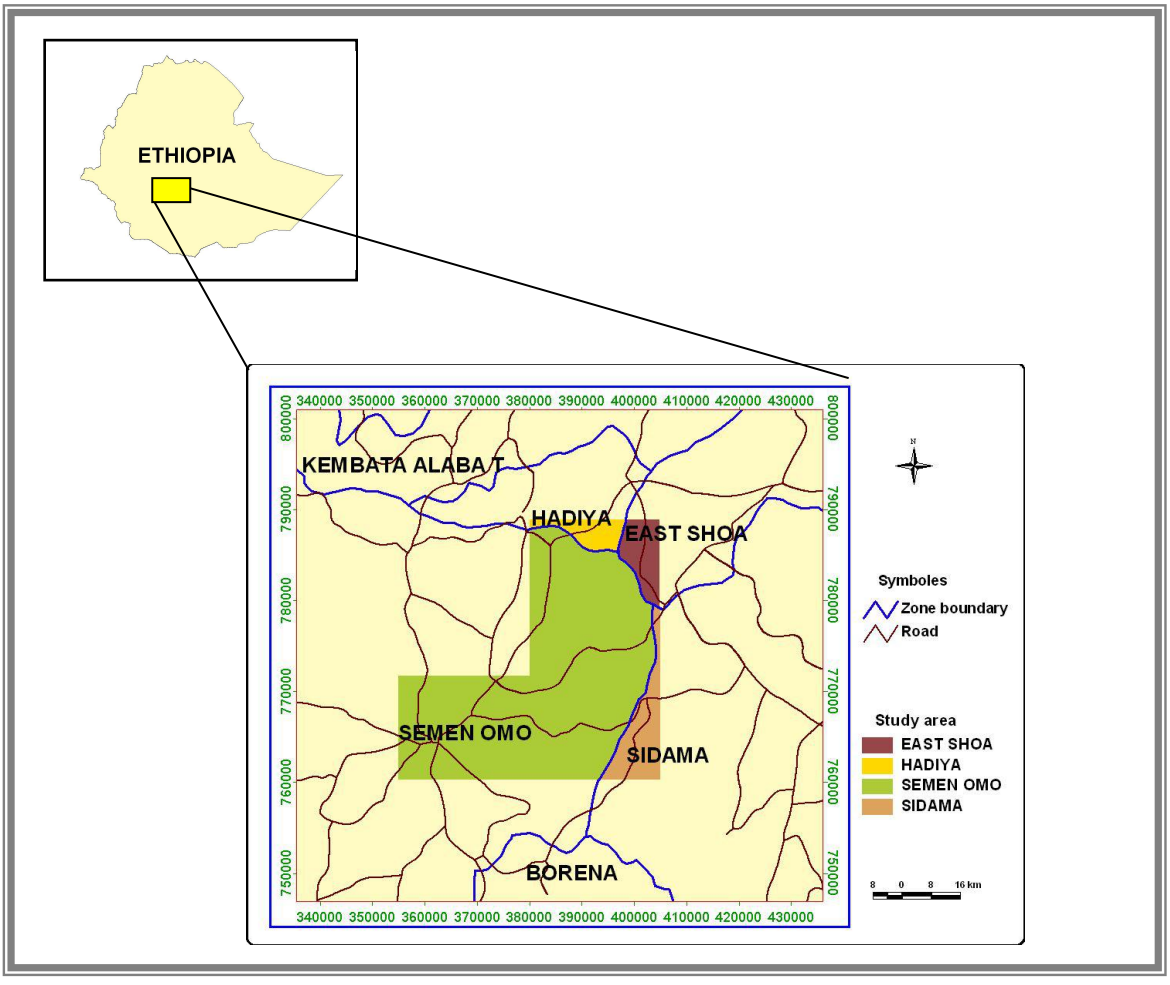

Figure 1.1 Location map of the study area

1.3 Topography and landform

The Region can be broadly divided into a number of highland and lowland zones. The highland-lowland boundary is found at about 1,500 m.a.s.l. The Rift Valley separates the Sidamo-Amaro Highlands in the east from the Highlands just to the west of the Rift Valley running southwestwards from Gurage to North Omo Zones. To the northwest are the Highlands Kaficho-Shakiso running southwards in to Bench-Maji Zone. In the south are the Omo and Sagen valley Lowlands in South Omo Zone (Woody Biomass, 2001)

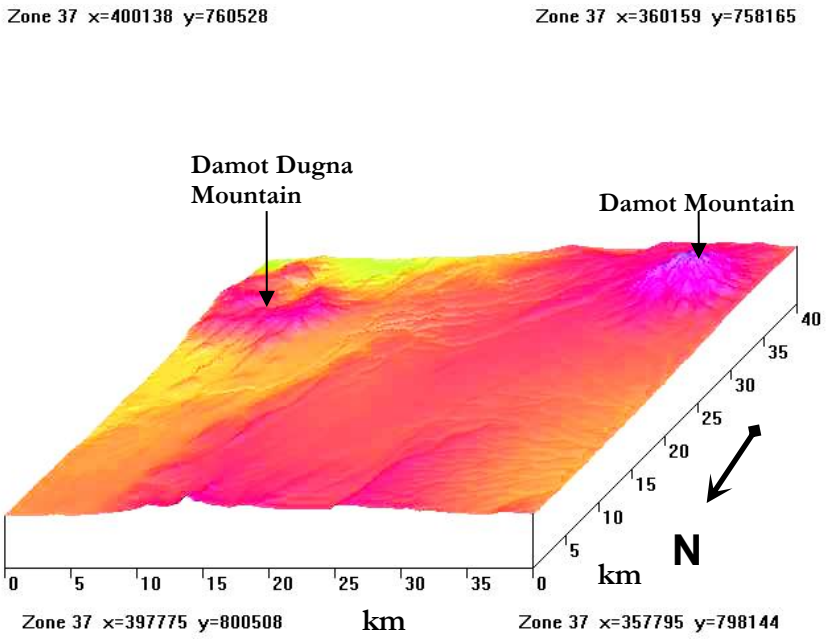

Figure 1. 2 3D-view of SRTM data at 90m resolution of the study area showing domes river cuts, tectonic structure ...etc.

The study area can be topographically considered as a water shade. It divides the Blate drainage basin to the east from the Omo drainage basin to the west. The altitudes range from 1500 m.a.s.l. at Blate River and 2800 m.a.s.l. on top of Damot Mountain. In general, the study area has a rugged topography with volcanic highs, valleys, flat lands and various tectonic structures (Figure1.2).

1.3.4 Soil

According to the map produced by ethioGIS, the study area comprises 12 soil types such as calcaric flubisols, calcaric fluvisols, calcic fluvisols, chromic lavisols, chromic luvisols, chromic vertisols, dystric fluvisols, dystric nitisols, eutric nitisols, pelic vertisols and vitric andosols (Figure 1.3). The classification is made based on 'The FAO-UNESCO Soil Classification System: The World Reference Base for soil resources'. According to FAO (2001), most soil profiles can be named without difficulty but some more complex situations require additional classification guidelines therefore, the WRB prefers to name soils as they occur, i.e. with present-day characteristics and functional behavior, rather than emphasizing their (supposed) genetic history.

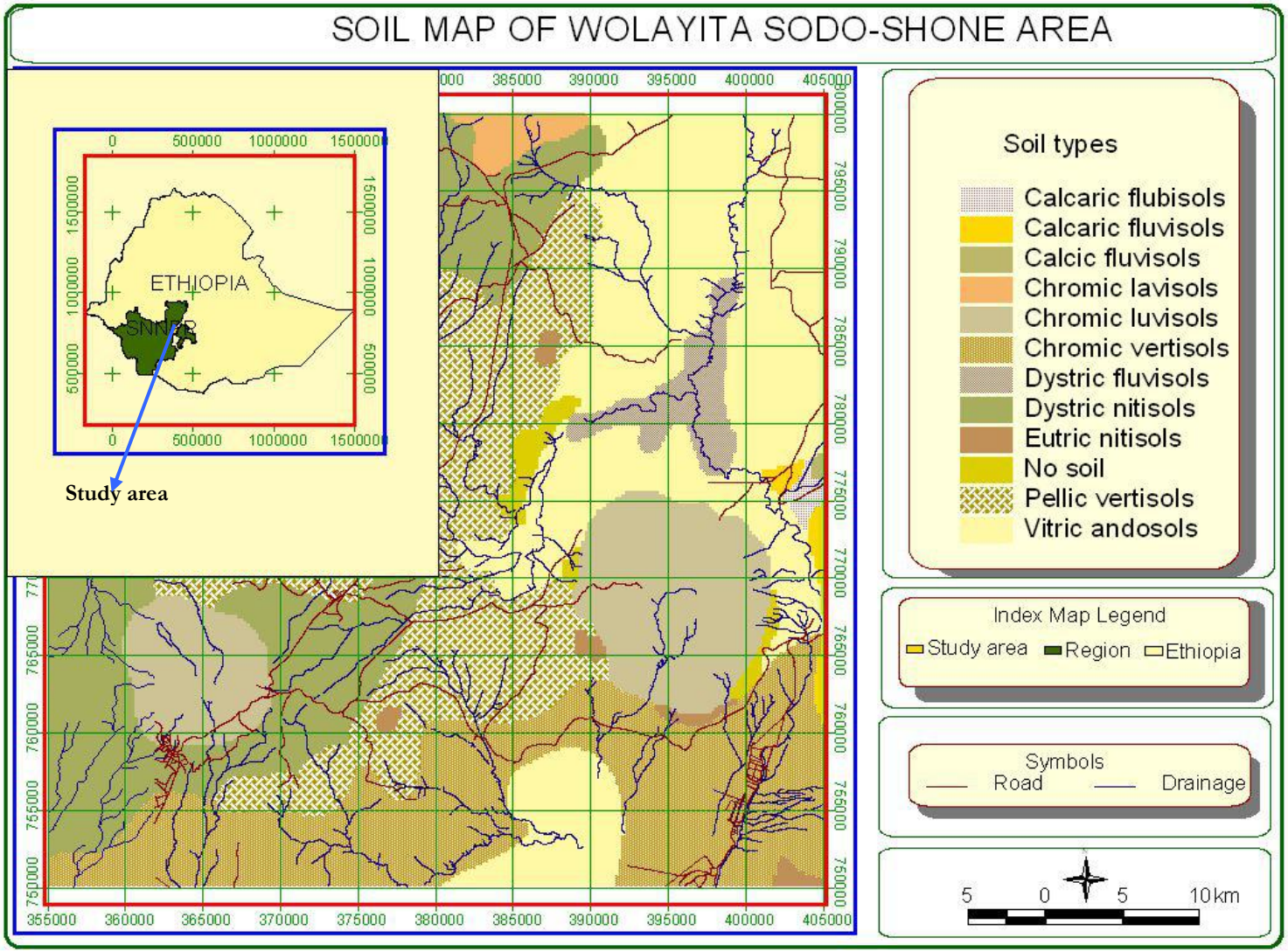

Figure 1.3 Soil map of Wolyita Sodo-Shone area

1.3.5 Geology

1.3.5.1 Regional Geology

The area is covered by welded tuff of 4.2 ma age at Wegebeta caldera, situated at the western margin of the Main Ethiopia Rift (MER) (WoldeGabriel et al, 1990). Rhyolite lava situated at a distance of 10 km to the southeast of the caldera is 3.6 m. y. old. At Mount Damot, more than 35km south of the Wegebeta caldera, there is a major trachytic center with a minimum age of 2.94 ma. The Damot's activity can be correlated with that of the trachytic centers on the eastern rift shoulder. Along the two fault scarps at the Omo River canyon which is west of Damot, there is exposure of more than 1.2 km of volcanic rocks underlain by sedimentary rocks.

According to WoldeGabriel and Aronson (1987) the volcanic rocks along the eastern canyon wall are dominated by rhyolite, trachyte, basalt, and pumiceous pyroclastic flows that are unconformably overlain by vitric tuff, basalt, and welded tuff in ascending order. The rift floor along the Blate River drainage system is blanketed by welded tuff, lacustrine strata, and fissural basalt and maars (Di paola, 1972; Zenettin et al, 1978)

1.3.5.2 Geology of the study area

Part of the study area that embraces Sodo town and Damot mountain, is located on the western margin of the main Ethiopian rift whereas the other part, Blate river basin and the surrounding area, is situated on the main Ethiopia Rift floor. Generally the area is characterized by NNE-SSW trending major step faults of the rift system. Some minor faults trending NE-SW and numerous lineaments are also found in the area. One of the study areas, Shone, is situated in the down throw side of a normal fault. Old caldera like structure is also found east of Damot Mountain. In general the study area is tectonically active and structurally controlled.

The area comprises various lithologic units originated from the rift formation or the local development of the domes. The area is mainly dominated by rift floor ignimbrites (ignimbrite-1) that cover more than 50% of the area. In most of the areas, this ignimbrite shows weathering at varying intensity. Most of the degraded area falls in the places where this lithology is exposed. There are also other ignimbrites which originated from intrusion of Damot and Damot Dugna (ignimbrite-1 and ignimbrite - 2 respectively). Damot mountain is predominantly covered by trachytic flow of two

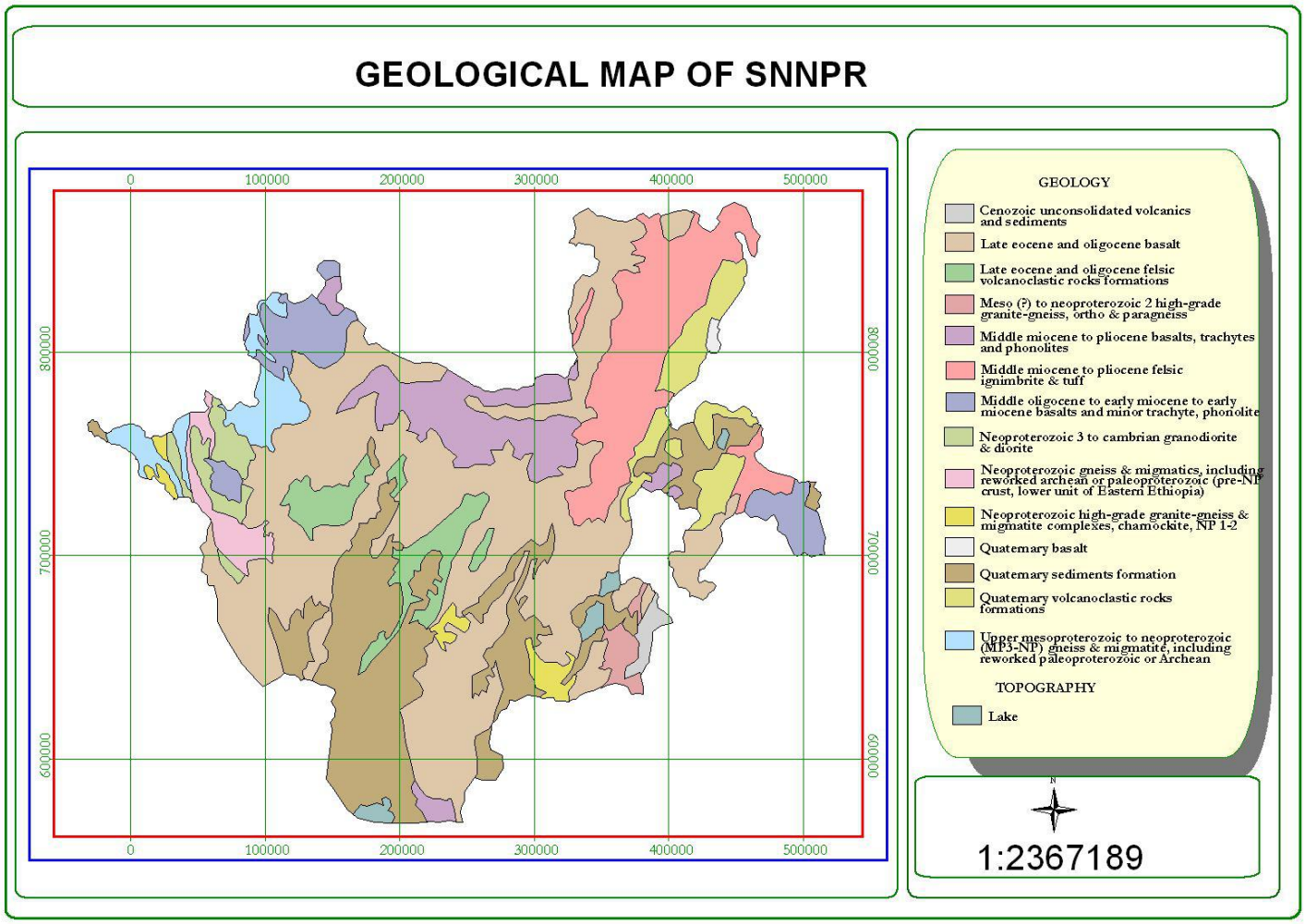

Figure 1.4 Regional Geological Map of SNNPR (After Solomon et al., 2004)

types (trachyte -1 and trachyte -2) while the top part of Damot Dugna is covered by rhyolitic flow. Some small scoria cones are also mapped north and south of Damot Dugna.

The Damot Mountain is constituted by three rock units among which the two types of trachytes were investigated petrographyically:

The lower trachyte (trachyte-1) is porphyritic trachytic basalt constituted by phenocrysts of plagioclase (~75%) with typical euhedral, hexagonal crystals of average length of 1-2mm. The crystals show characteristic twinning; Quartz crystals (~20%) of subhedral shape are observed in addition to rare k-feldspar (~5%). The matrix is constituted by fine grained plagioclase laths set in darker materials which could be basic minerals (such as olivine and pyroxenes).

The upper trachyte (trachyte-2):- is porphyritic with typical characteristics of trachyte. It consists of plagioclase feldspar comprising about 50%, 35% quartz, and relatively more abundant k-feldspar (~15%). fine grained plagioclase laths that set in darker materials constitute the matrix.

Ignimbrite-2:- This pyroclastic material is rhyolitic in composition. Rare plagioclase crystals were observed in a juvenile glassy matrix of rhyolitic in composition.

Geology of Damot volcanism

Damot mountain is a dome like structure where trachyte predominantly covers the area. Two types of trachytes and ignimbrite are formed during three stages of eruption (Figure 1.5). An ignimbrite is exposed at the eastern and south eastern foot of the mountain due to a road cut. This ignimbrite is not exposed on the other sides of the mountain, as it should have been covered by trachytes that erupted after wards. The dome has an asymmetric shape that is highly skewed to west- northwest due probably to dominant flows of trachytic material towards one side.

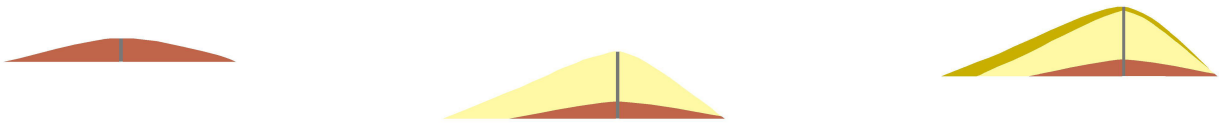

A. 1st step: eruption of pyroclastic material. B. 2nd step: trachytic material covers the underlying trachyte pyroclastic material C. 3rd step: coming out of the other

Figure 1.5 rough sketches that show the volcanism of Damot cross section from NE-SW direction. A and B were inferred from the geologic map that is produced for this research.

The trachytes which predominantly cover the volcanic dome in its northeastern, northern and western parts give the current asymmetrical shape of Damot (Figure 1.6).

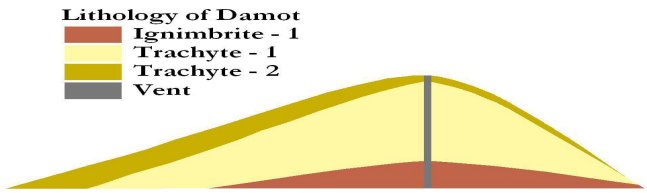

Figure 1.6 Damot Mountain before faulting and weathering

Since its formation, various geomorphic processes including faulting weathering and erosion occurred on the dome resulting in its current physiography (Figure 1.7).

Since the dome is situated in the western part of the main Ethiopian Rift (MER) margin, several normal faults trending NNE-SSW and NE-SW cut it in various localities.

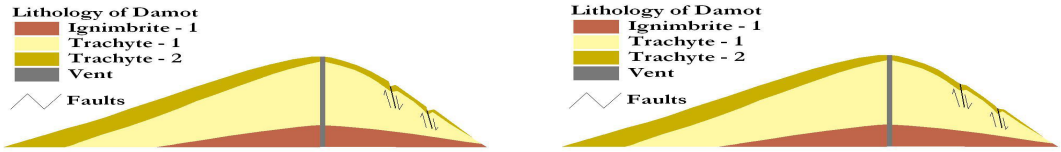

Figure 1.7 Geomorphic processes on Damot mountain

1.3.6 Drainage

Drainage pattern of the study area is influenced by various factors, mainly by lithology and structure. The drainage pattern of the study area can be grouped in two parts. The first part that includes Mount Damot and Damot Dugna area has a radial drainage pattern. The remaining part comprises the commonest dendritic drainage pattern. The presence of uniform type of lithologic unit, rift floor ignimbrite, is responsible for such type of drainage pattern. There is also some drainage which is controlled by structures in the area between the two domes (Damot and Dugna).

1.3.7 Land use / Land cover

The dominant landuse system in the area is mixed cropping of perennial and annual crop (cereal cultivation). The annual crop comprises teff, maize, wheat, onion, potato and other variety of vegetables. Enset (false banana), coffee, eucalyptus, sugar cane, banana and avocado are some of the perennial crops. Enset is the main and dominant source of food in the region. Next to enset, eucalyptus is becoming extremely dominant and it is considered as a perennial crop given that it is fast growing and it does not need much of the farmer's effort to grow. It is considered as an important means of income. Most of the natural forests are being replaced by this plantation, especially; the riverine trees are subjugated by eucalyptus. About 16 landuse/landcover classes are mapped during this study using Remote Sensing and GIS with the help of field survey. The details are explained in chapter 3.

1.3.8 Weather and Climate

The climate in the region is controlled by the topography since temperature is inversely related to altitude. In the lowlands mean annual temperature range between 22°C to 27°C while in the highlands up to 3,000 m.a.s.l., it varies between 10°C to 22°C.

From 33 years of climatic data, it is deduced that the study area is characterized by mean annual temperature of 10°C to 15°C and maximum mean annual temperature of 22°C to 31°C with the exception of 1986, where the maximum temperature rise up to 35°C (Figure 1.8).

The monthly mean rainfall data for 33 years and 30 years were analyzed for Wolayita Sodo and Shone area respectively. Monthly average rainfall in Wolayita Sodo and the surrounding areas ranges between 50mm-150mm (Figure 1.9) while in Shone and the surrounding areas it ranges from 80mm-200mm (Figure 1.10).

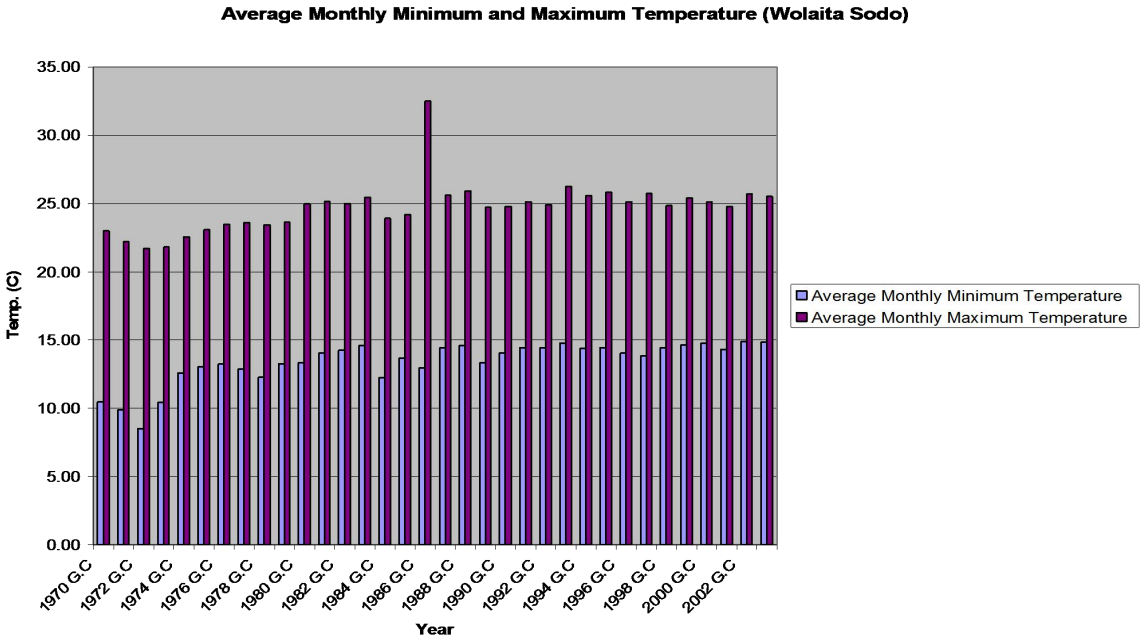

Figure 1.8 Average monthly minimum and maximum temperature of Wolayita Sodo area

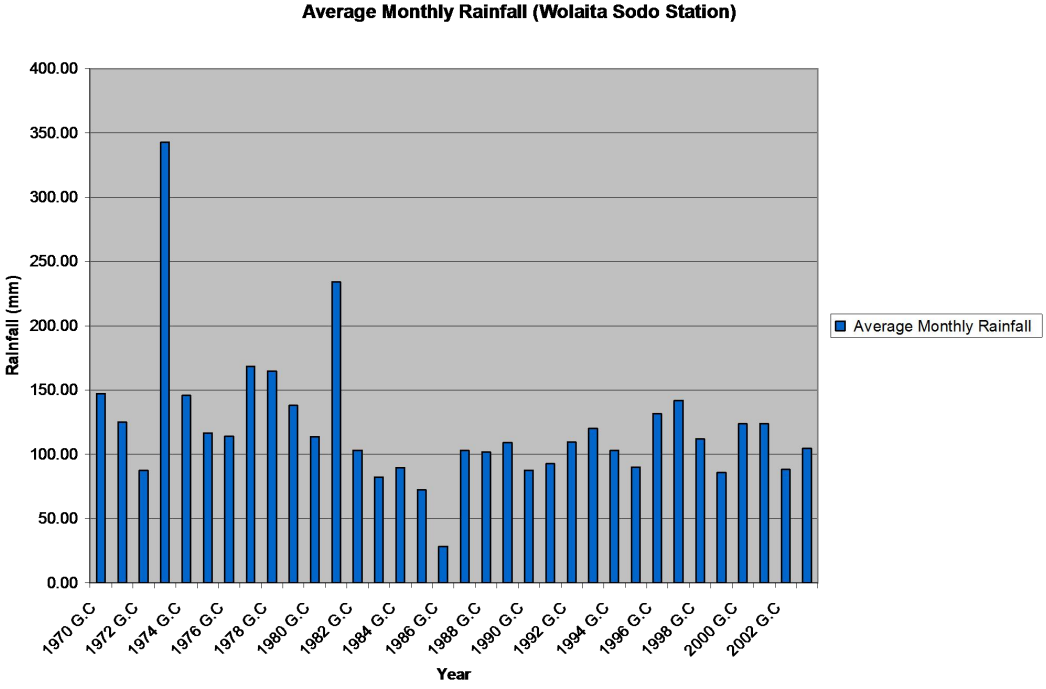

Figure 1.9 Average monthly rainfall of Wolayita Sodo area

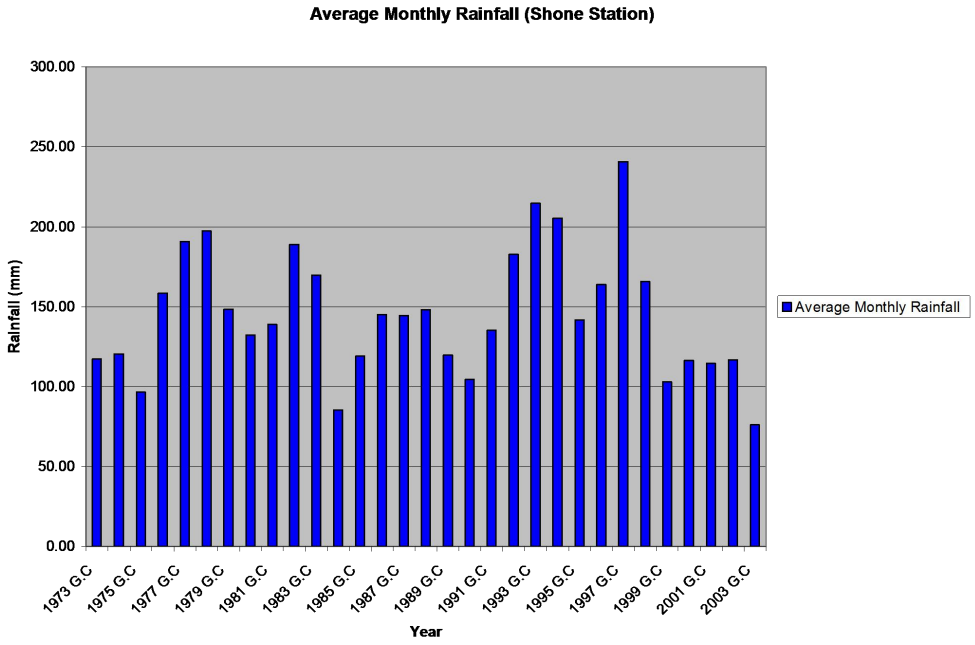

Figure 1.10 Average monthly rainfall of Shone area

1.3.9 Population

In Ethiopia, population census has been taken at two times, in 1984 G.C and 1994 G.C. The data has been projected for the desired year.

The population estimates presented for July 2002 are derived by projecting the 1994 census. Therefore, the total projected population of the country for July 2002 is estimated to be 67,220,000 persons. Out of the 67,220,000 persons, the population of rural area comprise 56,913,000 and 10,307,000 are urban. Urban areas refer to all capitals of regions, zones and woredas, and it also includes localities with urban kebeles, whose inhabitants are primarily engaged in non agricultural activities. The total estimates presented for the Southern Nations, Nationality & Peoples Region for the same year is 13,293,010. Out of this figure 6,606,005 are male whereas the 6,687,005 are females.

Most of the statistical results in this issue are based on the results of the October 1994 national population and housing census of Ethiopia. The present annual rural growth rate is estimated at 2.66 percent. If this rate of growth is maintained, the rural population will double in 26 years. The urban rate of increase is 4 percent per annum, and will double in about 18 years (Woody Biomass, 2001).

The overall population density in the region is approximately 118.3 persons per sq. km (Annex 1). This makes the region a highly populated one in the country except Addis Ababa, Dire Dawa and Harari regions since they are almost totally urban areas.

1.3.10 Presentation of the study

Apart from part-I (chapter one) that deals with general description of the study area; this study has two main parts and a conclusion part. The first part deals with the land degradation hazard around Wolayita Sodo-Shone area while the second part deals with the landslide problem around Sodo (mount Damot) area. Part I include from chapter two to chapter six. Chapter two deals with introduction on land degradation problem and clarifies the threat of land degradation in global, national and regional perspective. It also deals with the previous works on land degradation in Ethiopia and the reason why it is necessary to study the problem in the area. Appropriateness of GIS and RS for land degradation study and the objectives (both general and specific) of the study are also included in this chapter. Chapter three deals with the application of Remote Sensing and GIS for the problem at hand. In this chapter the methods used, the available data sets, image processing and interpretation are well explained. The maps produced and mapping techniques are also part of this chapter. Soil horizon analysis sampling, and the laboratory results are parts of chapter four. Chapter five deals with land degradation mapping and analysis including the rate and intensity of degradation. Chapter six focuses on integrated GIS analysis for causes and factors of land degradation and present the final land degradation susceptibility mapping. Part II mainly discus the evaluation of landslide problem in the study area. Previous works on landslide in Ethiopia, background on landslide problem in the study area, purpose of the study of the problem in the area, awareness of the community, appropriateness of GIS and RS for landslide study and the objective of the study are also discussed in this chapter. Moreover, the data and methods used factors of landsliding and their weighting using GIS and landslide hazard mapping are some of the parts that are explained in this chapter. Finally in part-IV, conclusion and recommendations of part I and part II are discussed together.

PART-II

Land Degradation Analysis Around Shone – Bilate Area

Chapter-2

Introduction on Land Degradation Problem

2.1 The threat of land degradation: global, national and regional perspective

Land Degradation is becoming a major worldwide problem. Developing countries are more affected than the developed countries due to their poor farming practice, lack of knowledge, poor infrastructure, increasing population, increasing demand for land and the absence of strong environmental policy itself.

The human population in hilly and mountainous regions of developing countries is growing rapidly (Templeton and Scherr, 1999). As a result agricultural lands in these hilly areas are degrading at an alarming rate due to the use and/or misuse of land (and other resources) beyond its capacity. The natural conditions of this land may have been suitable for agricultural purposes provided that the climate is regular and soil degradation is well controlled through proper land use management.

In Ethiopian highlands land degradation has become sever environmental problem. A number of factors contribute to unsustainable land management in this country. According to Berry (2003), with steady growth in population, clearing of woodland for agriculture has been a continuous process at an estimated rate of 62,000 ha per year. Moreover, Methods of crop production are conducive to soil loss and, dung and crop residues are needed for fuel, reducing their use as fertilizers. In order to conserve land and improve degraded ranges, it is necessary to analyze the land conditions and the cause of land degradation. For this purpose Remote Sensing and Geographic Information Systems serves as extremely useful tool for carrying out time sequential analysis of land condition.

Land degradation is a composite term; it has no single readily-identifiable feature, but instead describes how one or more of the land resources (soil, water, vegetation, rocks, relief) have changed for the worse. It is clear that the impact of land degradation is a drain on economic growth in rural areas and has an affect on national economic growth patterns (Leonard, 2003). Land degradation is the declination of productive capacity of the land. However, it is difficult to assess by any single

measure the productivity of land. Hence, we have to use different indicators of land degradation, including:

- Decline in yields of a crop may be an indicator that soil quality has changed, which in turn may indicate that soil and land degradation are also occurring. Especially, if the area was fertile with a good production history;
- The condition of the soil is one of the best indicators of land degradation. For example decrease in depth of the soil profile, change in landscape etc.;
- Land slides and other hazards in the area are also indicators of land degradation;
- Land degradation that is occurring upslope can be marked by accumulation of sediment against a down slope barrier.

2.2 Previous works on land degradation in Ethiopia

Research works concerning degradation in Ethiopia have been conducted both at the regional and local levels. Regional study includes that of Berry (2003) who studied the extent and impact of land degradation in Ethiopia. In this regional work, he studied the impact of the problem, its cause, cost of the impact, cost improvement measures and cost of policy reform and institutional development. Sonneveld and Keyzer (2002) evaluated the future impact of soil degradation on national food security and land occupation in Ethiopia.

Local level Studies especially on the northern highlands of Ethiopia, includes that of Fitsum Hagos et al.,(2002), which dealt with the nature of land degradation problem and its causes under miscellaneous conditions of the highlands of Tigray based upon review of existing studies, interviews with key informants, and analysis of secondary data. The effective policy, institutional and technological strategies to improve productivity and to restrain land degradation and poverty in the highlands of Amhara were discussed by Lakew Desta et al. (2000).

Bezuayehu Tefera et al. (2002) discussed the nature and extent of land degradation in Oromiya region. They develop some testable hypotheses about the possible pathways for overcoming land degradation problems and improve agricultural productivity in the region. In their research, they also evaluated the causes of land degradation and identified knowledge gaps.

All the above works stressed the fact that land degradation is becoming an important issue in Ethiopia. The previous studies mostly concentrated on northern parts of the highlands of Ethiopia since it is the most degraded area in the country. The Southern part of Ethiopia is considered as fertile and did not receive much attention yet, though it is degrading at an alarming rate. There have not been serious studies in the region regarding the problem at hand. The use of Remote Sensing and GIS for evaluating land degradation in the study area in particular and the country in general are either absent or scanty. It can be safely concluded that the area is totally unexplored and virgin to scientific works when it is compared with the intensity of the problem and the available studies. Though there are some reports available from local and regional offices and local NGOs prepared on the basis of specific interests. Therefore they are not of much relevance to the problem at hand.

2.3 Why it is necessary to study the problem in the area?

The study area is becoming highly eroded in a very frightening rate. We can see degraded lands on the process of changing to badlands in many part of the area. The resistant parts which could withstand the erosion are observed in most places as standing protruded from the surrounding degraded part. By coming out with such reality they pass on an immense message for the observer, that nature sculptured them as monuments for the land which is dying with hasty rate. Moreover, the study area is an excellent site where natural and human induced or anthropogenic factors work jointly to result such a staggering environmental damage.

Southern Nation's National Peoples Region is the most populated region in the country where lack of farm and grazing land is palpable. Natural forests are decreasing in alarming rate. Since the area is situated in the western margin of the Ethiopian Main Rift system, it is structurally controlled (geological structures) and tectonically active. Generally, it is a place where most favorable factors of land degradation coincide in space making the present study area candidate for analysis using advanced technology.

2.4 Appropriateness of GIS and RS for land degradation study

Satellite remote sensing of the earth began in the 1960s when the technical capabilities of satellite operating in Earth orbit converged with the increasing ability of computers to manipulate large quantities of data (Bernhandsen, 1999). From the mid-1970s, specialized computer systems have been developed to process geographical information in various ways (Bernhandsen, 1999). Over the

application of remote sensing and GIS in environmental studies has become very important for mapping and monitoring land degradation and other hazards over broad spatial and spectral resolution using multi-temporal images.

Quantifying the amount of soil lost and calculating the rate of degradation is easier when it is done through Remote Sensing and GIS application. In order to compute the rate and amount of soil loss in the study area multi-temporal images (satellite images of different dates) were of enormous help. To obtain more reliable and accurate data, it is better to use as many temporal images as possible with a certain interval of generation including images older than the degradation process. In addition, the availability of spectral and spatial data resolution makes remote sensing more appropriate for this specific study. The spectral data provide enough spectral separability between different surface features related to gully formation processes. Whereas the spatial resolution of the sensor determines the scale at which the data may be useful for gully analysis and mapping. More often, gullies usually develop into large badland areas, which are easier to map from remote sensing data. Individual gullies in the study area are elongated, narrow features that are difficult to map using the conventional method. Therefore, the application of Remote Sensing and GIS makes it possible to delineate consistently the smallest of the ground features of interest over a selected area.

2.5 Objectives both general and specific for the study

In relation to the above condition, this study has three main objectives:

- to apply integrated approach of Remote Sensing and GIS technique to evaluate the extent and cause of land degradation
- to use integrated techniques of Remote Sensing and GIS for land degradation susceptibility mapping and
- to recommend conservation and prevention strategy techniques

The specific objectives of the- study are:

- to investigate the causes of land degradation
- to quantify the amount of soil loss
- to identify the physical processes associated with initiation and development of land degradation

- to assess changes in the degraded areas through time
- to assess the knowledge and attitudes of the farming community
- to identify the possibilities for rehabilitation of degraded areas
- to leave a base line data for future researcher purpose since the area is not much explored

Chapter 3

Remote Sensing and GIS Application

3.1 Methods Applied

3.1.1 Data sets

Data layers that are used for assessing the problem include GIS layers, remotely sensed data, in-situ references and some auxiliary data layers.

GIS data Layers: Five GIS data layers are used in this study including, landuse/cover map, lineament map (faults, caldera like structure and some linearly aligned features), lithological map, slop map and drainage map of the area.

Remotely sensed data: Raster layers of multi-temporal data of the area extracted from the full scene of path 169 and row 55 imagery includes:

- 7 bands extracted from ETM+ (Enhanced Thematic Mapper Plus) image of Landsat 7 acquired on February 14, 2001, with a spatial resolution of 15m for band 8 and 30m spatial resolution for the rest bands excluding the thermal bands.
- 7 bands of Landsat TM images of Landsat 5 acquired on January 21, 1995 and the same number of bands of Landsat 5 TM image acquired on December 22, 1984 with spatial resolution of 28.5 m.

Field data and Ancillary Data layers: Several data have been used in addition to the vector and raster layers. In-situ data collected in the field using GPS (Global Positioning System) include:

- points collected for profiling to quantify soil loss from the selected sample sites,
- Points collected for sample site locations; and
- Points collected from the ground truthing of the land use/land cover map and geological map

Many ancillary data that contribute to complete analysis include

- Four topographic maps covering the study area fully or partially at a scale of 1:50,000, published in 1978
- SRTM data (Space Shuttle Topography Mission)

- DEM (Digital Elevation Model) of the area
- Hard copies of satellite images with different combination of color composite and different scale were used during field survey.
- Metrological data (monthly mean rainfall, monthly minimum temperature, monthly maximum temperature)
- population census data
- seismic data of the area
- Publications and reports at local and regional level concerning related topics.

3.1.2 Software

The following software were used in this study:

ENVI 3.5:- for image processing of the 3 date images in order to make it ready in usable form to other softwares for further processing;

Arcview 3.2:- to produce all the thematic layers using onscreen digitization from the processed and well enhanced satellite images, for quantifying the rate and amount of soil loss;

Cartalinx: - to digitize and edit contours, roads and drainages from the topographic maps at 1:50,000 scale.

Microdem: - to generate and display 3D view of the area by using the SRTM and DEM data, to do profile and cross section to identify structures such as faults, linear features etc.

Idrisiw: for rating, weightings, final integration of data and maps.

3.2 Image processing and interpretation

3.2.1 Image processing

Image processing is a vital part of most remote sensing operations. All digital imageries were processed using different processing techniques so that they can be applied to the problem at hand. In this case, more than just color composite image is required and more complex processing is needed in order to produce a final product (reliable result). All relevant images processing techniques were applied on ETM+ of landsat 7 and 2 dates' image of TM landsat 5.

3.2.1.1 Pre processing

Pre-processing generally precede other image processing operations. The amount of pre-processing required will vary with the sensor type and the quality of the digital data, and also with the use to which the imagery is put (Legg, 1994). The pre-processing performed includes:

Image rectification (Georeferencing):- When a polar orbiting satellite passes overhead in slightly eccentric orbits in order to obtain repeat coverage of each part of the world at roughly the same local sun time, images will never be aligned in a correct north-south direction. So image rectification is a must to correct each line of the images that is slightly offset from the line before it to compensate for the earth rotation. This earth rotation correction transforms all the images used from a square or rectangular image into a rhomboidal image. This helps to improve the relative positional accuracy of features in the image. It does not modify the original pixel values.

Band 8 of ETM+ image is used to georeference and resample the other images since it has a spatial resolution of 15 m. Band 8 of ETM+ were georeferenced using image to map registration. More than 15 well distributed ground control points were collected. All ground control points are representative and well distinguished both on the image and map. The RMS error obtained from the georeferencing of the three date image is less than 2. The georeferenced image of band 8 of the ETM+ image serves as a base image for further georeferencing of bands of ETM+ images other than band 8 and the remaining two images of TM Landsat imagery taken on two different dates. The remaining bands of ETM+ image were rectified using image to image registration by using band 8 as a base image. ETM+ image has a spatial resolution of 15 m for panchromatic data and 30 m for remaining six bands except the thermal band which has 60 m. The rectified images were resampled to a 15 m spatial resolution to increase the interpretability of the image in order to use them both as digital images and hard copies. Seven bands of Landsat TM image of 1984 and 1995 are also georeferenced based on band 8 of the ETM+ image and resampled to a 15 m resolution. The spatial resolution of TM image before the resampling process was 30m for band 1, 2, 3, 4, 5 and 7 whereas band 6 which is the thermal band has 120 m resolution.

Subsetting/resizing data: - A full scene of Landsat TM image has 185 by 185 km^2 ground coverage similar to ETM+ image of Landsat 7. Consequently, the original images are larger than the area of interest which is not more than 1750 square km. Based on this fact subsetting or resizing is

crucial. Sub setting of the study area has been done by using two step processes. First a smaller area which contains the area of interest resized from the full scene of the original image. After resizing the image, the area out of interest was masked out using a vector file imported to the working environment of ENVI 3.5 from ARCVIEW 3.2.

3.2.1.2 Processing

Image Enhancement: - For a better interpretability, the images were contrast stretched, using histogram equalization to increase the original low dynamic range of the image to a full dynamic range of the system.

Color composites: - Examination of data band by band at a time does not extract the maximum information needed for this study. Color composite images are most useful to extract the information needed regarding land degradation. Because inter-relationships between different wavelengths are very important in the recognition of features and cover types. The composite image was obtained from three bands of data assigned at a time to the RGB of the color monitor.

For a Landsat TM image there are eight hundred and forty possible band combinations. But out of all these combinations, a few of them are considered useful for this particular work. These particular combinations were chosen on the bases of how much the interest of the study is fulfilled and how much of the needed information is well extracted. Some of the color composites used include 543, 453, 432, 523, 754, 457, 4/5+5/6+6/7, and 5/4+7/4+3/7.

Decorrelation stretching: Extensive inter-band correlation is a problem frequently encountered in the analysis of multi-spectral image data (Lillesand & kiefer, 2000). In most satellite images, correlation between different bands of the sensor is very high. The generalized reflectance (albedo) of most surfaces, in particular, rocks and soils, varies relatively little with wave length between different surface types, and spectral differences are relatively subtle compared with the total reflectance. If correlation between bands can be minimized, spectral differences can be emphasized and the interpretability of the image is increased using decorrelation stretching such as PCA (principal component analysis) or IHS (intensity hue and saturate).

After applying PCA, only PC1 (with the highest variance) gives the best result for general aspect of geology while PC2 and PC3 (lesser amount of covariance) can enhance some geological features.

After performing the PCA, the PC images are combined to form a color composite which helped in mapping some of the different thematic maps produced.

Ratio images: The inter-relationship between different bands of data may often be rather subtle, and techniques other than production of color composites may be necessary in order to reveal them. It may also be desirable to remove some components, such as illumination due to topography or solar elevation, which is common to all bands of an image thus band ratioing is most preferably applicable. In this study some ratios (one band divided by another) and normalized ratios such as NDVI are used. Some of the band ratios used includes 3/7, 7/3, 5/4, 4/5, 4/7, 5/2, 5/6, 6/7, and 7/4.

Ratioed image according to Lillesand & Kiefer (2000), are often useful for discriminating subtle spectral variations in a scene that are masked by the brightness variation in images from individual spectral bands or in standard color composites. It can be also used to generate false color composites by combining three monochromatic ratio data sets.

Linear filtering and edge enhancement: In order to increase the visual interpretability of an image, it is often necessary to artificially sharpen the image.

In order to enhance edges a high pass directional filter at an angle of 45^0 was applied to band 7 of ETM+ image (Figure 3.2). This helped to emphasize areas of abrupt change relative to those of gradual change resulting in an edge enhanced image. The enhanced image is then added to the original image to result in an intensified boundary and line information. Geological structures which were not well observed and that seemed indistinct appeared evidently visible after the implementation of the filtering process. A simple formula was created to sum the filtered and original image:

B1+B2= the resulting edge enhanced image

Where: B1 represent the directionally filtered image and

B2 represent the original image

For the directional filtering, a 3x3 convolution matrix was used. The kernels used contain zero on the diagonal values while the upper matrix contain negative values and the lower matrix contains positive values.

-1.4142	-0.7071	0.0000
-1.0000	0.0000	-1.0000
0.0000	0.7071	1.4142

Table 3.1 A high pass filter

These kernels are ENVI's default directional filter (Table 3.1). Application of the filter resulted in removing the low frequency components of the image while retaining the high frequency (local variation). It can be observed in the summed image below clear linear features and boundaries (Figure 3.1 & Figure 3.2) of the high pass directional filter.

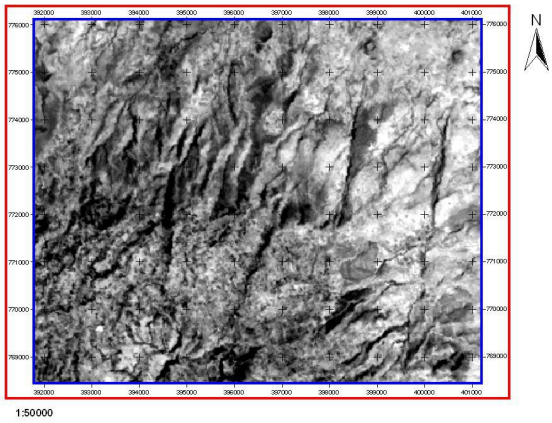

Figure 3.1 Original image before processing

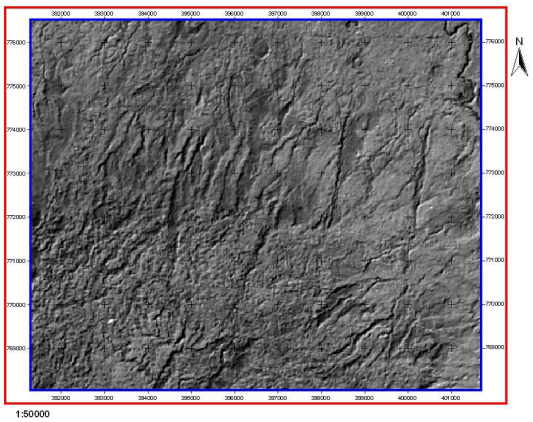

Figure 3.2 Image after processing

3.2.2 Image Interpretation and Mapping

3.2.2.1 Interpretation

Visual image interpretation is a crucial step that follows image processing. All image processing techniques help to make features that are present in the image visible and well enhanced for information extraction based on visual analysis or interpretation of the data. During visual image interpretation, interpretation elements such as tone, shape, size, pattern, texture, site and association provide great help in recognizing certain objects. These objects are identified by their relative brightness, shape, spatial arrangement and geographic location. Visual interpretation is done using a single band and color composite of multi band combination which resulted from the different image processing techniques. Morphological features and tectonic structures were also visually interpreted in 3D view using MICRODEM and 3dem software.

3.2.2.2 Mapping

The result of the interpretation is made explicit by digitizing the geometric and thematic data of different layers. Onscreen digitizing on ARCVIEW 3.2 software was carried out to digitize 2D features such as points, lines and polygons.

The maps that are produced as a result of image processing and visual interpretation include:

1. Landuse/land cover map: - by selecting appropriate color composite image, hard copy prints were produced to undertake landuse/landcover mapping through visual interpretation. For this purpose, hard copies of the relatively recent LANDSAT ETM+ image with different color composites were of great help. The false color composites used for landuse mapping comprises the bands 543, 453 & 432. Landuse categories can often be distinguished quite well by assigning a combination of Landsat TM bands 543 or 453 to RGB (Bakker et. al, 2001). False color composite 453 in RGB order (Figure 3.4) highlights vegetation differences. Natural forest appears reddish brown; grassland is green to yellowish green and bare soil white to light green. Irrigated crops show shades of red whereas degraded areas appear light purple. After producing the hard copies of the images, the landuse mapping was conducted in the field during preliminary field checking by taking as many representative sample sites as possible. By taking these representative samples as bases, the landuse map was prepared using on screen digitization with the help of 543 and 453 color composite ETM+ images. Before finalizing the landuse map, detail field checking (verification) was necessary. On this step, five representative sites were taken for each landuse class based on which ground truthing was conducted by using the landuse map that was prepared during the preliminary field checking. Subsequent to the final field checking, all the necessary corrections were made and the final landuse map was produced (Figure 3.3).

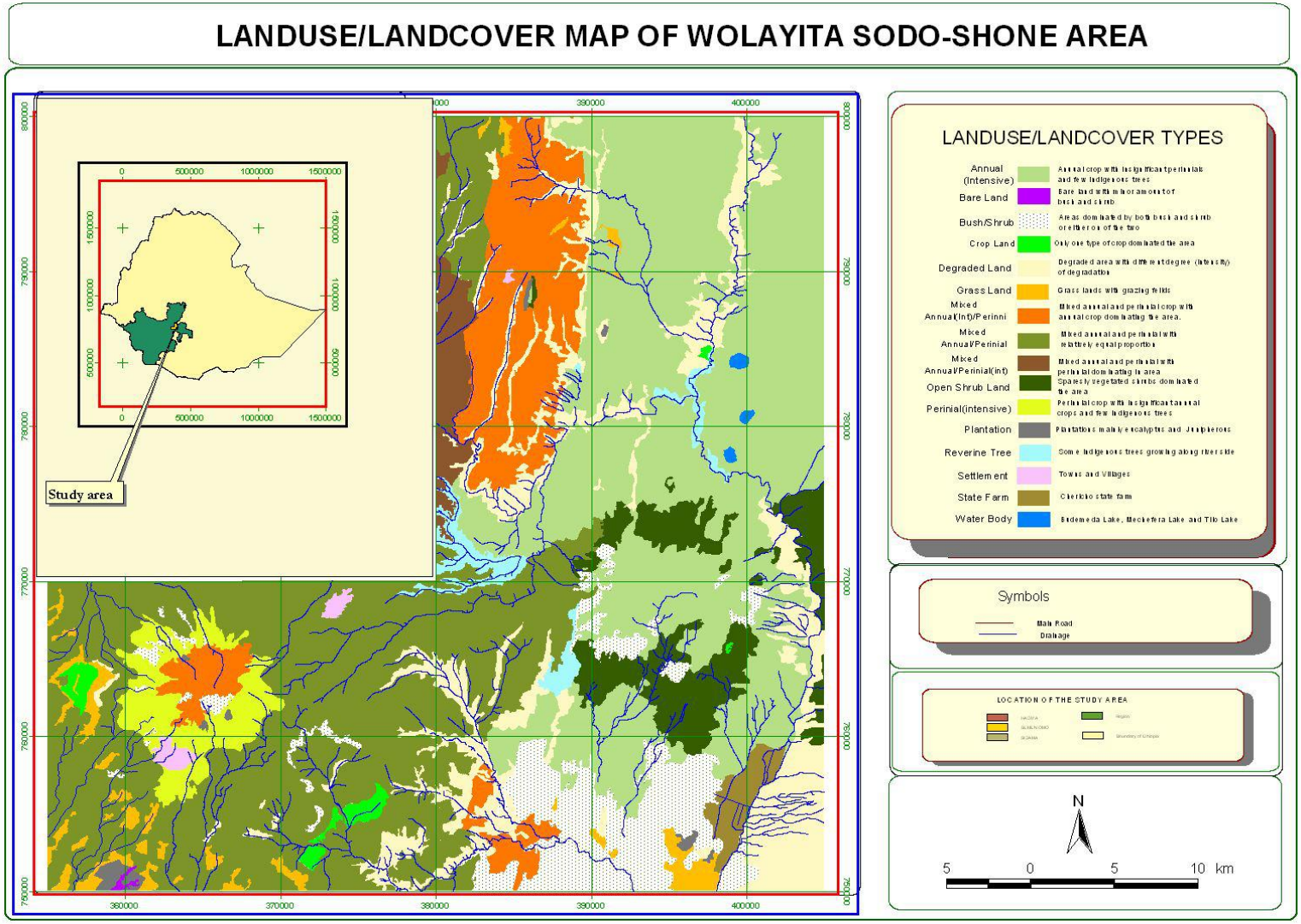

Figure 3.3 Landuse/landcover map of Wolayita Sodo-Shone area

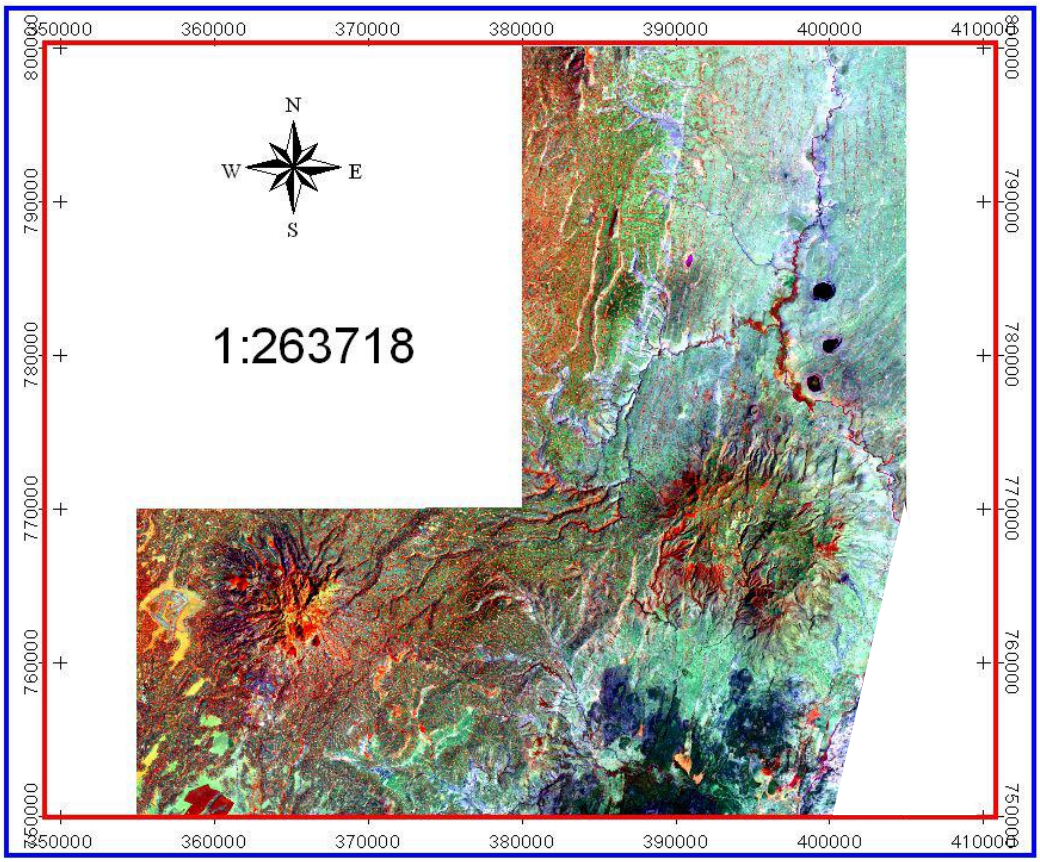

Figure 3.4 False color composite 453 in RGB order

2. Geological map:- For lithological mapping, since the mid infrared band 7 is specifically designed to be sensitive to clay minerals and indirectly to their parent materials, composites including bands 7 and 5 with one visible band (usually 3) are frequently used. In addition to the 753 (RGB) combinations, a ratio and PC's bands are also used for further interpretation of lithologic units. By combining the PCA 1, 7/3 ratio image and the sum of band 3 and band 7 in RGB order, more distinct lithological boundaries were observed. The lithological map shown in Figure 3.5 is a result of visual interpretation of a hard copy and digital data of band 753 color composite (RGB) followed by detail field checking. The visual interpretation was done on a hard copy at a scale of 1:100,000.

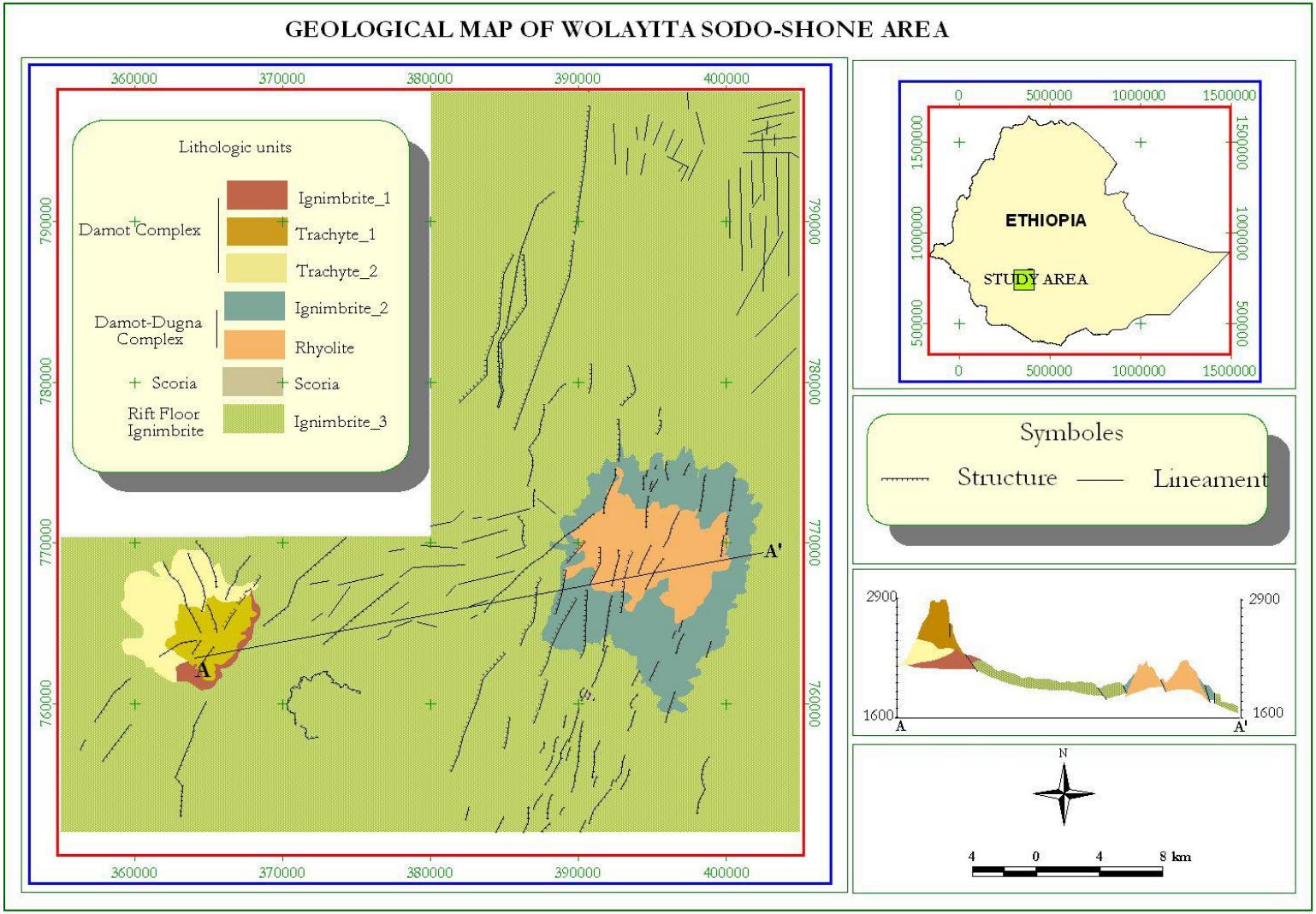

Figure 3.5 Geological map of Wolayita Sodo-Shone area

3. Structural map of the Area: - since the study area falls partly in the western margin and partly on the Ethiopian Main Rift (MER), it is highly affected by tectonic structures. Most of the geological structures are normal step faults trending NNE-SSW to NW-SE as that of the Main Ethiopian Rift (MER). These faults are commonly arranged in side-steeping an en-echelon style (Tesfaye Korme, 1999). These geological structures were mapped using a directional filtered monochromatic band 7 of the Landsat ETM+ image. This filtered image was added to the original band 7 image in order to avoid confusion of tectonic structures with man made linear infrastructures (features). The downthrown and up thrown parts were also identified from the difference in tonal variation with neighboring pixels. Geological structures facing away from the direction of illumination showed low reflectance in the visible and near infrared. This can be attributed to a shadow effect caused by the depth and surface irregularities of the dawn thrown and up thrown part that traps the incoming light and reduces the reflectance. Since the illumination direction of the ETM+ image used is from E-W, faults that have down throw towards west appear darker and those facing east appear lighter. Moreover, cross checking was conducted using 3-D views of SRTM data with the help of MICRODEM. SRTM (Figure 3.6) data clearly shows the presence of tectonic structures especially

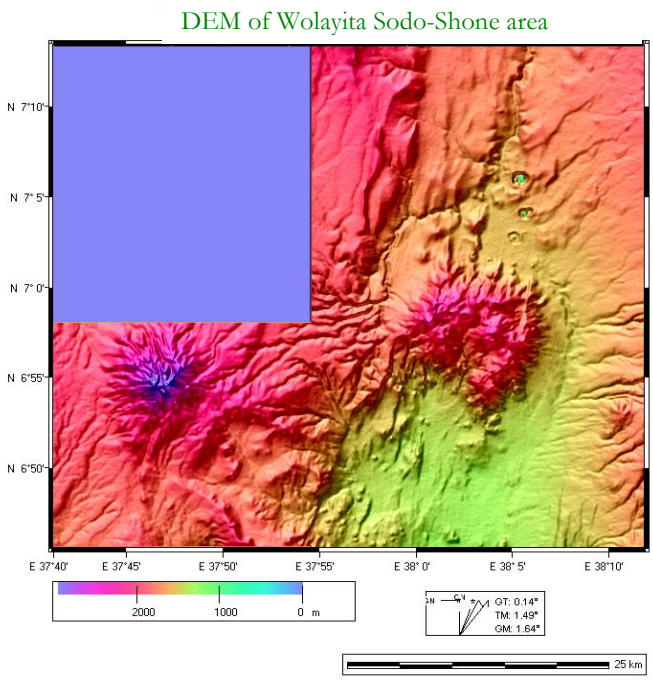

Figure 3.6 DEM of the study area (x4 exaggeration factor)

faults with their direction of throw clearly identified. Finally, all these sets of information were integrated with field check to produce the final structural maps. Between Mount Damot and Mount Dugna, there is a half caldera-like structure. It is more enhanced and mapped using non-directional filter. Some lineaments trending in different directions than the common NNE-SSW were also visually interpreted and mapped.

4. Drainage Map: - drainage lines were digitized from a 1:50,000 scale topographic map of the area. The drainages were digitized from 4 topographic sheets and were edited using Cartalinx software. The digitized and edited drainage maps were exported to ARCVIEW shape file where all drainages from each topographic map were merged for further analysis. The digitized drainages draped on the satellite images of ETM+ show a very slight offset, probably due to the error encountered during digitization (RMS error for each drainage digitized from each topographic maps were less than 3.0) or due to temporal difference (the topographic map was produced in 1978 G.C. Whereas the image used to drape the drainage is taken in 2001). The drainage may have changed its course very slightly within this interval of time.

Chapter 4

Soil horizon analysis and sampling

4.1 General

Soil is regarded by geologists as the accumulation of loose weathered material which covers much of the land surface of the earth to a depth ranging from a fraction of an inch to many feet (Whitten and Brooks, 1972). It is the end product of weathering of different types of rocks through different chemical, physical and biological processes. When Rocks those are formed at high temperature and pressure brought up to the surface, and exposed to low temperature and pressure condition they decompose into minerals that form soil. Human's life depends on the use of this soil for their daily needs though they do not sufficiently take in to account of its slow formation and fast consumption.

In this study the nature of the soil has its own great contribution for the problems which are the initiatives of the research. So in order to characterize the nature and type of the soil and to assess its input to the problem at hand, 8 samples were taken during the field survey and analyzed through laboratory work to get the necessary results (Annex 2). Out of the 8 samples, 5 samples were taken with especial interest to the land degradation part while the rest 3 samples were analyzed and interpreted to get substantiation for the landslide part.

Classification for the analyzed samples was done using Unified Soil Classification System (USCS) based on the distribution of various particle sizes and the plasticity characteristic of very fine particles. According to this classification system, more than half of each sample is smaller than No. 200 sieve opening (0.075mm), thus soil of the area falls in to CL, MH, and CH group.

Where,

CL= Inorganic clays of low to medium plasticity, gravely clays, silty clays, sandy clays, lean clays

MH= Inorganic silts, micacous or diatomaceous fine sandy or silty soils, elastic silts

CH= Inorganic clays of high plasticity, fat clays

The soil profile observed around shone (Figure 4.1) indicates that organic soil is found on top overlaying the red soil next the pumice layer followed underlain by the thin ash layer. The bottom part is weathered ignimbrite overlain by the pumice and ash layer.

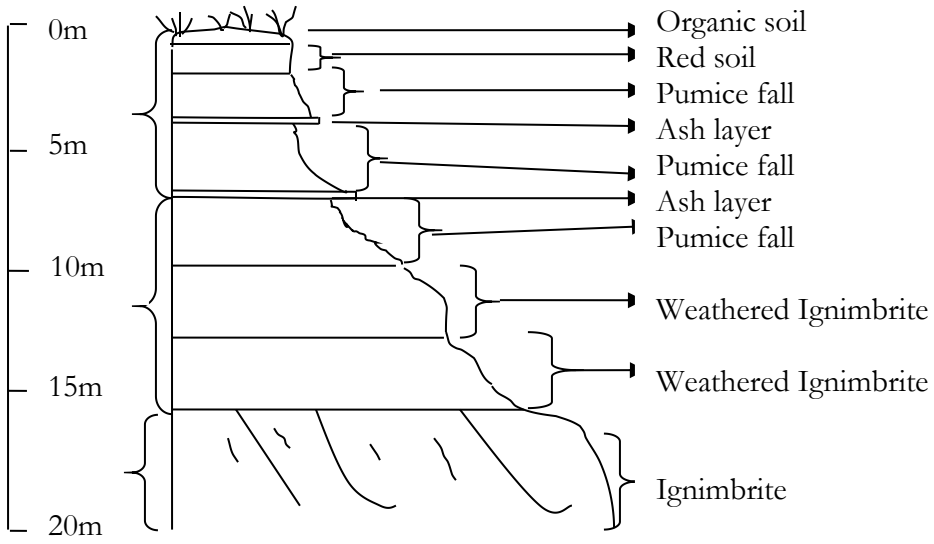

Figure 4.1 Soil profile around shone area

4.1.1 Field sampling

During the field survey samples which are believed to be representative were visually interpreted and taken for further laboratory analysis. Disturbed samples were taken from accessible outcrops on the surface to very shallow depths. Representative sites where intensive degradation with differential weathering occurred and where all the soil horizons are clearly visible were selected for sampling purpose. Samples were taken from 4 successive layers in order to identify the nature and type of each soil layer, and to investigate the cause for the differential weathering occurred on the different layers.

4.1.2 Soil sample analysis

Essential soil tests were performed on eight soil samples at the Soil Mechanics Laboratory of the Faculty of Technology of the Addis Ababa University. Out of the nine samples, five were taken with special interest for land degradation study. Simplified index tests (Gradation analysis and atterberg limits) were conducted to characterize the physical property of the soils (Annex 2).

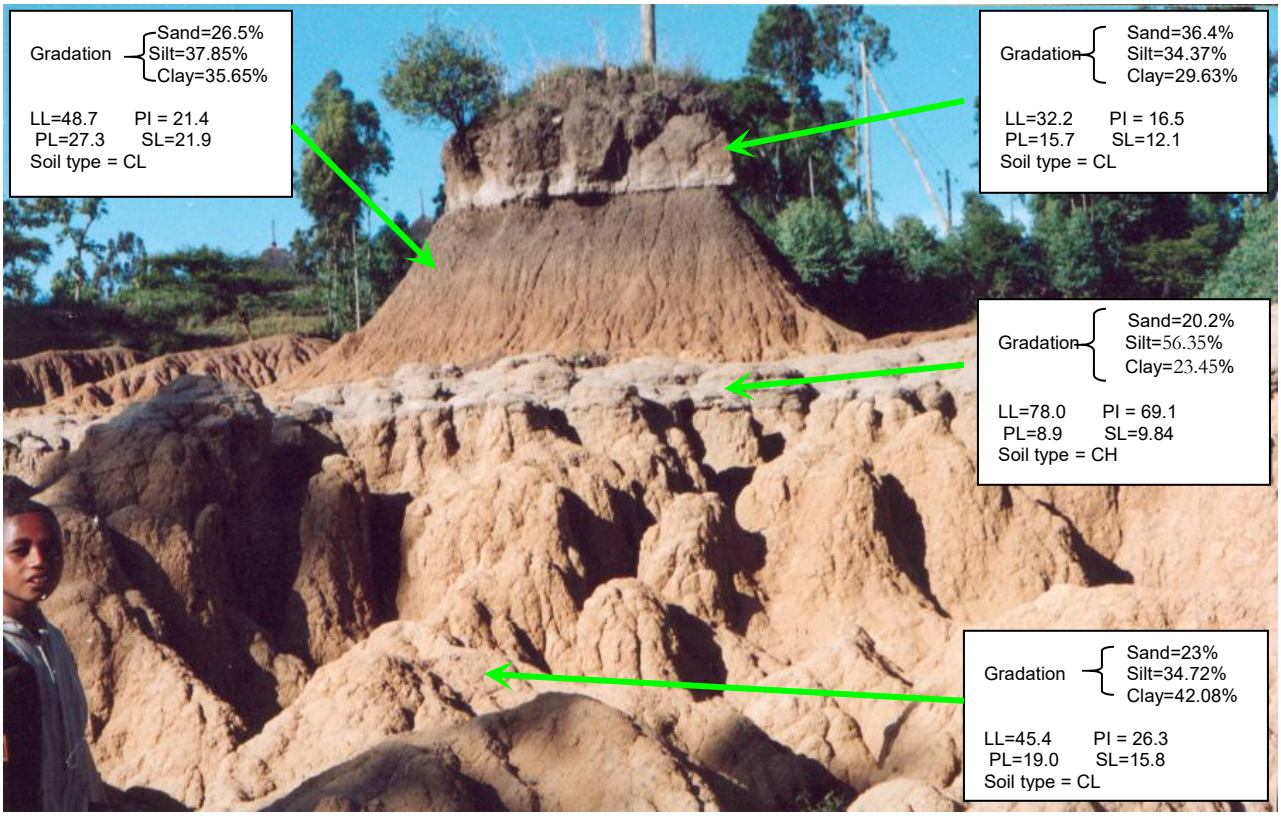

Figure 4.2 Highly eroded and degraded area around Shone show fully exposed soil profile

4.1.2.1 Gradation test

Gradation refers to the distribution of grain size and it is presented in the form of a cumulative grain-size curve in which particle size are plotted logarithmically with respect to percentage (by dry mass) total specimen plotted to a linear scale (Earth manual, 1998). It helps to understand the particle size distribution within a given sample and helps to determine percentage of gravel, sand, and fines in soil. Based on the understanding of gradation test, a soil can be said to be well graded, poorly graded and gap or skip graded. A well graded soil is the one which has a good representation of all particle sizes from gravel to clay. Where as poorly graded or uniform soil comprises particle size of about the same size. There is also a case in which an absence of one or more intermediate sizes is available. This kind of soil is known as a gap or skips gradation. The hydrometer analysis and sieve analysis carried out were helpful to characterize the grain size distribution of the samples from the study area.

Sieve analysis: - Sieve analysis was conducted to identify the percentage of particles greater than 75-μm (200) sieve. According to this test, percentage of sand in the study area ranges between 8.5% - 26.5% except sample 1 which contains about 36% sand (Table 4.1 & Figure 4.2).

Hydrometer analysis: - was done for the particles finer than 75-μm (200). For these fine particles of soil, plasticity characteristics are determined by performing the Atterberg limit tests. These tests were performed to determine the moisture content of a soil at liquid, plastic, semisolid, or solid state.

Sample No	Location	Depth of sampling	Liquid limit (%)	Plastic limit (%)	Plastic index (%)	Shrinkage limit (%)	Classification based on USCS	Grain size (%)
1	Cheleleki	30cm	32.2	15.7	16.5	12.1	CL	Sand: 36.40 Silt: 34.37 Clay: 29.23
2	Cheleleki	1m	48.7	27.3	21.4	21.9	CL	Sand: 26.50 Silt: 37.85 Clay: 35.65
3	Cheleleki	1.5m	45.4	19.0	26.3	15.8	CL	Sand: 23.20 Silt: 34.72 Clay: 42.08
4	Cheleleki	2.5m	78.0	8.9	69.1	9.84	CH	Sand: 20.2 Silt: 56.35 Clay: 23.45
5	Adilo	30cm	68.7	26.3	42.4	38.38	CH	Sand: 13.10 Silt: 15.27 Clay: 71.63

Table 4.1 Soil test results

4.1.2.2 Atterberg Limits

Atterberg limit test is one of the physical property tests that are used to determine whether the sample's fines are silt or clay based on their behavior.

The physical properties of most fine-grained soils, and particularly clayey soils, are greatly affected by moisture content (Earth manual, 1998). The moisture content of the soil samples taken from the field is determined using their liquid limit, plastic limit, shrinkage limit, and plasticity index (Table 4.1 & Figure 4.2).

Liquid Limit (LL):- The minimum water content at which clay deforms under its own weight and changes in to a liquid is its liquid limit. For three fifth of the samples tested the liquid limit is less than 50% while Sample no 4 and 5 have 78.0 and 68.7 respectively.

Plastic Limit (PL):- is the minimum water content at which plastic deformation is possible. The plastic limit is less than 30% for all soils analyzed. Moreover Sample No 4 has surprisingly lower plastic limit than the rest of the samples.

Shrinkage Limit: - refers to the water content that is just sufficient to fill the pores when the soil is at the minimum volume and it is attained by drying. It also indicates the boundary between the semi-solid and solid states. The shrinkage limit of the samples analyzed ranges from 9.84-38.38.

Plasticity index (PI):- is the difference between liquid and plastic limits, and represents the range of moisture content over which soil is plastic.

As moisture content increases, the consistency stage of a soil changes from solid state to liquid state passing through the semisolid and plastic state respectively. As the phase of soil water content advanced from liquid state to solid state; the volume of the material decreases, the consistency changes from slurry to very hard while the shear strength increases.

4.1.3 Soil classification

According to the gradation test results the soil samples taken for the area affected by degradation ranges from silty clay to fine clay. The analysis confirmed that more than 50% of each of the samples passes No. 200 sieve. This shows that the soil of the area is dominated by the finer soils such as silt and clay (Table 4.1 & Figure 4.2).

According to the Unified Soil Classification System (USCS), there are two major divisions namely fine grained soils in which more than half of material is smaller than No. 200 sieve and coarse-grained soils where more than half of material is coarser than No 200. Since all the soil samples percentage passing greater than 50% passing No. 200 sieve, the samples are classified as fine grained. Within this division the three samples (sample No 1, 2 and 3) have a liquid limit of less than 50% and their plasticity index ranges between 26.3-16.5, there for their typical class belongs to silty clays (CL). Whereas, sample No 4 and 5 have a liquid limit of 78.0 and 68.7 respectively. Their plasticity indexes are 69.1 and 9.84 respectively. Based on this fact they are classified as inorganic clays of high plasticity or fat clays.

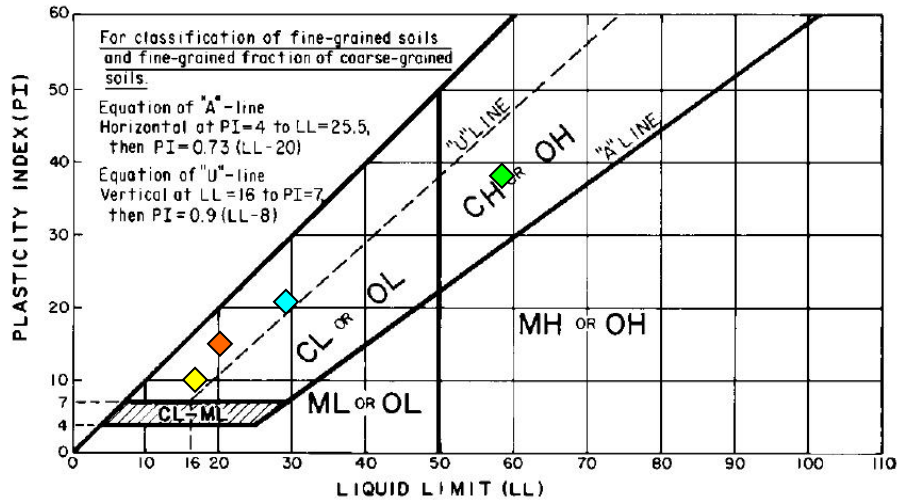

◇ Sample No 1 ◇ Sample 2 ◇ Sample 3 ◇ Sample 5

Figure 4.3 Samples plotted on the Plasticity chart

4.1.4 Implication of test results to degradation

The test results show that most of the soil layers belong to silty clays (Figure 4.3 & Annex 3). However the different soil layers show different liquid limits. The resistant layer shows a relatively high liquid limit of 78.0% while the friable and degraded layers show about 45% liquid limit on average. Similarly shrinkage limits are proportionally lower for resistant layer and higher for the highly eroded layers. These clearly indicated that the differential weathering is directly related to the differential properties of the soil layers, where the layers with smaller shrinkage limit and higher liquid limit are very hard to firm soils with higher shear strength resistant against erosion. The soil layers underlying and overlaying these resistant layers are softer and are sensitive to change in moisture content which facilitates their erosion. There for, these differential properties of the soil layers lead to differential weathering and erosion of the area resulting the degraded lands. However, it must be noted that the triggering factors of the degradation could be the structural weaknesses along faults and subsequent drainage patterns.

Chapter 5

Land degradation mapping and analysis

5.1 Introduction

Soil erosion is considered to be the major cause of soil degradation in Ethiopian highlands (Solomon Abate, 1994). Soil integrates a variety of important natural and artificial processes involving vegetation growth, overland flow of water, recharging media for ground water, and landuse and land management. Soil degradation is, in itself, an indicator of land degradation. But, in the field, additional variables are used as indicators of the occurrence of soil degradation. Some of the indicators seen in the area include:

- Soil erosion by water such as rill, sheet and gully erosion;
- The productive capacity of the land declining as a result of reduction in soil fertility that results from the washing away of organic matter;
- Loss of vegetation cover;
- Increased stoniness and rock cover of the land: the bed rocks are exposed at the surface in most places; and
- loss natural beauty of the area

5.2 Types of degradation

Land degradation refers especially to soil degradation in the area of study. Three types of degradation namely rill erosion, sheet erosion and gully erosion are observed in the area. Most research on soil erosion in Ethiopia deals with sheet and rill erosion (Nyssen et al. 2003). But in the specific area of study, gully erosion which is the dominant type is given more emphasis.

Sheet erosion: Sheet erosion is the first stage of gully formation (figure 5.1). It occurs when the infiltration capacity of soil is exceeded by the amount of rain water resulting in surface flow, detaching fine particles from the upper loose soil. It involves the removal of a uniform thin layer of soil by raindrop splash or surface run off. This thin layer of topsoil often disappears little by little, making it difficult to monitor for the reason that the damage is not instantaneously traceable. This insidious process is often unnoticed until the subsoil is exposed. Most of the areas are characterized by removal of organic matter and vegetation cover is decreasing, aggregates are breaking down and in many parts crusts are formed which air and water can no longer penetrate.

Figure 5.1 Bed rock exposed due to sheet erosion

Rill erosion: Rill erosion often occurs and is commonly seen in areas of recently cultivated soils following high-intensity rainfall. It is easily identified as a series of small channels or rills up to 25-35 cm deep. In the study area, land degradation mainly affects places where the land use type is dominated by annual cropping, due to the fact that running water forms small gutters (rills) that transport much soil from the cultivated area. Once water starts to form rills, erosion intensified and soil particles tend to move off the field entirely. As water moves down slope, it will get more energy; will run ever stronger and deeper to transport huge amount of soil.

Gully erosion: This is the most dominant type of erosion observed in the area (figure 5.2). Most of the gullies in the area have elongated shape with varying width and depth. This type of gully is formed when water widens and deepens the walls and floors of creeks or small rills as it moves all the way through it baring the bed rock and transporting ever more soil. Usually, rill erosion develops into gullies with time which is evidenced in the study area. Major concentrations of high-velocity run-off water in these larger rills remove enormous amounts of soil. This results in deeply incised gullies occurring along depressions and drainage lines. Deep wide gullies, sometimes reaching 30-35m deep, are limiting the use of the land in the study area by disrupting normal farm operations.

Figure 5.2 The most dominant type of erosion in the study area

5.3 Rate of degradation

Intense land degradation is evident in the study area. The rate of degradation is increasing with time due to various reasons. One of the objectives of this study is to calculate the rate of degradation in the study area in areal base. However, due to the absence of base line profile data, it is not possible to calculate the degradation in volumetric base.

Processed satellite images of three different years were resized from the original path 169 raw 55 images to use them for this analysis. Smaller area of about 640 square kilometer that is representative of the degradation was selected from the whole study area based on the intensity of the problem. The images used include landsat 7 of 2001 and two different date images of landsat 5 taken in 1984 and 1995. Color composite images of bands 743 in RGB order were used in order to map the degraded areas from the three dates image.

It should be noted here that the images available are of 1984, 1995, and 2001, with different intervals (11 years and 6 years) among them. This may complicate the interpretation of the rate of degradation. Moreover, the calculation is empirical and it considers natural and human induced factors as constant.

Areas that are affected by degradation were onscreen digitized for each available three dates images using Arcview GIS 3.2 software. This is intended to calculate the rate of degradation through time in areal base. The degraded areas were zoomed until the boundary of the degraded areas become clearly visible. Therefore, the digitization process was performed with maximum care to minimize the errors encountered during digitization. The vector layers that represent degradation were imported to IDRISI 32 and converted to raster format. Using IDRISI's analysis module, the total area of the degraded and non-degraded land were calculated for each year (Table 5.1). In 1984 the total area that is affected by degradation within the 640 square kilometers area was only 38.4 square kilometers (Figure 5.3) which is 6% of the total representative site. However, this amount has increased to 58.1 square kilometers (9.1%) in 1995(Figure 5.4). In 2001(Figure 5.5), this value has grown to 76.1 square kilometers (12.0%).

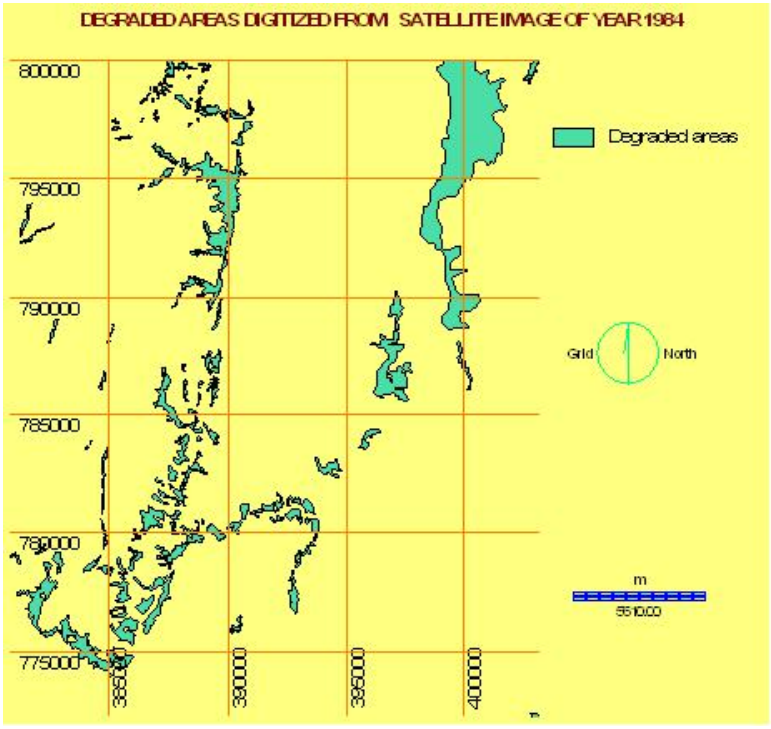

Figure 5.3 Vector map of the degraded area digitized from the 1984 TM landsat image

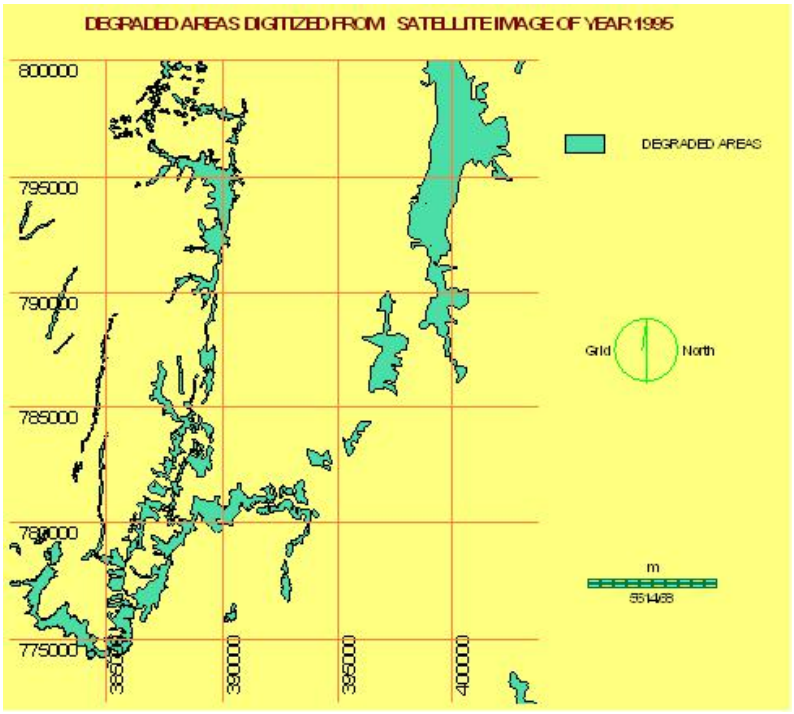

Figure 5.4 Vector map of the degraded area digitized from the 1995 TM landsat image

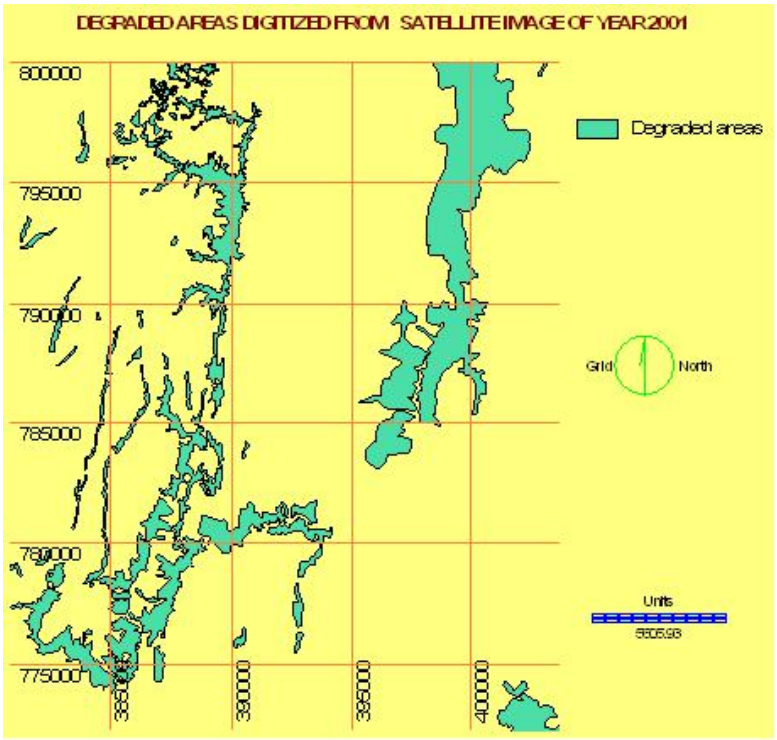

Figure 5.5 Vector map of the degraded area digitized from the 2001 ETM+ landsat image

Year	Degraded area (km^2)	Non-degraded area (km^2)	Degraded area (%)	Non-degraded area (%)

1984	38.4	601.6	6	94
1995	58.1	581.9	9.1	90.9
2001	76.7	563.3	12.0	88.0

Table 5.1 Degraded and non degraded areas in square kilometers for year 1984, 1995 & 2001

The change in a time series of the degraded areas was produced using CROSSTAB module in IDRISI 32. This module helps for cross-classification of images in which the categories of one image are compared with those of another. Cross-classification can be described as a multiple overlay showing all combinations of the logical AND operation and the result is a new image that shows the locations of all combinations of the categories in the original images (IDRISI, 1990-2000). The result of this operation is an image that comprises different categories such as classes that are present in both images, classes that are present in the first image only, classes that are present in the second image only and classes that are not present in both images.

Cross-classification was analyzed between the 1995 and 1984 rasterized map of land degradation. Then area is calculated for the cross classified image using ANALYSIS module so that the change with time series is calculated. The cross-classified image resulted from the analysis has 4 categories. From the description of these categories (Table 5.2, Figure 5.6), it can be concluded that there are areas with positive change, negative change and no change within the specified time series in the selected sample site. The green color in the image represents non degraded areas that have not changed between 1984 and 1995 with respect to the change parameters considered. It covers about 581.9 square kilometers of land. The negative change areas that are represented by blue color indicate the additional degraded areas from that of the 1984 image. It covers about 31.4 square kilometers area. Whereas, the class represented by red color covers 26.7 square kilometers area. It characterizes 4.17% of the total sample site.

Category	**Areas in (km^2)**	**Area in (%)**	**Legend**	**Remark**
1	581.9	90.92	0 | 0	classes of non-degraded areas in both images
2	31.4	4.9	1 | 0	classes that are present in 1995 image only
3	11.7	1.8	0 | 1	classes that are present in 1984 image only
4	26.7	4.17	1 | 1	classes that are present in both images

Table 5.2 Areas calculated from the cross-classified images of 1984 and 1995

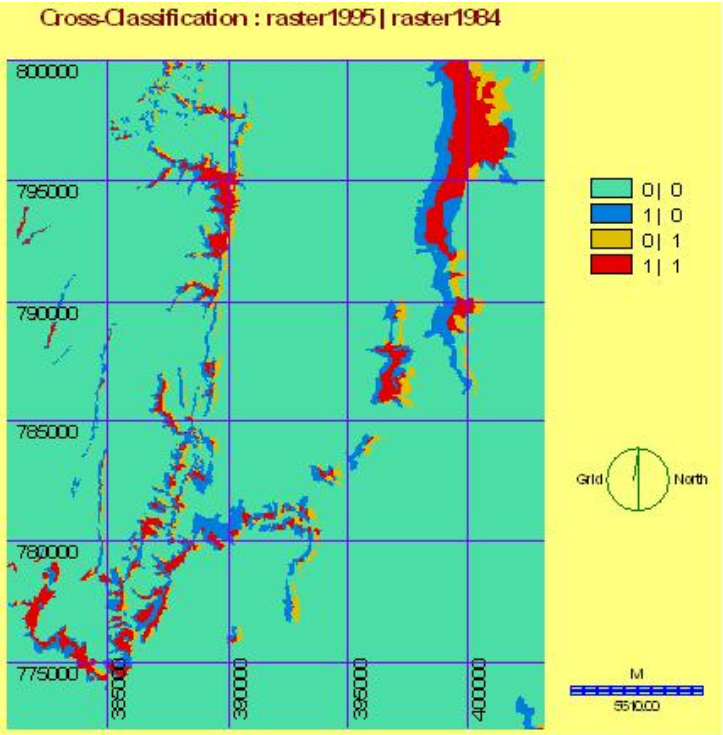

Figure 5.6 Cross-classified image from the 1984 and 1995 images.

The analysis shows that there are areas with positive change in which degraded areas seemed to be cover by vegetation. The areas that show positive change are represented by yellowish color and cover about 1.8% of the total sample area. This positive change might have been due to encroachment of weeds and some other types of vegetation to the abandoned degraded lands.

Cross-classification was also applied for the images of 2001 and 1995 (Fig 5.7). Within the given period of time 25.1 square kilometers of degraded land is added to the existing degraded areas. This increase of degraded area is a negative change and represented by blue. The green color that stands for non-degraded areas in both image covers 569.8 square Kilometers of the total sample site. Whereas red color stands for the degraded areas that do not show change within the given interval. It covers about 51.6 Square Kilometers or 8.06% of the total area. An area that was degraded and seems to be covered by vegetation is represented by yellow color and covers about 1.01% of the total area (Table 5.3).

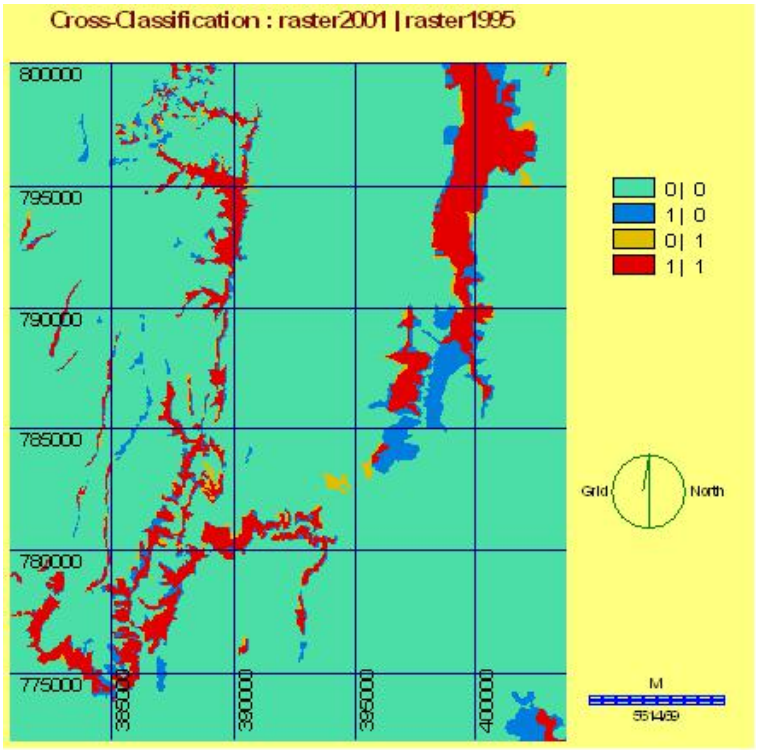

Figure 5.7 Cross-classified image from the 2001 and 1995 images.

Category	Areas in (km^2)	Area in (%)	Legend	Remark
1	569.8	89.03	0 | 0	classes of non-degraded areas in both images
2	25.1	3.92	1 | 0	classes that are present in 2001 image only
3	6.5	1.01	0 | 1	classes that are present in 1995 image only
4	51.6	8.06	1 | 1	classes that are present in both images

Table 5.3 Areas calculated from the cross-classified images of 2001-1995

After performing the cross-classification between 1995 and 1984 images and 1995 and 2001 images, rate of change in degraded areas is calculated. The average rate of degradation from 1995 to 1984 is given as 1.8 sq. km/yr [(58.1-38.4) sq. km/11yrs] while the average rate of degradation between 2001 and 1995 is given as 3.1 sq. km/yr [(76.7-58.1) sq. km/6 yrs]. This shows that the degradation problem is becoming serious since recent times. From these figures it can be seen that the rate of degradation is increasing nearly in alarming rate. If this trend is considered to be true since 2001, it can be safely concluded that in the last 3 years a roughly equal amount of degraded land between that of 1995 and 2001 (about 25 sq. km) has been added to the already degraded land, resulting in a totally degraded zone of about 100 sq. km. (about 17% of the sample site) at this moment.

5.4 Intensity of degradation using cut and fill method

Calculation of the amount of soil lost from the study area is conducted on 5 representative sites, selected based on the intensity of the problem, their areal extent and accessibility to the main road. The amount of loss within the sites is estimated through cut and fill analysis using arc view 3.2 software. During the field survey, profiling was done for the whole representative site using GPS reading taken at every 5-10 m interval depending on the relative roughness of the area. For somewhat rough area where a brisk altitude change exists within very short distance, GPS readings were taken at even at less than 5 m interval, whereas for a relatively flat area at 5-10 m intervals reading were carried out.

All GPS reading were organized in a database. By considering relatively uneroded areas as a plane to represent the area before the degradation, volume loss is calculated by subtracting the plane surface from the presently existing degraded area. This gives an estimated result of net loss of the soil (Table 5.4). The data and the 3D view of the area (Figure 5.8, 5.9 & 5.10) show that the area is intensively affected by erosion.

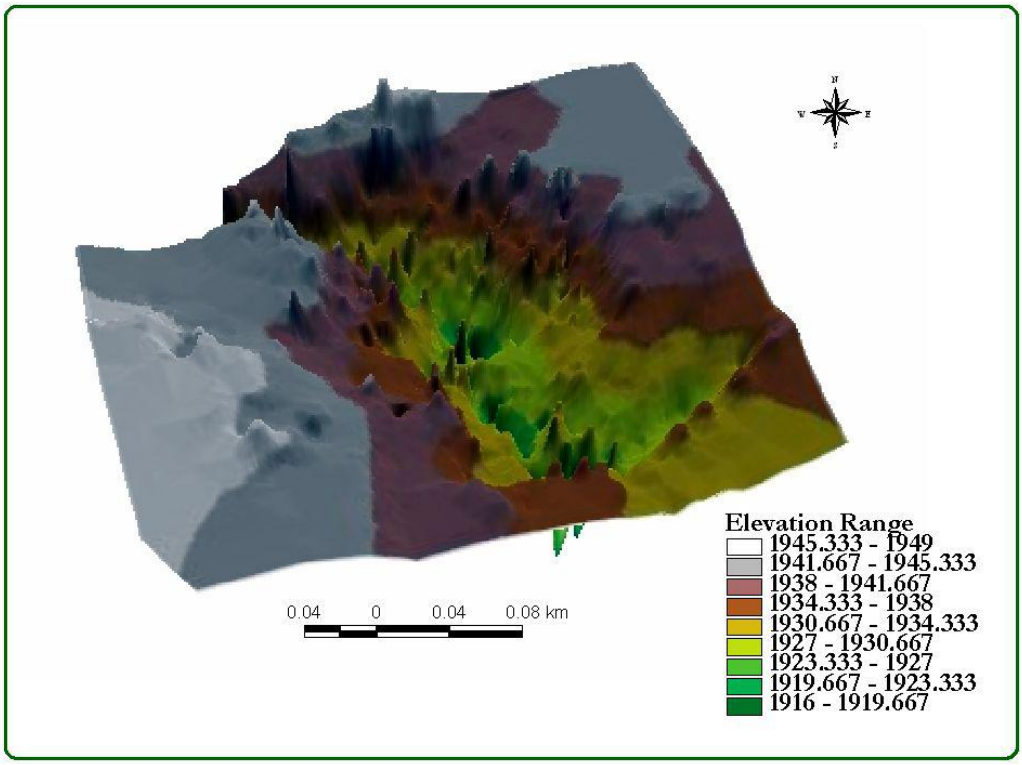

Figure 5.8 3D view of the surface data for the sample site 3 (exaggeration factor X4).

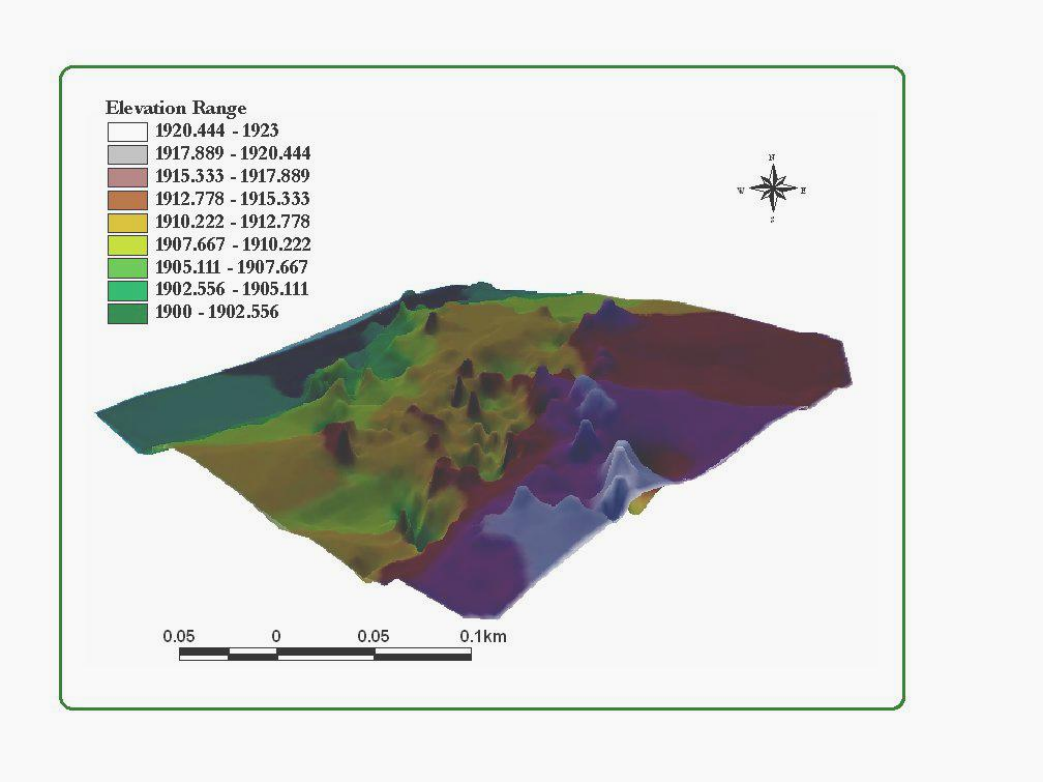

Figure 5.9 3D view of the surface data for sample site 4 (exaggeration factor X4).

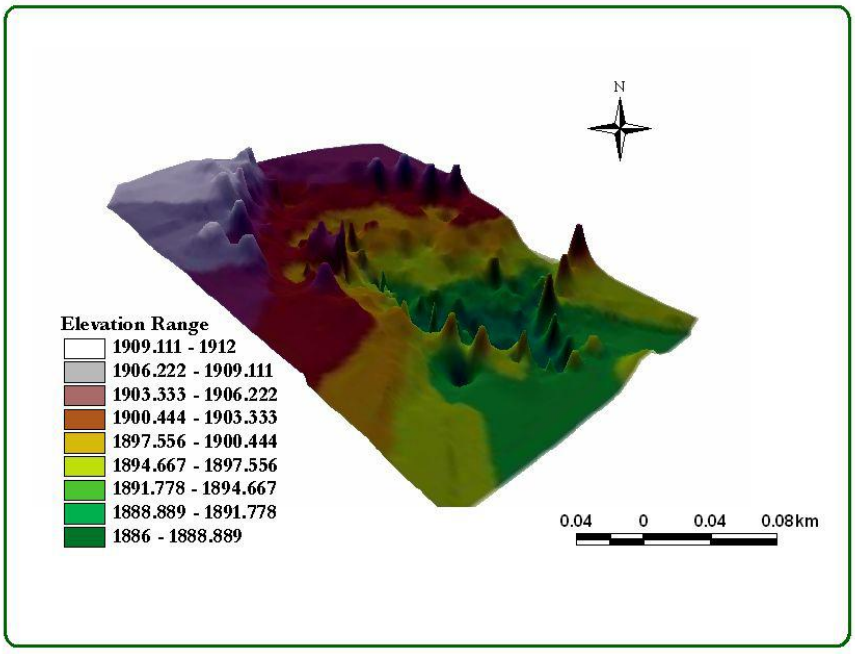

Figure 5.10 3D view of the surface data for sample site 5 (exaggeration factor X4).

Sample site	Location (UTM)		Net loss (m^3)	Sample area (m^2)	Net loss/area
	Easting	Northing			
1	381006	779139	914,273	101,368	9.02
2	382543	788440	145,440	79,221	1.8
3	386576	796510	363,693	67,340	5.4
4	389038	797677	789,867	84,456	9.35
5	388183	786874	272,545	58,856	4.6
		Total	**2,485,818**	**291,241**	**8.53**

Table 5.4 Estimated values for the amount of soil lost in the study area

As it can be seen from the table, large amount of soil is lost from such a small area without consideration of the time taken, since there is no base line survey data to calculate the rate of degradation in volumetric base. However, the rate of degradation is calculated on areal base using three date multi-spectral satellite image as it is explained in the previous part.

Chapter 6

Integrated GIS analysis for causes and factors of land degradation

6.1 Introduction

Land degradation is caused by communal interaction of various factors. The process and exact mechanism of land degradation are still not well understood; hence prediction of this hazard is quite difficult. Therefore, there is a substantial degree of uncertainty involved in any hazard evaluation process (Saha et al. 2000). Out of the various methods of data integration for land degradation and landsliding application, in this study, the qualitative hazard analysis using relative weighting rating system has been adopted with the help of the field observation. This method is adopted since it is commonly applied in most studies (Birhanu et al. 2001, Dragan et al.2003, Saha et al. 2000, Tenalem Ayenew and Barbieri, 2004, and Peter V. Gorsevski et al., 2000).

Several factors contribute to the exiting land degradation in the study area, which would also have the potential to prolong their effect to lead to a bad land with an intensively degraded environmental condition. As discussed in the previous chapters, the degradation in the area has been resulted from two main impacts, namely natural and human induced factors. Within each impact there are a number of factors that contribute to the degradation process such as structure, lithology, landuse, slope, soil, drainage, and climate factor. Each factor that contributes its exertion in this precarious distraction has its own degree of impact.

The factors that are very important in aggravating the land degradation in the area can be reclassified into two major groups as back ground factors and triggering factors. The background factors are inherent to the geology of the area like geological structures and lithology while the triggering factors can be subdivided into major and minor triggering factors. The major triggering factor is drainage where as slope and landuse factors are considered as minor. However, it has to be noted that the "minor and major" classification is relative. All the factors are important in activating the degradation of the area with slight degree of variation in importance. By assessing the degree of impact of each factor, the land degradation susceptible areas are mapped with their degree of vulnerability, for further reclamation activities. Since several factors are involved in the process, integrated GIS analysis using IDRISI 32 was used to perform all the integration approach of multi criteria evaluation (MCE).

MCE module is a decision support tool for Multi-Criteria Evaluation. A decision is a choice between alternatives based on a certain criteria. During Multi-Criteria Evaluation, an effort is made to combine all the factors as a set of criteria to accomplish a particular composite basis for a decision according to the specific objective which is to delineate land degradation prone areas. Hence a decision is needed to make a choice of what areas are the most prone for land degradation. So criteria images such as land use type, lithology, slope angle, proximity to structures and drainages; were combined to form a single suitability map from which the final land degradation susceptible area is decided.

All the factors used in this analysis are standardized by using a byte binary format with a standard scaling that range from 0-255. This scaling is achieved using the module FUZZY as discussed in detail below. Once the standardized factor images have been created, a set of weights were developed that indicate the relative importance of each factor to the decision under consideration.

6.2 Factors controlling degradation in the study area

Factors that are considered significant in advancing the degradation process and used in the integration analysis are discussed in detail below.

6.2.1 Geological structure factor

Geological structures are weak zones that range from a few meters to many kilometers in length. The identification and mapping of geological structures and lineaments of the area has been done using the stretched ETM+, band 7 image of the year 2001. The stretched band 7 image was exported (saved) from ENVI 3.5 format to ARCVIEW 3.2 .bil format. Then on screen digitization was performed to create a new vector layer of the geological structures. Subsequently the geological structural map was imported to IDRISI 32 where the integration processes was performed.

The geological structural vector map was converted to their raster equivalents, in order to perform integration successfully to pixel by pixel base, and 50m cell size is assigned so that it is compatible with all the necessary layers.

No.	Major factors	Sub factors	Rating
1	Drainage	the drainage impact is expected to decreases further away from the drainage line	0-255 (fuzzy boundary) High value means high impact and vise versa
2	Geological structure	the impact of geological structures is expected to decrease further away from the geological structures	0-255(fuzzy boundary) High value means high impact and vise versa
3	Lithology	Rift floor Ignimbrite (Ignimbrite-3) Ignimbrite 1 Ignimbrite 2 Trachyte 1 Trachyte 2 Rhyolite Scoria	255 200 200 150 150 100 100
4	slope	as the slope angle increases the impact is also expected to increase	0-255(fuzzy boundary) High value means high impact and vise versa
5	Landuse/Landcover	Degraded Land Annual Intensive Mixed Annual (int) /Perennial Bare Land Mixed Annual/Perennial State farm Grass land Crop land Plantation Riverine trees Mixed Annual/Perennial (int) Water body Perennial intensive Bush/shrub Open shrub land Settlement	255 225 225 200 180 160 50 225 75 140 160 100 160 125 200 75

Table 6.1 Major factors and sub factors used for analysis with their corresponding ratings

For the purpose of this work, distance is assigned to measure the Euclidean distance between each cell and the nearest of a set of neighbor cells. It helps to measure the distance of each point by taking the geological structure as a starting spot. Away from the geological structures the distance will increase. Thus distances derived from the images with rectangular cells are correctly calculated.

Fuzzy boundary is established for each distance class in order to avoid sharp boundaries. Hence, transition between high degrees of importance to less importance for each distance class is gradual. The impact of the geological structures simultaneously decreases with increasing distance away from the structures thus monotonically decreasing type of fuzzy membership curve has been chosen.

Based on this the output scale is assigned from 0-255 indicating a continuous increase from less impact to high degree of impact (Figure 6.1). Given that only two control points are needed to determine the shape of the fuzzy curve.

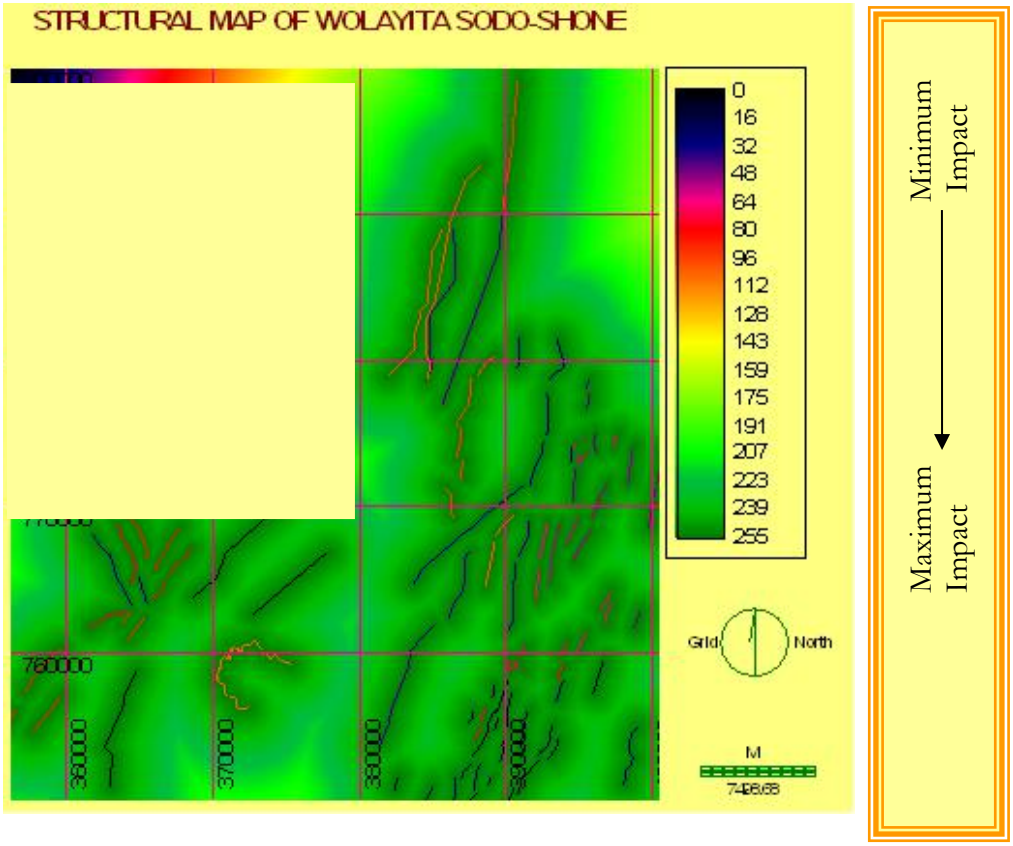

Figure 6.1. The reclassified structural map of the study area overlaid by the vector structural layer

6.2.2 Drainage factor

The study area has a radial and dendritic drainage pattern. It is observed during field survey and from interpretation of band combinations, intensive degradation is concentrated along river curses and their tributaries.

The drainage network of the study area is digitized on screen using 1:50,000 topographic maps. This drainage map is imported to IDRISI 32 and converted to raster format for advanced processing. Just like the procedures followed to structural map, distance is assigned by taking the drainages as starting point. Since the impact of the rivers decrease with increasing distance away from the rivers, monotonically decreasing type of fuzzy membership curve is preferred. Subsequently 0-255 output

scale is assigned to indicate a continuous increase from less degree of impact to high degree of impact Figure (6.2).

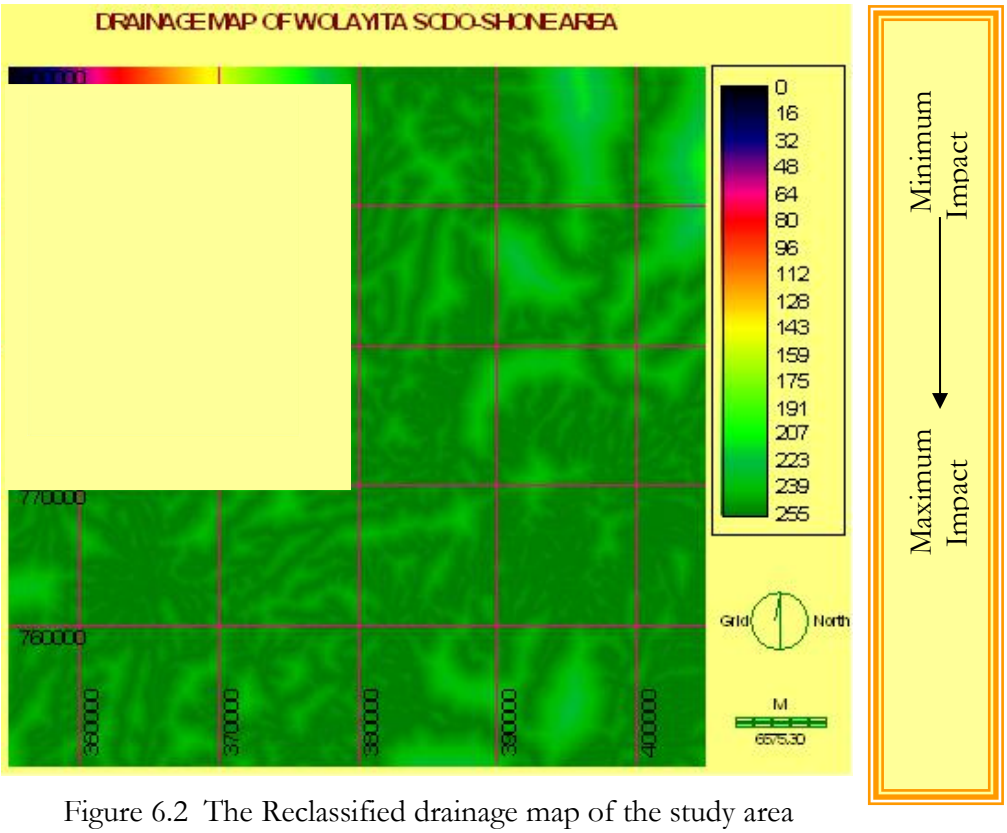

Figure 6.2 The Reclassified drainage map of the study area

6.2.3 Lithologic factor

Four lithologic units are represented in the area. These units are grouped into three complexes; Damot complex, Damot Dugna complex and the rift floor ignimbrite. Damot complex includes two types of trachyte (trachyte-1, trachyte-2) and Ignimbrite (Ignimbrite-2) while rhyolite and (ignimbrite-1) are represented in Damot Dugna complex. These units are affected at varying intensity of degradation.

All the lithologic units were mapped from the visual interpretation of satellite images of 753 & 721 colors composite and intensive field checking. The lithologic units are digitized on screen from which a lithologic map was produced, and imported to IDRISI32, then converted to raster layer.

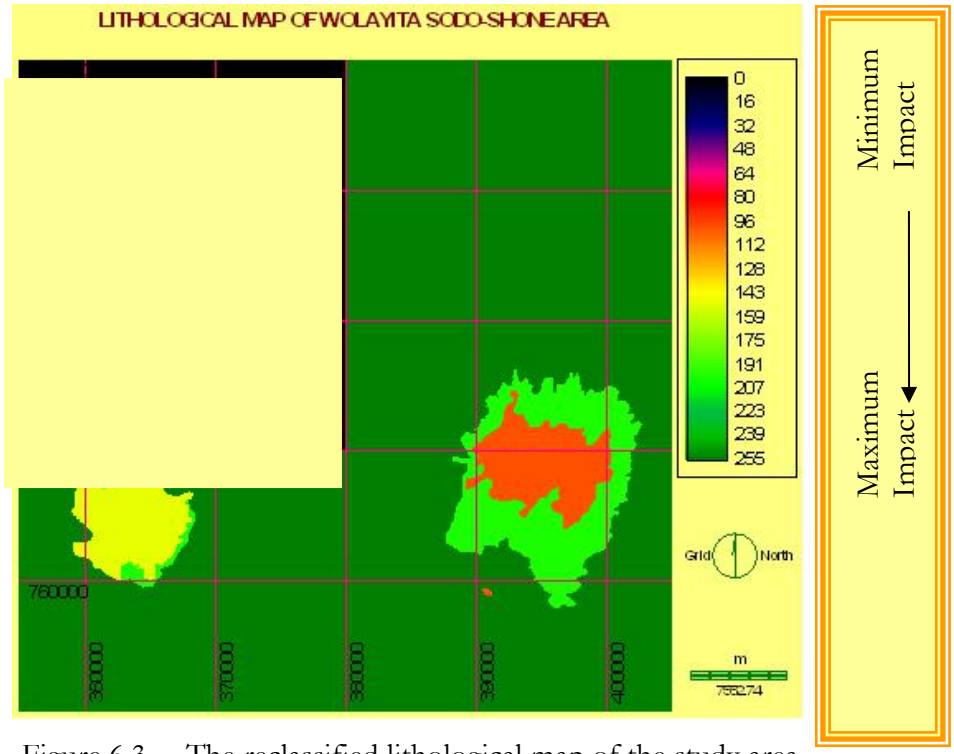

Figure 6.3 The reclassified lithological map of the study area

The lithologic image was reclassified (Figure 6.2) so that the data stored in the images or attribute value files classified into new integer categories ranging from 0-255. These values are priority values in which high value refers to high priority. Priority values ranging from 0-255 (Table 6.1) are assigned to all the factors so that the integration process would be performed with factors having the same integer ranges.

Largest part of the study area is covered by highly weathered and fractured rift floor ignimbrite (assigned as ignimbrite-3). Almost all the gullies observed in the area are situated in this rift floor ignimbrite. Therefore, high priority value is given to this unit while a very low priority value is given to the rhyolitic unit since it is strong and not a single gully is observed in this unit (Table 6.1).

6.2.4 Slope factor

The study area has rugged topography that varies from a relatively flat to mountainous areas. The slope of the area ranges between 0 to 60 degree in flat and mountainous area respectively. The slope of the area is derived from DEM of 20m resolution. Contours were on screen digitized from 4 topographic map of scale 1:50,000 at 20m interval using CARTALINX software. The data is exported to ARCVIEW 3.2 for further processing. These contour lines are imported to IDRISI 32

where the digitized contours as vector lines are rasterized with LINERAS operation and interpolation is performed using INTERCON operation. INTERCON interpolates a raster Digital Elevation Model (DEM) from the digitized contours using linear interpolation between each contour line. Finally, the resulting model was filtered to produce a smooth model using the 5x5 mean (low pass) filter to remove some of the angularity of the linear interpolation. Mean filters are commonly used to simplify an image. The output value after applying the mean filter is the sum of the products of each pixel value and its corresponding kernel value. The kernel that is set by default is given in Table 6.2.

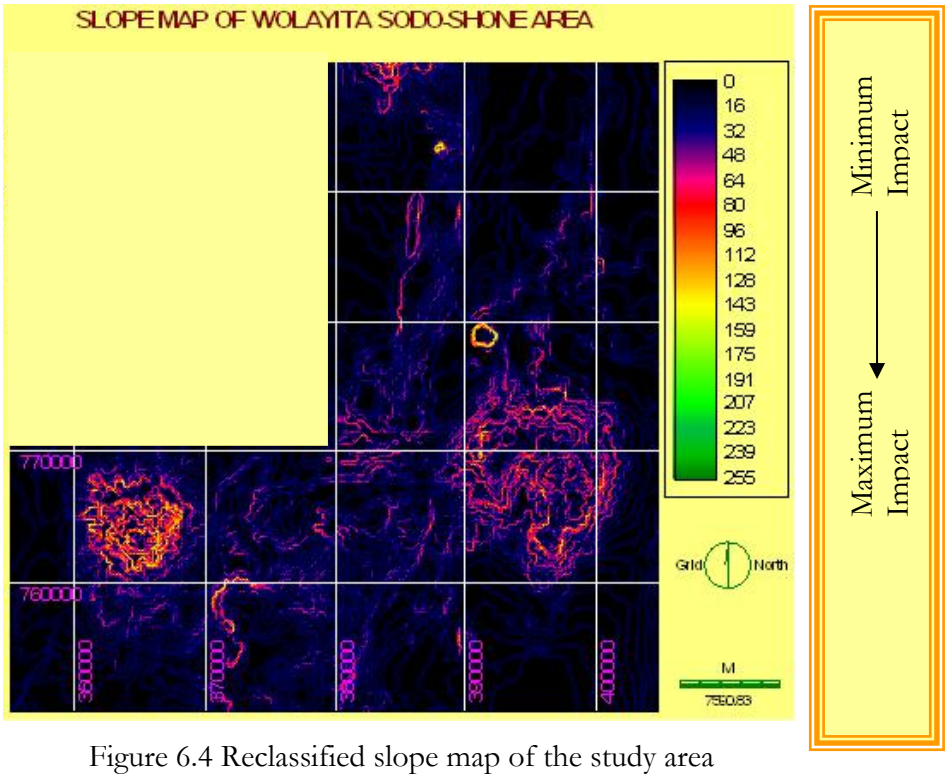

Figure 6.4 Reclassified slope map of the study area

Slope is calculated using SURFACE operation from the DEM of the area. For the calculated slope, a fuzzy boundary with monotonically increasing type of fuzzy membership curve was chosen since the impact of the slope for the degradation increases with increasing the angle of the slope and vise versa. Besides, output scale ranges from 0-255 is assigned to indicate a continuous increase from less impact to high degree of impact (Table 6.1 & Figure 6.4).

1/25	1/25	1/25	1/25	1/25

1/25	1/25	1/25	1/25	1/25
1/25	1/25	1/25	1/25	1/25
1/25	1/25	1/25	1/25	1/25
1/25	1/25	1/25	1/25	1/25

Table 6.2 IDRISI's default law pass filter

6.2.5 Landuse/landcover factor

The landuse/landcover, of the study area is dominated by mixed annual perennial crop type. Yet the crop type mapped as annual intensive or perennial intensive is a relative concept. It is difficult to find

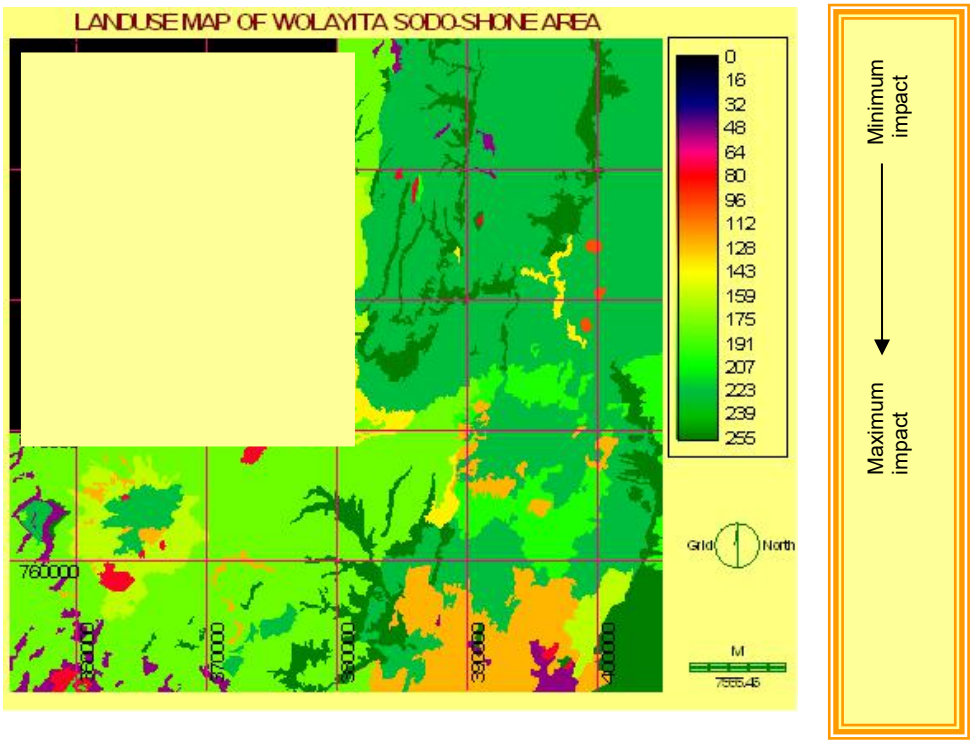

Figure 6.5. The reclassified Landuse/Landcover map of the study area

a pure annual or perennial crop field over a large area. Sixteen landuse/cover types are visually interpreted from digital and hard copy of bands 543 color composite of ETM+ image at RGB order. Intensive field survey and mapped during the field survey. The resulting landuse map is re-checked and ground truthed during the final field trip and digitized using ARCVIEW 3.2. The land use map is imported to IDRISI 32 and converted to raster format.

The available landuse/landcover units have varying impact in aggravating the land degradation in the area. The rasterized map is then reclassified into new integer categories ranging from 0-255. These values are priority values in which high value means high contribution (Table 6.1).

6.3 Weighting

In order to apply a multi-criteria evaluation, a set of relative weights for the available factors that are responsible for the degradation have been developed using WEIGHT module of IDRISI32. The weights are developed by providing a series of pair wise comparisons of the relative importance of each factor to the suitability of pixels for the degradation as proposed by Saaty (1997) under the Analytical Hierarchy Process (AHP). Saaty (1997) developed a procedure for obtaining a ratio scale for a group of elements based upon a complete paired comparison of the elements taken two at a time. These are then analyzed to produce a set of weights that sum to 1 (Table 6.3).

	Drainage	**Structure**	**Lithology**	**Slope**	**Landuse**
Drainage	1				
Structure	0.333	1			
Lithology	0.2	0.333	1		
Slope	0.1428	0.2	0.333	1	
Landuse	0.1111	0.1428	0.2	0.333	1

Table 6.3 Pair wise comparisons of the relative importance of each factor

The matrix (Table 6.3) contains the name of the factors that are labeled in the same order across the columns and down the rows with the lower half of a symmetric matrix of the pair wise comparisons. The cells in the matrix consider the relative importance of the row variable to its corresponding column variable for each likely pair of comparisons. Since the upper right triangular half is symmetrically identical with the lower-left, only the lower-left triangular half is evaluated. Each factor that is responsible for the degradation is rated according to the following 9-point scale (Figure 6.6):

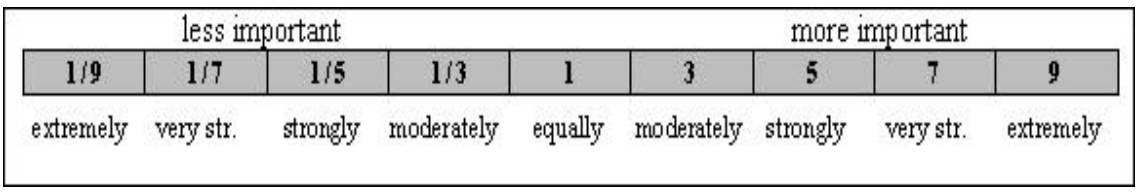

Figure 6.6 The continuous rating scale proposed by Saaty (1977).

Factors	**Factor Weight**

Drainage	0.4275
Structure	0.2744
Lithology	0.1762
Slope	0.0811
Landuse	0.0408

Table 6.4 The eigenvector values obtained for the factors

The weighting is given based on the relative importance of causative factors derived from field knowledge hence it is subjective. The observation made during field survey, confirmed by visual interpretation made from satellite images indicate that almost all of the river banks are eroded and intensively degraded. This shows how significant the influence of drainage is and that it is a major triggering factor which generates the hideous result. Running water has indisputable impact in eroding and transporting enormous amount of soil. Therefore, highest weight is given for the drainage layer during the multi criteria analysis (Table 6.4).

The existing rivers and their tributaries have also indirect impact in aggravating land degradation by creating local slopes which facilitate movement of soils down slope by gravity. However, when it is weighed against the other factors, the contribution of the local slope is minimal. Accordingly, minimum weight (Table 6.4) is given for the slope factor since it is taken as a minor triggering cause in accelerating land degradation.

As it is observed in the field, the presence of the geological structure at most of the areas aggravated the land degradation. The structural weakness can be taken as a back ground factor because it is inherent to the geology of the area. Since half of the study area is situated on the western margin of the rift valley and the rest on the main Ethiopian rift system, it is highly affected and controlled by tectonic structures trending NNE-SSW and NE-SW direction. So these tectonic structures have a tremendous impact on degradation. This is easily judged from the visual interpretation of color composite satellite images and field verification. It can be seen from the images that all the gullies in the area have narrow and elongated shapes with most of them trending NNE-SSW and NE-SW direction parallel to the geological structural trends, showing the importance of the geological structures for their occurrence. The faulting exposes the highly weathered ignimbrite and the pumice layer. As a result, some of the faults planes are extremely weathered and eroded.

The lithologic units are other background factors that assist the degradation process together with the major and minor triggering factors. These units have varying level of fracturing and weathering that guide the way for further degradation process. The concentration of degradation mainly in the rift floor ignimbrite is strong evidence that the lithology has a significant impact on land degradation. From the picture below, we can see that there is a clear contact between a thin layer of basaltic flow and the rift floor ignimbrite. The part which is covered by the thin basaltic flow is relatively not affected by the degradation whereas the rift floor ignimbrite is highly eroded (Figure 6.7 & 6.8).

Figure 6.7 A thin basaltic flow that is relatively unaffected by land degradation

Figure 6.8 Rift floor ignimbrite affected by intensive degradation

Intensity of soil erosion varies with different sort of landuse/land cover type. Crop lands are the most susceptible areas to erosion. Large amount of soil can be eroded and transported from farm lands especially after harvesting, where the tillage soil left bare for a certain period of time till the next cropping season comes. Generally, repeatedly cultivated soils, fallow soils or soils that are bare through overgrazing by stock animals are particularly vulnerable and have major impact for the on going processes. The eastern, north eastern and south western part of the study area is the most affected by degradation as they are dominated by annual crop and mixed annual intensive with lesser amount of perennial crops. Areas covered with perennial crops, natural vegetation and plantations have a minimum or negligible degradation. In addition to these landuse/landcover types, road cut also aggravate land degradation (figure 6.9).

Figure 6.9 Land degradation aggravated by road cut

6.4 MCE

Multi-Criteria Evaluation (MCE) primarily concerned with how to combine the information from several criteria to form a single index of evaluation. Criteria are divided into factors and constraints. Factors are defined as spatial features which influence the suitability of a spatial unit for the given objective. Constraints are areas which have no suitability. Using Multi-Criteria Evaluation (MCE) with a weighted linear combination procedure, continuous factors are combined by applying a weight to each factor according to its relative importance and summed the results to yield a suitability map.

WLC (Weighted liner combination) is characterized by full tradeoff between factors and average risk. Factor weights, in WLC determine how individual factors will tradeoff relative to each other. In this case, the higher the factor weight, the more influence that factor has on the final suitability map. Along with full tradeoff, this combination procedure is characterized by an average level of risk, as it

is exactly midway between the minimization (AND operation) and maximization (OR operation) of areas to be considered suitable in the final result.

All the factors and their resulting weights processed so far were used as input for the MCE module with weighted linear combination procedure. In using this procedure, 5 factors with their respective weights (Table 6.4) and 1 constraint were used as inputs. A binary constraint map used to exclude the area that is not of interest for the current analysis. As it can be seen, the area of interest for analyzing land degradation has an inverted L-shape. Thus, the upper left part of the study area need to be excluded from the analysis by applying a constraint layer. This constraint layer is formed by digitizing the boundary of the study area including the discarded upper right part. The digitized boundary layer was reclassified by assigning 1 for the area of interest and 0 for the discarded part. Each factor was multiplied by its factor weight (Table 6.4) and then added to the results through the application of WLC procedure. The constraint layer is then useful in multiplying 1 by the values resulted from multiplication of factors by their weight for the area of interest and 0 for the discarded part (figure 6.10). Therefore the resulting map includes (figure 6.11) the summed result of each factor multiplied by its factor weight while the excluded areas contain 0 values.

The final land degradation susceptible map (Figure 6.11) was produced through series of comparisons (figure 6.12) to obtain a ratio scale for a group of factors based upon a Complete paired comparison of the elements taken two at a time using the formula n(n-1)/2 comparisons for n elements as proposed by Saaty (1997). Out of all the comparisons, the map presented manifests the field observations. The map indicates that drainage is the major triggering factor followed by structure and lithology while slope and landuse have minor triggering impacts.

Figure 6.10 Illustration of the multi-criteria analysis with all the factor and constraint maps used

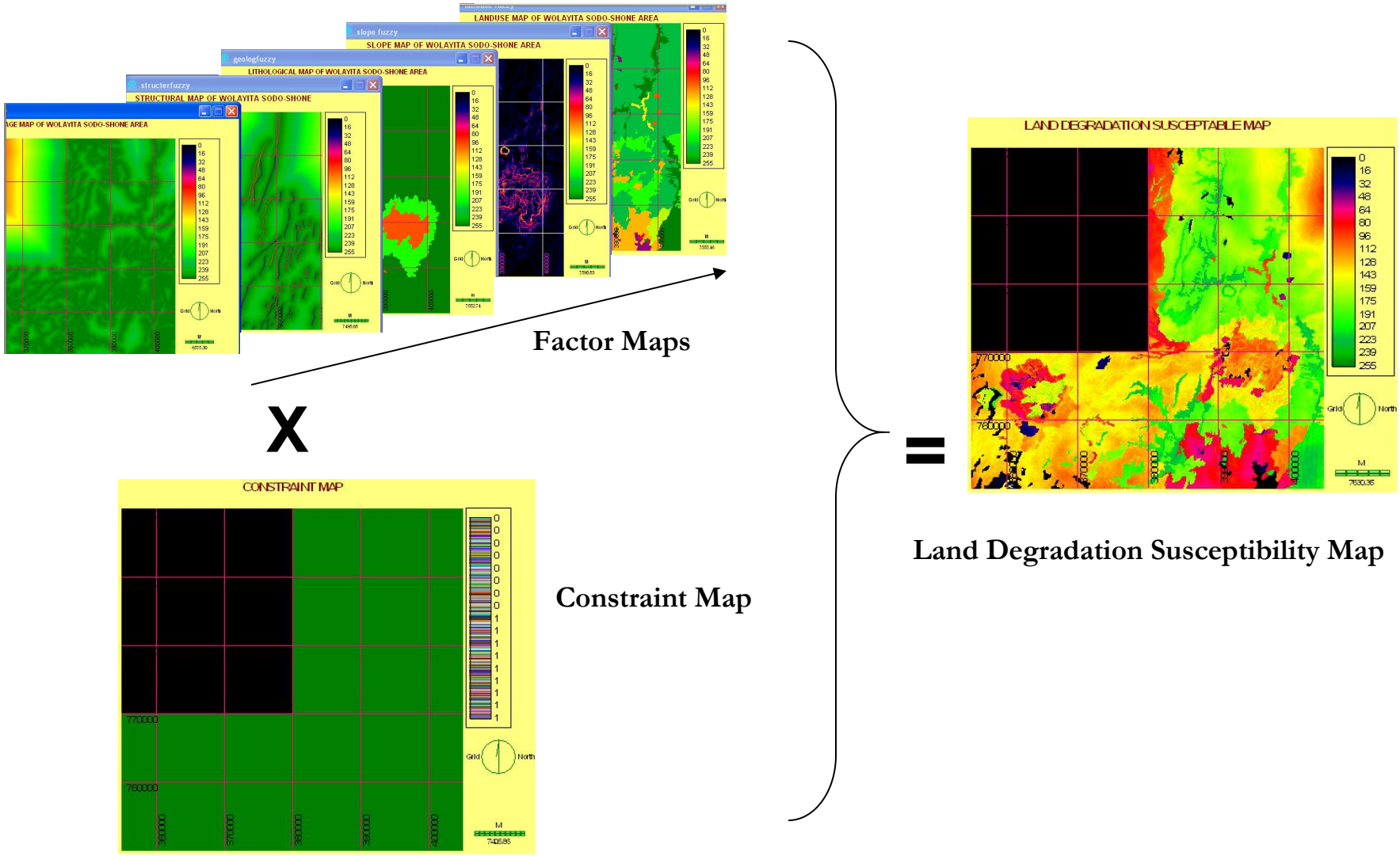

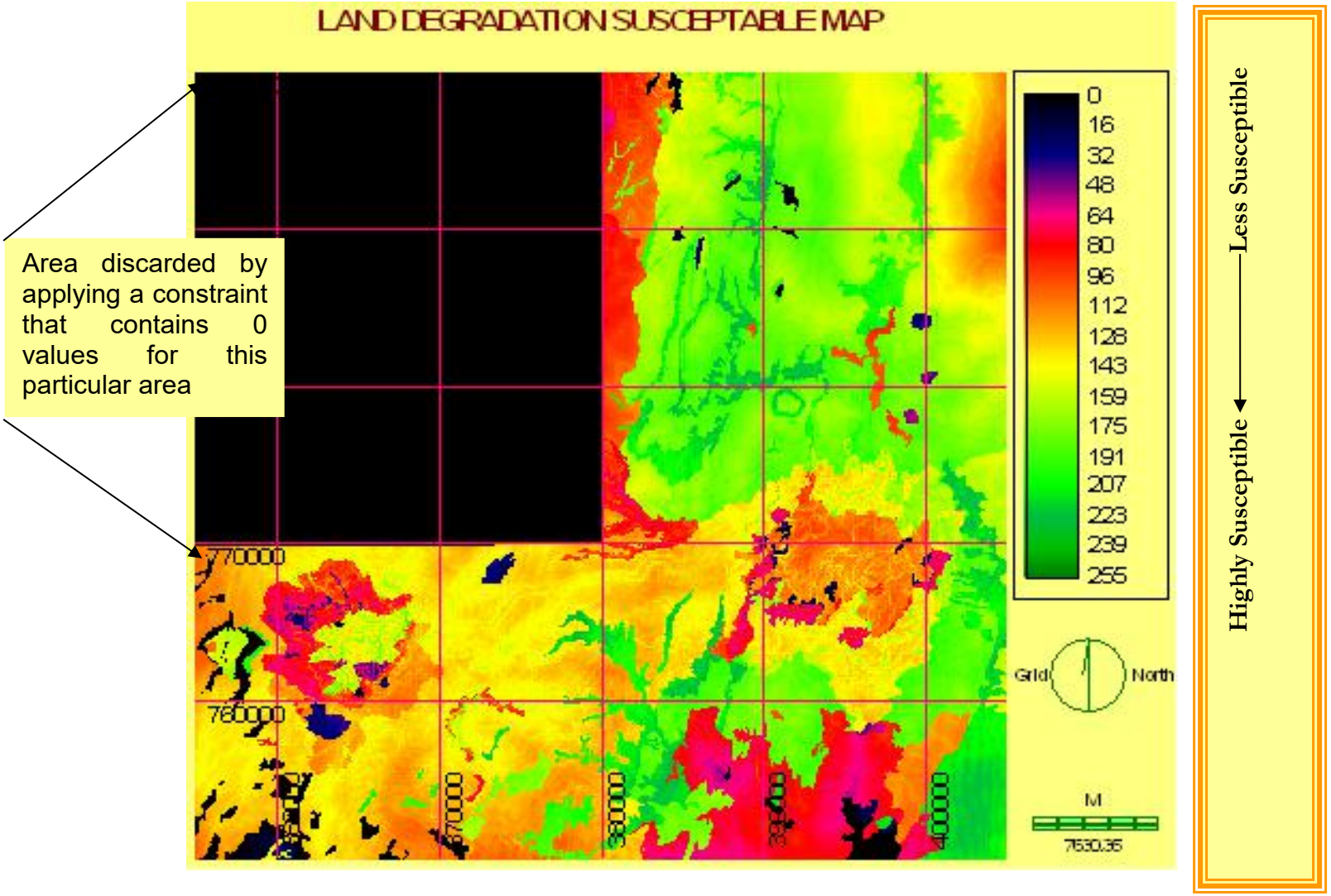

Figure 6.11 Land degradation susceptible map of Wolayita Sodo-Shone area

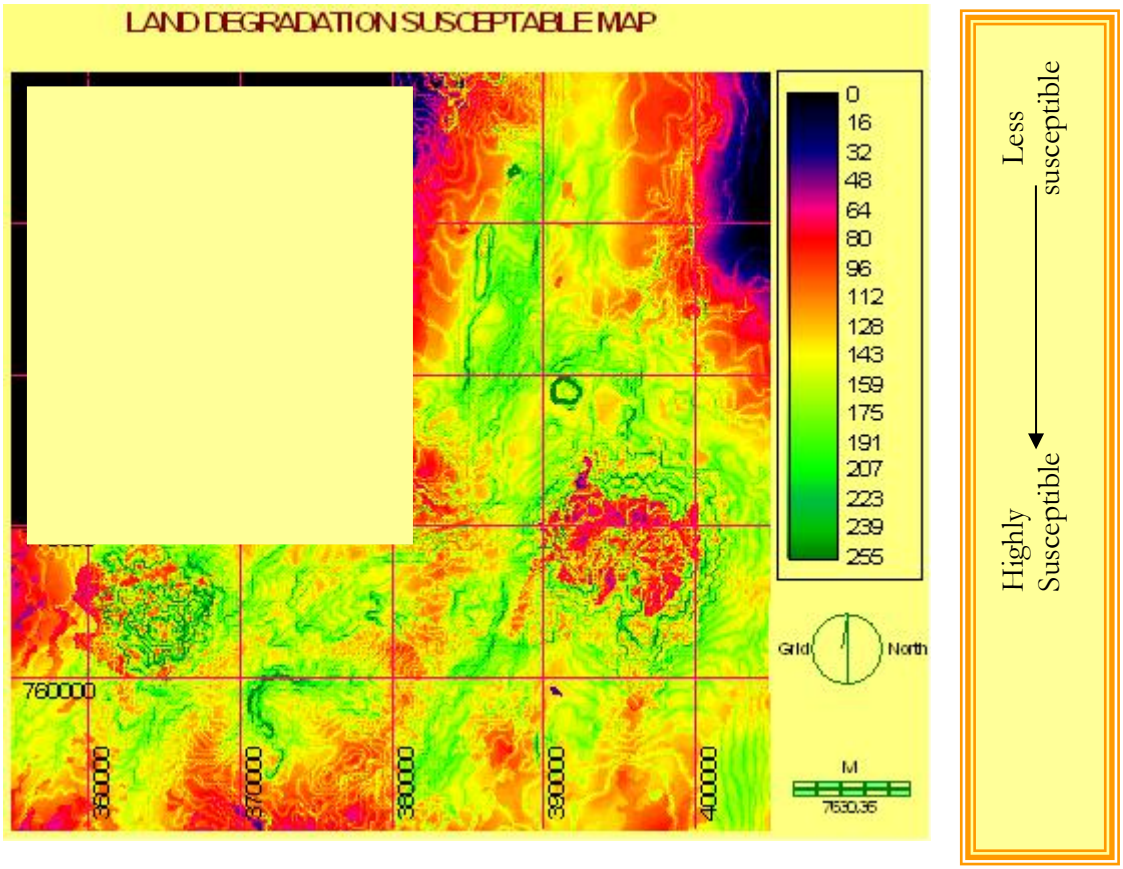

Figure 6.12 Land degradation susceptible map of the study area produced by taking slope as a major triggering factor

6.5 Awareness of the farming community

The farmers of the area, who depend on the degraded land and low crop yields with difficult farming operations, are the direct victims of the degradation process that is occurring. But the awareness that they have is insignificant when compared to the intensity of the problem. It can't be said fully that all the farmers do not have any understanding about the situation.

Informal interview was conducted to assess the awareness of the farming community. Most of the farmers believe that the cause for the degradation is deforestation and the nature of the soil. Together with intensity of rainfall which usually repetitively causes flooding is believed have a major impact on the washing and transporting of the upper soil.

In few areas terracing was observed to prevent the transportation of soil from sloppy parts. The farmers are also well aware of the increasing rate of formation of the gullies. As it is explained by one of the farmers, one of the selected sample sites for profiling in order to analyze the amount of soil lost from the gullies was a field that used to serve the community as grazing land and an open area.

Very few areas with gullies are fenced and left as area of enclosure. These rehabilitation and prevention works are done with the help of local agricultural offices and local NGOs that work close with the community. Some training is also given to the farmers by the DA's (development agent). But still the awareness that is created and the work that have been done is not even close to the need when compared to the intensity and distraction of the problem.

Thus, serious attention has to be given and farmers should get enough knowledge about the problem on prevention and rehabilitation strategy.

PART-III

LANDSLIDE AROUND SODO AREA

Chapter 7

Evaluation of Land Degradation Problem

7.1 Introduction

Landslides are serious geological hazards common in many parts of the world. They constitute a major hazard to population, property and infrastructure in many hilly and mountainous areas (ROSIN and HERVA´S, 2005). They cause billions of dollars worth damage of properties and thousands of deaths and injuries each year worldwide. Annual global economic losses due to landslides are estimated to be in the order of two to five billions of US Dollars (Schuster, 1994).

Landslide is an example of land degradation in action. Though in the longer term, the area of landslide may regain its productivity, the disadvantages of a landside usually outweigh its advantages.

Most land slided materials move so rapidly that they can destroy property and take lives suddenly and unexpectedly. Nearly all events of landslide occur during periods of intense rainfall. One of the triggering factors of landslides is rainfall as it percolates and enters natural or man-made slopes (Tewodros AYELE and VLČKO, 2002). Rainfall-induced landslides pose significant hazards in many parts of the world especially in the mountainous areas in a rainy environment, due to their highly frequent occurrences (WANG and SASSA, 2002). Among those hazardous rainfall-induced landslides, fluidized landslides are the most dangerous and damaging, because they usually occur unexpectedly, and are characterized by rapid movement and long run-out distance. In areas where the vegetation cover is sparse and cleared, a minor amount of precipitation may initiate landslides. Mudflows are common types of fast-moving landslides. They are rivers of earth and other debris saturated with water. They develop when water rapidly accumulates in the ground, such as during heavy rainfall episodes changing the earth into a flowing river of mud. They usually start on steep hillsides as shallow landslides when the soil get liquefied and accelerate to speeds. The consistency of mud flow ranges from watery mud to thick rocky mud. They continue flowing down hills and through channels, clearing every thing that came along their path, growing in volume with the

addition of water, sand, mud, boulders, trees, houses (cottages) and other materials. When these materials added with the flow, their destructive power may increase greatly.

Almost 60% of the total population in Ethiopia lives in highlands with an altitude of more than 1750m (Lulseged Ayalew, 2000). The study area, Damot Mountain and the surrounding villages belongs to the highlands with average altitude of 2400m. Damot Mountain is frequently affected by landslide hazard. However, the available information on landslides in the area is still inadequate.

Land slides and rock falls are two of the most damaging natural hazards in Ethiopia (Lulseged Ayalew, 2000). A significant factor for the mass movements in the study area is the modification of natural slope to suit the need of human interest for farm and grazing land. Deforestation has also cause sever change in vegetation cover and soil erosion of the area. Most of the indigenous trees are disappearing and replaced by eucalyptus in some part of the study area.

Since the advent of regularly acquired Synthetic Aperture Radar (SAR) and high spatial resolution optical imagery from space platforms (often also providing stereoscopic capability), remote sensing is increasingly used not only to assist in landslide investigations by deriving area-wide land use, geological and geomorphological information in landslide-prone areas, but also for direct delineation of landslide surface boundaries and monitoring their activity (ROSIN and HERVA´S, 2005).

In this study, in line with the already established techniques, integrated GIS and Remote Sensing approach was used to point out the landslide hazard zones. The quantitative relationships between landslides and the triggering factors are established by the help of Multi-criteria Evaluation. The affecting factors such as lithology, geological structure, slope angle, slope aspect, drainage and Landuse/Landcover are weighted based on their relative importance in aggravating the landslide. This approach is used to produce the landslide susceptibility maps and landslide hazard zonation by integrating the different weighted factors. Information on these maps could be useful for explaining the existing landslide, making emergency decisions and mitigation of future landslide hazards.

7.2 Previous work on landslides in Ethiopia

The magnitude of landslide occurrence and its resulting damage has been increasing from time to time. Many researchers tried to assess the cause and factors that trigger landslide in the highlands of

Ethiopia. But when it is compared to the damage it is causing in human life and property, the attention given to study the problem is not proportional.

Nevertheless, some works on landslide in Ethiopia include:
Lulseged Ayalew (1999), has conducted research on the effect of seasonal rainfall on landslides in the highlands of Ethiopia. He tries to elaborate the relation between the mechanism of landslide and rainfall and suggested an empirical relationship that could help in assessing the problems of instability.

Tenalem Ayalew and Giulio Barbieri (2004), have conducted an inventory of landslides and susceptibility mapping in the Dessie area, northern Ethiopia. In their work, a method of landslide susceptibility mapping that adapts to the area of the hillside is presented.

Lulseged Ayalew (?), has studied the causes and mechanisms of slope instability in Dessie town. In his work he tries to examine the relationship between slope instability and seasonal rainfall in the area. By taking the variation in moisture content of soil, the rate of daily precipitation, the amount of cumulative precipitation, and mean annual rainfall as variable, he derived a simple equation that is useful to determine the likelihood of landsliding.

Lulseged Ayalew and Berihanu Temesigen (1995) assessed slope movements from Gohatsion to Dejen, Abbay (Blue Nile) Gorge and Kefyalew Tefera (2001) has conducted a study on landslide assessment of Dessie town and performed engineering geological mapping of the area.

There are also a few studies that have been conducted in the southern part, where the study area belongs to. Berhanu Temesigen et al. (2001) used GIS and Remote sensing methods for natural hazard assessment to the landslide in the Wondo-genet area. In their work they evaluated the occurrences of landslides and their relationships with various event controlling parameters using GIS and Remote Sensing techniques. Finally, a landslide hazard zoning was done through the statistical relationships of the parameters with landslide occurrence that were converted into risk susceptibility priority numbers.

Asfawosen Asrat et al. (1994) conducted a study on land movement of November 10, 1994 in Goffa District, Northern Omo zone, Southern Ethiopia.

7.3 Background on land slide problem in the study area

Ethiopia is one of the 3rd world countries where people suffer from various man made and natural hazards. Malaria, HIV and drought take the lead in such developing countries in annihilating human life, destroying property and curtail the economic growth of the countries. Accordingly a better consideration is given for such catastrophic event. Even though its impact is local unlike the above hazards, Landslide is killing vast number of human life and destroying a great deal of property. However, little attention is given to this hazard.

The study area is situated in Southern Nations Nationalities and Peoples Region. The region is densly populated and intensively cultivated. The average population density is 118.3 persons/sq. km. The annual population growth rate is increasing. This leads to lack of land for farming and grazing and people are forced to encroach to steep areas where natural hazards such as mass movements are common. Damot Mountain is one of these places with high population density and intensive cultivation. Almost every single hectare of land is cultivated or explored for various purposes.

Damot Mountain is mainly covered by thick soil cover of faty clays that overlies trachytic flow. During rainy seasons, precipitation infiltrate in to the thick clay soil. The clay soils swell up on wetting and crack upon drying. Water infiltrates through the cracks and accumulates as it comes across scorched surface on the impermeable trachytic material causing an increase in pore water pressure within the soil profile. Increased pore water pressure or greater water absorption may weaken inter-granular bonds. It also reduces internal friction of the soil and therefore attenuates the cohesive strength of the soil and ultimately the stability of the slope. Subsequently, the accumulated water saturates the overlying soil material. Once the amount of water exceeds the saturation level, the soil started to move downward as mud flow. At this level, seconds are enough to destroy property and human life.

Mud flow, rock fall and creeping are the most common mass movements in the study area. In Gurmu Wayide kebele, 11 people were killed by a mud flow that occurred on November 17 1993 (figure 7.1). According to the local people, the disastrous mud flow occurred at night following intensive rainfall that lasted for hours. The movement occurred only within 3 minuets period. The local people planted eucalyptus trees on the spot where the sliding occurred to prevent further

sliding. But the trunks of the growing eucalyptus trees bend down slope (Figure 7.3) indicating soil creep, implying that the area is still active and prone to such events. Most of the

Figure 7.1 Mudflow that killed 11 people

Figure 7.2 Landslide scar that damage property

landslide scars present in the study area that cause such disasters are very small. The width of the scar that kills 11 people in Gurmu Wayide kebele is about 21 m while the depth after the flow is about 8 m. The slope angle measured on the spot of the sliding is about 21^0.

Figure 7.3 Tilting of tree trunks indicating of soil creep, on Damot Mountain.

In addition to the intensive rainfall, the presence of springs above the landslide scar may have triggered the mud flow. The spring water seeps into the soil and move laterally till it approaches a perched zone to accumulate. When the stress exceeds the frictional and cohesive force of the soil, it flows as mudflow.

The thick clay soil cover played an important role in triggering mass movement to already prone areas. During the field survey, in areas near to the landslide scar, no well developed soil horizon is

observed, a typical characteristic of repeated landslide history. The soil outcrop close to the foot of the mountain comprises larger boulders, pieces of wood and other transported materials (Figure 7.4).

Figure 7.4 Transported materials as a result of mass movement

The settlement type that dominates steeper parts of the slope has an immense contribution in aggravating landslide (Figure 7.6). In order to avoid strong wind on the top flat part of the mountain, the locals prefer to settle on the steep slopes with high susceptibility to mass movement. The landslides occurred at these areas could also be partially attributed to the settlement conditions.

In Damot Wajo keble, a locality known as Tejo, 5 people were killed at their sleep because of the mudflow that occurred at about 2:00AM on July 19, 1996 E.C (figure 7.5). In addition to human causalities, enormous amount of property including residences and cultivated crops (mainly "enset") were destroyed. The landslides were small scale with the width of the scars ranging from 3 to 5 m. The disaster was due to the fact that settlement of the houses that was located on the sliding axis.

Figure 7.5 Mudflow that killed 5 people

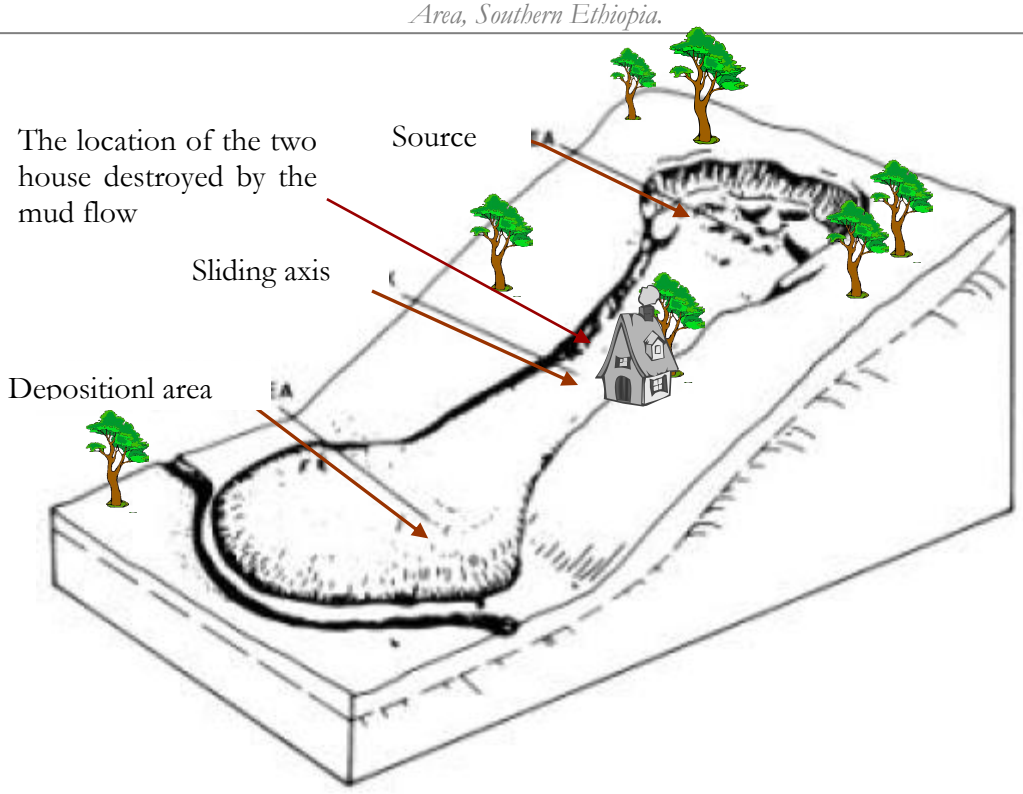

Figure 7.6 Schematic diagram that shows the sliding that killed 11 people in Gurmu Wayde keble.

Southeast of Damot Mountain there is a weathered semi-circular caldera like structure of about 7-8km diameter. A few landslide scars and rock fall were observed at the walls of the structure indicating unstable slope condition. This instability could be attributed to the precipitation and the steepness of the slope of the wall of the structure. There are also several places where rock fall and landslide occurred and destroyed cultivated lands (figure 7.7). However since they didn't interfere with humans' life they are left disregarded. In most of the places mass movements are given importance and attention, only if they interfere with humans' life, otherwise the community did not pay much attention. So there are lots of scars of rock fall and landslide that are left unrecognized in many parts of the study area.

Figure 7.7 Rock fall on Damot Mountain

In addition to Sodo area, in the surrounding woredas and kebeles', there are many of reports of damage on human life and properties caused by landslides and rock fall. According to information gathered from Ethiopia News Agency (ENA) regions branch office at Sodo town, the area has experienced a frequent occurrence of mass movements. On October 3, 1994 E.C., in Boloso sore kebele four family heads were displaced from their homes and 15 hectares of crop was damaged following intensive rainfall that last for hours. Seven people were also killed and enormous cultivated land damaged at chemu kare kebele as a result of landslide occurred at a river junction. The types of crops and property damaged include banana, coffee, maize, godore, eucalyptus trees and residences. Kuch wored (ocholbo) is also one of the places with history of landslide occurrence. In this area, the landslide that occurred on October 9, 1992 E.C. caused damage on farm land and human life. In offa Bosso woreda 2 persons were killed, one injured and property destroyed, on April 30, 1993 E.C. around 3:00 pm as a result of sliding triggered by heavy rainfall.

7.3.1 Types of landslides in the area

Two types of mass movement are observed in the area: mud flow and rock fall. Mud flow is observed in gently sloping areas where the slope mainly ranges from 20^0-30^0. It is generally recognized that mudflows are induced by intensive rainfall. They are usually a result of high excess pore-water pressure generated during a process of liquefaction; hence the soil mass suddenly loses a large proportion of its shear resistance and flows in a way similar to a liquid. In addition to the mudflow, rock fall and soil creeping are common in the area. Rock fall is common in areas where the slope angle exceeds 40^0. Minor soil creep is also observed scattered in many places.

7.4 Purpose of study of the problem in the area

Detecting landslides and monitoring their activity is of great relevance for disaster prevention, preparedness and mitigation in hilly areas (ROSIN and HERVA´S, 2005). Landslide hazard poses a severe threat to human life, property and infrastructure, and becomes a major constraint on the development of the area. Attention should be given to understand landslide process and mechanism in order to examine threatening landslide hazard and predict future occurrence of landslides to reduce damage from such mass movements. Understanding the factors and mechanism of occurrence will help to control and prevent it, through various methods including

Landslides hazard zonation.

Following the factor/tradeoff weight value integration and landslide hazard zonation methods, key factors are defined, which provide useful information for identifying different levels of landslide hazards. Most landslides in the study area are triggered by intensive rainfall. But rainfall is not the only cause, several background and other triggering factors work simultaneously to cause the distraction.

The Landslide in the area could be attributed to natural and manmade factors and/or both. Natural factors include gravity, geological setting (lithology and tectonic structures like faults, volcano tectonic collapses, etc.), drainage pattern, topography (slope angle and slope aspect) and rainfall. Clearing of vegetation, cultivation on hill slopes, over grazing, construction of infrastructures and settlement are some of the human induced factor. On these bases, the study area is a suitable place to investigate and study in detail the available landslides and its susceptibility in the future.

7.5 Awareness of the Community

Informal interview was conducted during the field survey to assess how far is the knowledge of the community about the staggering environmental hazard including mass movements occurring around them. They were interviewed about what they think of the cause of the mass movement occurring frequently in their area, what type of measures they take to prevent the damage and so on. Most of the people attribute the problem to divine power. In Gurmu Wayide kebele, at the place where 11 peoples were killed by the mudflow from the two residences built side by side, the community thought that the reason is that God's punishment for their disobedience. According to some elders of the community, the two families destroyed by the accident were relatives and there was some disagreement between them and God punish them for that. Most of the communities agree with this idea while some of them don't have any clue what caused the mass movements. Almost all of them do not know what measure to take in order to prevent and mitigate the catastrophe. This proves clearly the lack of awareness to the people, how these hazards are occurring. Therefore it is essential to train the community to bring the awareness which can help in minimizing the frequency of hazards.

7.6 Appropriateness of GIS and RS for land slide study

GIS techniques could provide a powerful tool to model the landslide hazards, spatial analysis and prediction, as collection, manipulation and analysis of environmental data on landslide hazard can be accomplished much more efficiently and cost effectively (Carrara and Guzzetti, 1999 and Guzzetti et al., 1999).

Many GIS-based analysis models and quantitative prediction models of landslide hazard have been proposed since the beginning of GIS application in geohazards research in the late 1980s (Carrara, 1983; Van Westen, 1994; Carrara et al., 1991; 1995; Carrara and Guzzetti, 1999; Jade and Sarkar, 1993; Chung et al., 1995; Chung and Fabbri, 1998; Chung and Fabbri, 1999 and Chung and Fabbri, 2001). Overall, the application of remote sensing in environmental monitoring and assessment are virtually limitless, ranging from environmental impact assessment to emergency response planning, landfill monitoring, permitting and enforcement, and natural disaster mitigation, to name but a few (Lillesand and kiefer, 2000). Therefore, multi-criteria analysis based on the triggering factor and their relative weighting is one of the appropriate GIS-based techniques to zone landslide susceptible areas and to evaluate the existing ones.

7.7 Objectives

This study has two main objectives:

- to use integrated techniques of GIS and Remote Sensing to zone landslide susceptible areas
- to apply GIS and Remote Sensing technique to achieve land slide event mapping in the area

The specific objectives of this study include to:

- investigate the causes of landslide
- identify the physical processes associated with initiation and development of landslide
- do land slide event mapping;
- zone land slide susceptible areas
- assess the knowledge and attitudes of the farming community
- to provide a base line data for future research purpose since the area is not much explored; and
- recommend prevention and mitigation measures

7.8 Data and methods

7.8.1 Data Sets used

Several data layers were used to achieve the objectives of this research that mainly dealt with applying integrated techniques to evaluate the extent and cause of land slide in the area. Data layers that are used for assessing the problem include GIS layers, raster layers, in-situ references and some auxiliary data layers.

7.8.1.1 GIS Data Layers

6 GIS data layers were weighted and integrated to accomplish the final landslide susceptible map. The data layers used include:

- landuse/landcover map,
- lineament map,
- lithology map,
- drainage map,
- Slop angle and aspect map and of the area.

7.8.1.2 Remotely sensed data

- ETM+ image of Landsat 7 with a spatial resolution of 15m for band 8 and 30m spatial resolution for the rest bands acquired on February 14, 2001 were very helpful.

7.8.1.3 In-situ data and Ancillary Data layers

Several supplementary data layers were used in addition to the vector and raster layers. Data collected in the field using GPS (Global Positioning System) include:

- points collected for Landslide event mapping,
- Points collected for sample site locations and
- Some GPS points collected for ground truthing

Some of the ancillary layers include:

- topographic maps of the study area at a scale of 1:50,000 of 1978 E.C
- SRTM data
- DEM of the area
- Hard copies of ETM+ satellite images with different combination of color composite
- Metrological data (monthly mean Rain fall, monthly minimum temperature, monthly maximum temperature)
- population census data
- seismic data of the area
- publications and reports at local and Regional level concerning related topics.

7.8.1.4 Software used

The following were the soft wares used:

ENVI 3.5:- for image processing

Arcview 3.2:- to produce all the thematic layers through digitization,

-to edit and tag the onscreen digitized topographic map and drainage map

Cartalinx: - to onscreen digitize and edit contours, roads and drainages from the topographic maps at 1:50,000 scale.

Microdem: - to outlook 3D view of the study area by using the SRTM and DEM data, to do cross section of the topography, to identify structures such as faults and calderas.

Idrisi 32: - -to convert all the vector layers to raster format,

-to weigh all the available factor maps and,

-to do the final integration work.

7.8.2 Methods

Methods of work include:

- Mapping of landslide events using aerial photographs
- map young to old scars of landslides through field survey and using the most recent satellite images
- Predicting landslide sensitive areas and ranking the most susceptible areas using GIS analyses
- Ground truthing of Image interpretation
- Map preparation and production
- Interviewing of locals
- Extensive library work to review literature and previous works.

7.8.3 Image processing and interpretation

7.8.3.1 Image processing

Most of the image processing techniques that have been performed for this research work are explained in detail on part I of the thesis. The relatively recent ETM+ image of Landsat and aerial photographs of the area were used for visual interpretation of landslide scars. To locate and refer objects exactly as they are located on the ground, images have been geo-referenced based on a set of ground control points using the first order polynomial transformation and nearest neighborhood resampling method before interpretation (Berhanu Temessegen et al., 2001).

Image enhancement techniques were also applied to increase the visual interpretability of the images.

7.8.3.2 Interpretation

After performing the necessary image processing procedures, image interpretations were done on hard copy and digital data of ETM+ image of Landsat 7 in addition to aerial photograph of the area. Monochromatic band 7 and color composite images of three band images with RGB order that comprise band 7 were used. Even though it is possible to identify and classify the different themes in the image automatically, more accurate results are obtained by visually interpreting the images (Tesfaye Korme, 1999). Thematic layers such as landuse/landcover map, lithological map and structural map of the area were produced by visually interpreting different combination of color composite images. Landslide scars were also mapped using aerial photographs and color composite images which encompass the study area.

7.8.3.3 Landslide event mapping

The first fundamental step in this study is to do the event mapping from the landslides inventory data the procedures:

- identification of topographic features that indicate landslide scars on aerial photographs and satellite images;
- field verification of landside data indicated from the aerial photograph and satellite images; and
- Correcting and finalizing the event mapping and preparing the statistics for comparison with event controlling factors.

Landslide event mapping was done through interpretation of aerial photograph and the available recent year ETM+ image of Landsat 7. Photo geologic indicators such as abnormal topography, relatively lighter tone of the slide area than the adjoining stable area, vegetation differences, hummocky surfaces, concave slopes, detached large blocks of rocks have been used (Berhanu Temessegen, et al., 2001) to map old and recent landslide scars. Totally 21 landslide scars both old and recent were mapped using the existing images. Detail ground truthing was needed to check the mapped landslide scars and to include the landslide scars left unmapped from visual interpretation. The field checking was also helpful in mapping rock fall areas and for ground truthing of the other thematic layers. For determining the exact location of landslide areas and to produce landslide distribution map, GPS was used. Finally, the GPS points that represent the location of the landslide

scars and rock fall areas were fed in ARCVIEW 3.2 to provide the landslides distribution map and to use it with the other maps to determine the relative importance of landslide triggering factors.

7.8.3.4 Soil sample analysis

Three soil samples were taken during the field survey from the exact spot where the mudflows occurred. Particle size distribution of the samples was determined from a gradation test analysis. During this test the samples are dried and then shaken through a series of sieves having progressively smaller openings. Soil masses retained on each sieve was measured to calculate the percentage that passes the different openings. Atterberg limit test was also conducted on particles that pass standard 75-μm [No. 200] sieve and smaller, to identify the plasticity characteristics of very fine particles of the samples. Moreover, this test was carried out to determine whether the fines are silt or clay (Table 7.1).

Sample No	Location	Depth of sampling	Liquid limit (%)	Plastic limit (%)	Plastic index (%)	Shrinkage limit	Classification based on USCS	Grain size (%)
1	Tejo	50cm	43.3	24.6	18.7	18.70	CL	Sand: 13.60 Silt: 34.68 Clay: 51.72
2	Gurmu Wayide	40cm	74.4	54	20.3	32.44	MH	Sand: 10.10 Silt: 52.00 Clay: 37.90
3	Gurmu Wayide	50cm	59.6	43.2	16.4	32.58	MH	Sand: 11.10 Silt: 49.39 Clay: 39.51

Table 7.1 Soil analysis laboratory result

According to the unified soil classification system the samples analyzed were classified as CL and MH, i.e the samples range from inorganic silts to inorganic clays of low to medium plasticity. The samples comprises of small amount of sand that ranges from 13.6 -10.1 % whereas the silt and clay amount ranges 34.7 - 52.0 % and 37.9 - 51.7 % respectively. The dominance of clay in the soil is a background factor that supports the triggering factors in aggravating the mass movement in the area. The poor grading of particle size indicates the presence of weak soil structure which in turn has its own contribution in facilitating landslide.

7.9 Factors of land sliding and their weighing using GIS

Using GIS & RS techniques, six factor maps that had been recognized as important in causing the mass movement of the area were produced. These factor maps had been arranged and prioritized so that integration through MCE is possible. To apply each factor in this analysis each factor was

reclassified into several classes and assigned rating for each class based on their relative suitability for mass movement.

7.9.1 Classification of the factors to produce landslide susceptibility maps

During the field survey detail study was conducted to determine the priority arrangement of the important factors that trigger the mass movement in the area. The location of landslides, type of landuse/ landcover near the landslides, slope angle, slope aspect, lithology, geological structures, manmade infrastructures such as road construction on slopes, drainage pattern & water ways, etc. were identified.

Each factor map that is used in this analysis was reclassified into classes in order to make the same out put scaling of 0-255. This scaling is assigned based on the number of landslides occurred within a given type of class as obtained from the landslide event map produced in the field. As a result, the classes of each factor that had the maximum number of landslide events were given the maximum value of 255 or close to 255, whereas classes in which none or a few number of landslides occurred were assigned a minimum value of 0 or close to 0. Two types of reclassification were applied to classify each factor map into its classes with new output scale. The first type of classification is the Fuzzy type of arrangement which is applied to avoid distinct boundaries where continues scaling values ranging from 0-255 are assigned. The second type of classification where distinct boundary is assigned and each class has a distinctive rating value that makes it more suitable as compared to the other classes.

No.	Major factors	Sub factors	landslide occurrence	Rating
1	Slope Angle	as the slope angle increases the impact is also expected to increase	as the slope angle increases the occurrence assumed to be increase	0-255 (fuzzy boundary) High value means high impact and vise versa
2	Slope Aspect	North = 0-22.5, 237.5-360 North East = 22.5-67.5 East = 67.5-112.5 South East = 112.5-157.5 South = 157.5-202.5 South West = 202.5-247.5 West = 247.5-292.5 North West = 292.5-337.5 Flat = -1-0	1 - 2 - 3 7 6 2 -	100 50 175 50 200 255 225 175 10
3	Landuse/Landcover	Mixed Annual (int) /Perennial Perennial intensive Mixed Annual/Perennial	6 10 4	200 255 175

		Degraded Land Settlement Riverine trees Crop land Bush/shrub Plantation Grass land	- - 1 - - - -	75 75 100 50 50 50 25
4	Drainage	the drainage impact is expected to decreases further away from the drainage line	away from the drainages the landslide occurrence assumed to decrease	0-255(fuzzy boundary) High value means high impact and vise versa
5	Geological Structure	the impact of geological structures is expected to decreases further away from the structures	away from the geological structures the landslide occurrence assumed to decrease	0-255(fuzzy boundary) High value means high impact and vise versa
6	Lithology	Trachyte 1 Trachyte 2 Ignimbrite 1 Rift floor Ignimbrite (Ignimbrite-3)	7 6 3 5	250 225 175 200

Table 7.2. Various data layers and their relative rating

The slope factor map of the Damot Mountain is obtained from the DEM of the area, IDRISI 32 Surface module. DEM of the study (Figure 7.8) area is digitized using table digitizer from the 1:50,000 scale topographic map of the area at 20m contour interval. The digitized contour map was imported to IDRISI 32 software where the interpolation is performed.

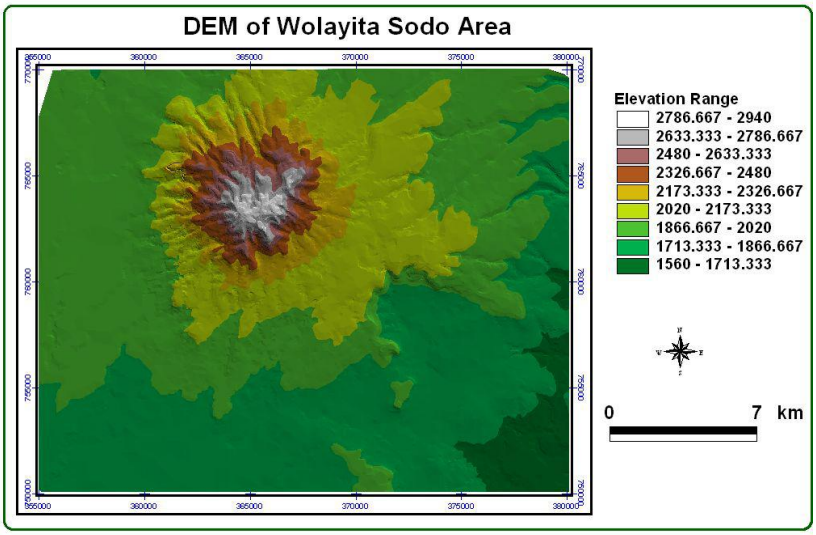

Figure 7.8 DEM of the area from where the slope angle and aspect map are derived

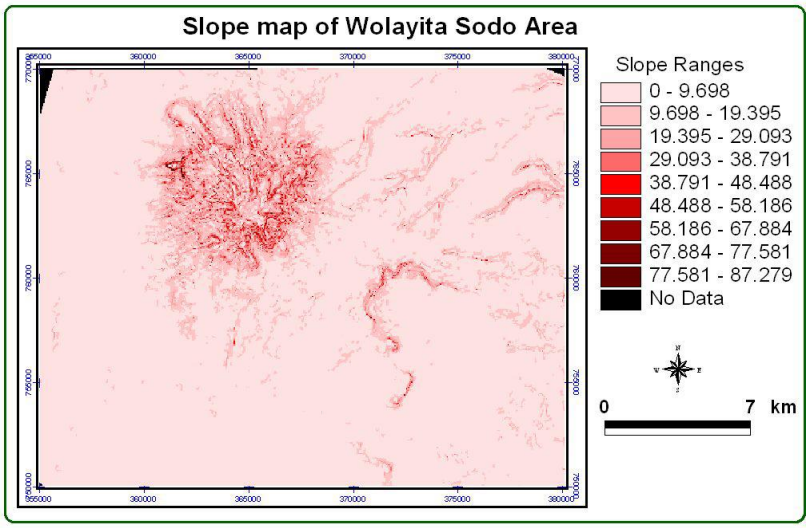

Figure 7.9 slope map of the study area

The slope surface map (Figure 7.9) was reclassified by assigning output values of continuous scaling ranges between 0-255. Small value indicates lesser impact while larger values indicate higher impact. Since the impact of the slope in triggering landslide increases with increasing the angle of the slope, a fuzzy boundary with monotonically increasing type of fuzzy membership curve is preferred. The slope of the area ranges between 0^0-60^0.

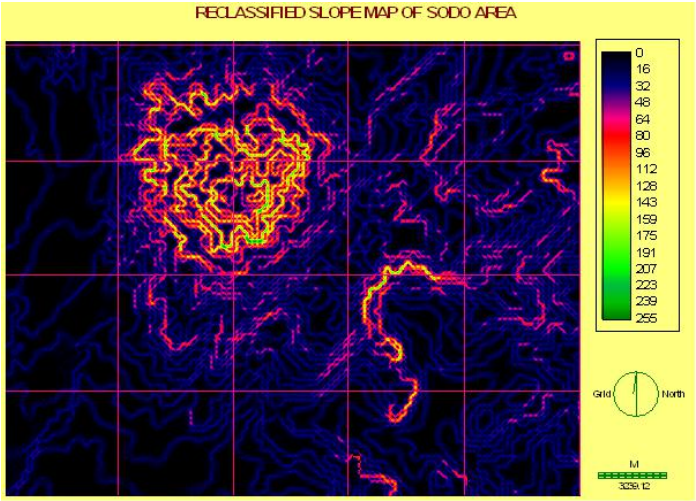

Figure 7.10 Reclassified slope map of the area

The landslide frequency is also controlled by the slope aspect. The slope aspect map (Figure 7.11) is derived from the DEM of the area just like the slope surface map produced using IDRISI 32. This

aspect map is subsequently reclassified into 9 distinctive classes. Out of the 9 classes, 8 of them are classified with 45° intervals while the 9th class that represent flat surfaces has only 0^0.

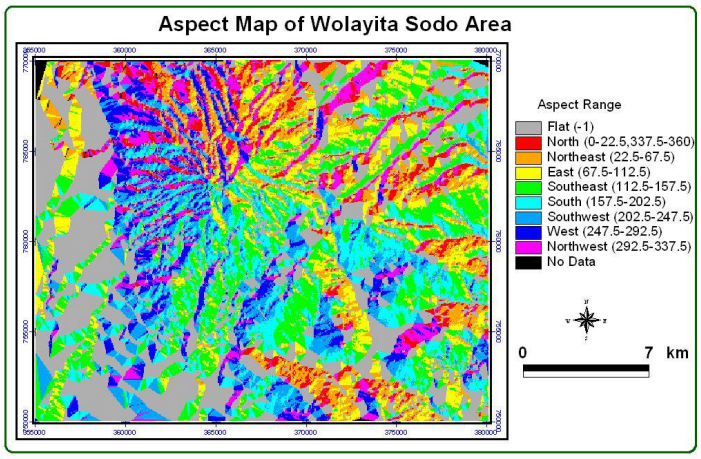

Figure 7.11 Aspect map of the study area

An out put value ranging from 0- 255 is assigned to each distinctive class based on the intensity of landslide occurrence available in each class (Figure 7.12). Higher value indicates repetition of landslide events in the specific class while small values indicate rare or no occurrence of landslide within the given class. Most of the landslides are concentrated in the west, northwest and southwestern part of the slope. Slope classes SW, W and the slopes facing NW have high rating values indicative of frequent landslide occurrence in the past. The shaded slopes have lower ground temperature, higher soil moisture, thicker soil layer (mainly clay), perennial intensive crop type, and higher rainfall amount, formed to be favorable for landslide occurrence.

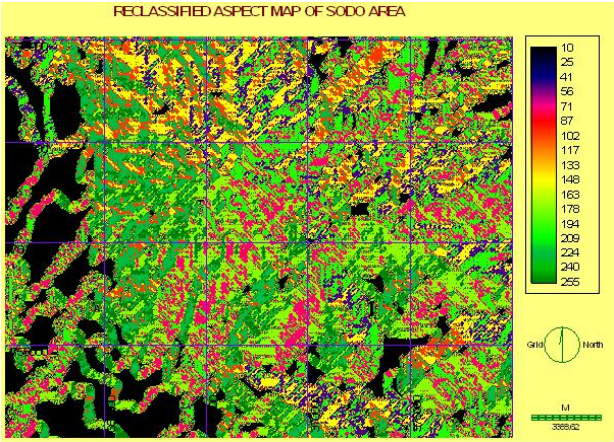

Figure 7.12 Reclassified aspect map of the area

Landuse/land cover map (Figure 7.13) of the area is produced from visual interpretation of digital and hard copy color composite image of band 543 (RGB order) of ETM+ Landsat 7. Each class was onscreen digitized using ARCVIEW 3.2 software. The digitized and edited final vector map of the landuse/landcover map was imported to IDRISI 32 software and converted to raster format. The rasterized landuse/landcover map has been reclassified using output scale that ranges from 0-255, the same as the other of factor maps (Figure 7.14). Higher values are assigned for the landuse/landcover classes with the highest number of landslide occurrence while the landuse/landcover classes with a few or no landslide record have a lesser value. The study area has been classified into ten landuse/landcover types. Out of these 10 types of landuse/landcover mixed annual/perennial class covers larger part of the study area. Perennial intensive landuse class has given the highest value (255) since it has the highest landslide record as obtained from the event mapping. While annual intensive mixed annual/perennial got the second highest value (225).

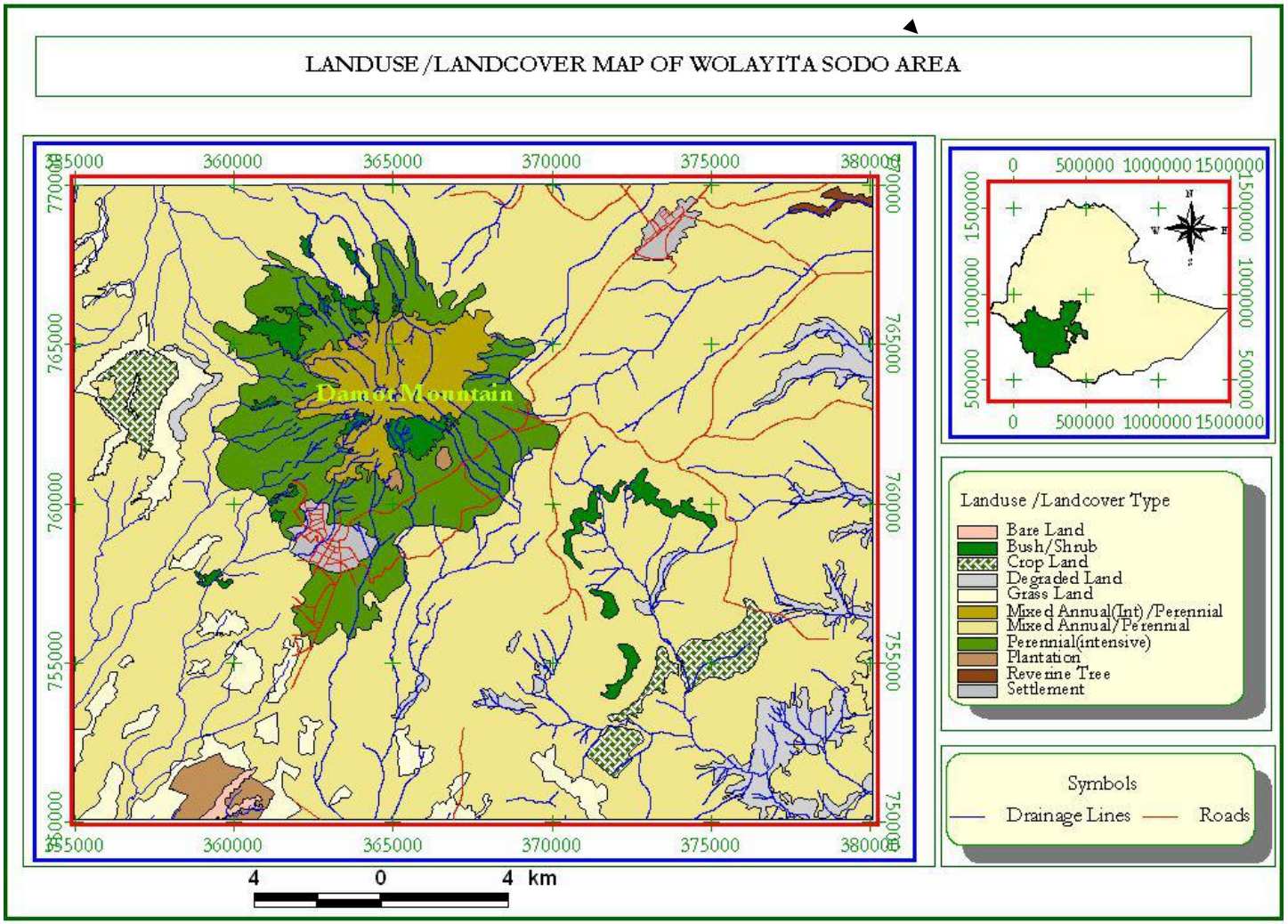

Figure 7.13 Landuse/Landcover map of Welayita Sodo area

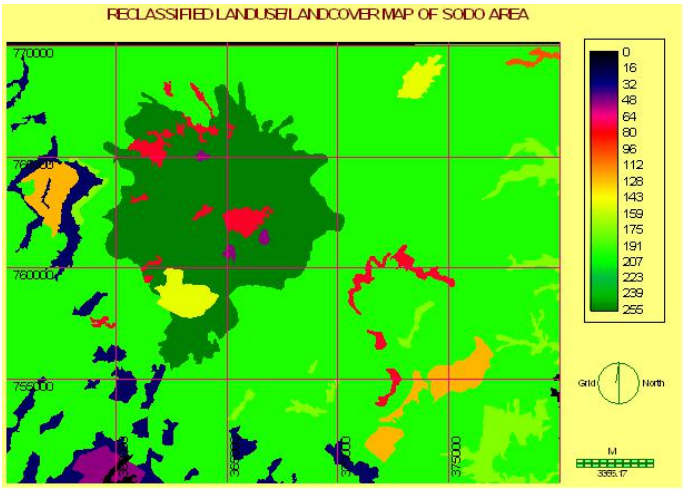

Figure 7.14 Reclassified Landuse/Landcover map of Mount Damot

The area of interest, Damot mountain, is represented by trachytic dome. Drainage pattern of the area has a radial pattern in which the tributaries originate at a concentric circle of small radius and grow into a wider circle as they get farther from their origin.

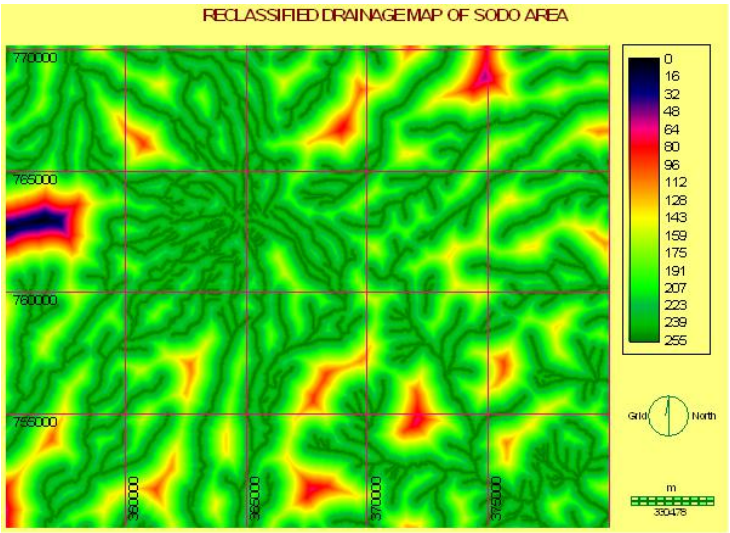

Figure 7.15 Reclassified Drainage map of Mount Damot

The drainage map of the area (Figure 7.16) was digitized using table digitizer from 1:50,000 scale topographic map through Cartalinx software. Subsequently this drainage map was edited through ARCVIEW 3.2 before it is used. The final edited drainage map was imported to IDRISI 32 and converted into raster format so that cell to cell operation is possible. Distance is calculated to measure the Euclidean distance between each cell and the nearest set of neighbor cells. The drainage

lines are a starting point for measuring the distance. Fuzzy boundary with monotonically decreasing type of fuzzy membership curve is established for each distance class in order to avoid distinctive boundaries (Figure 7.15). Away from the drainage lines, the impact of the drainage for triggering the landslide decreases, hence higher output values are assigned for the pixels near the drainage line while lesser values are assigned for the pixels far from the drainage line. This indicates transition between high degrees of importance to less importance for each distance class is continuous.

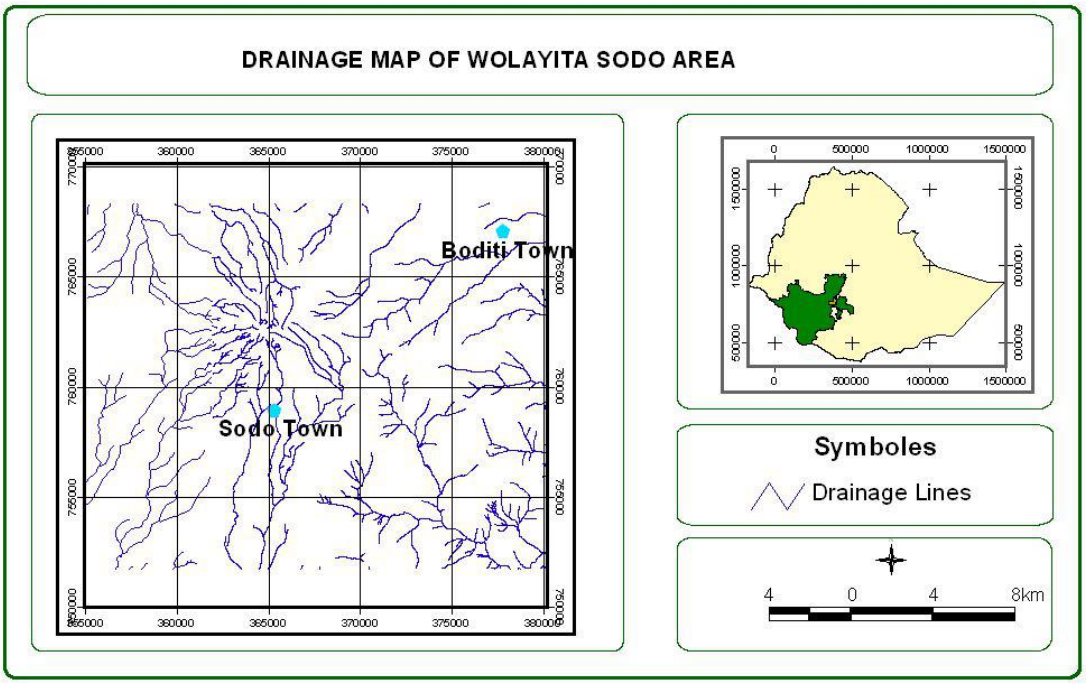

Figure 7.16 Drainage map of Wolayita Sodo area

Mount Damot is situated at the western boundary of the Main Ethiopian Rift System (MER). It is affected by different geomorphic processes. Faults that trend NNE-SSW are very common in the area. The structural map (Figure 7.17) is produced from processed satellite images. Directional filtering at an angle of 45^0 is applied to Band 7 of ETM+ image in order to emphasis linear features that trend at the same direction to the angle of the filter. The filtered image is summed to the original image to avoid confusion of the linear features with man made linear infrastructures. The enhanced structures were then onscreen digitized using ARCVIEW 3.2 software. The downthrown and up throw part of the faults were identified from the surface cross-section made by MICRODEM software and also all are ground truthed. The vector structural map has been converted into raster format through IDRISI 32 software. Moreover the distance of each pixel from the structures is

calculated using DISTANCE module. A fuzzy boundary is established between classes and a continuous scaling of 0 to 255 has been assigned (Figure 7.18). The impact of the structures usually decreases as the distance from the structures increases and vice versa. So monotonically decreasing type of fuzzy membership curve is chosen.

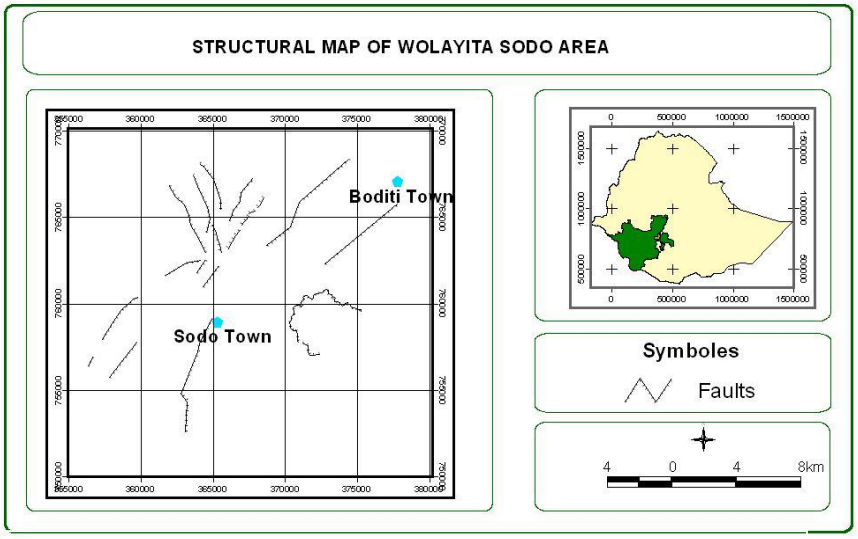

Figure 7.17 Structural (geological) map of wolayita Sodo area

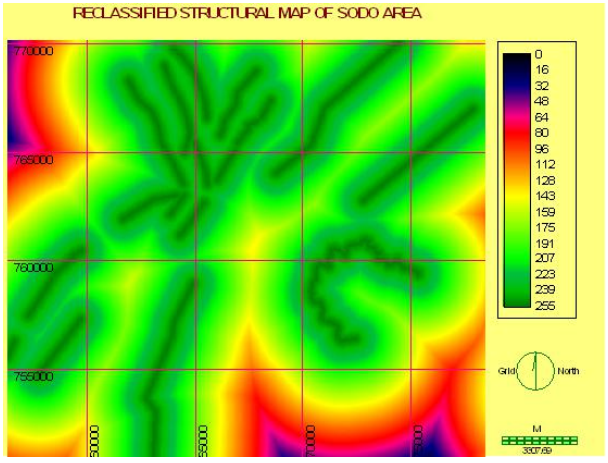

Figure 7.18 Reclassified Structural map of Mount Damot

The lithologic map (Figure 7.19) of the area constitutes 4 types of lithologic units. One of The study areas, Mount Damot, is a trachytic dome that is mainly covered by trachyte flow and ignimbrite. The relatively flat area surrounding Damot Mountain is covered by highly altered and fractured rift floor ignimbrite.

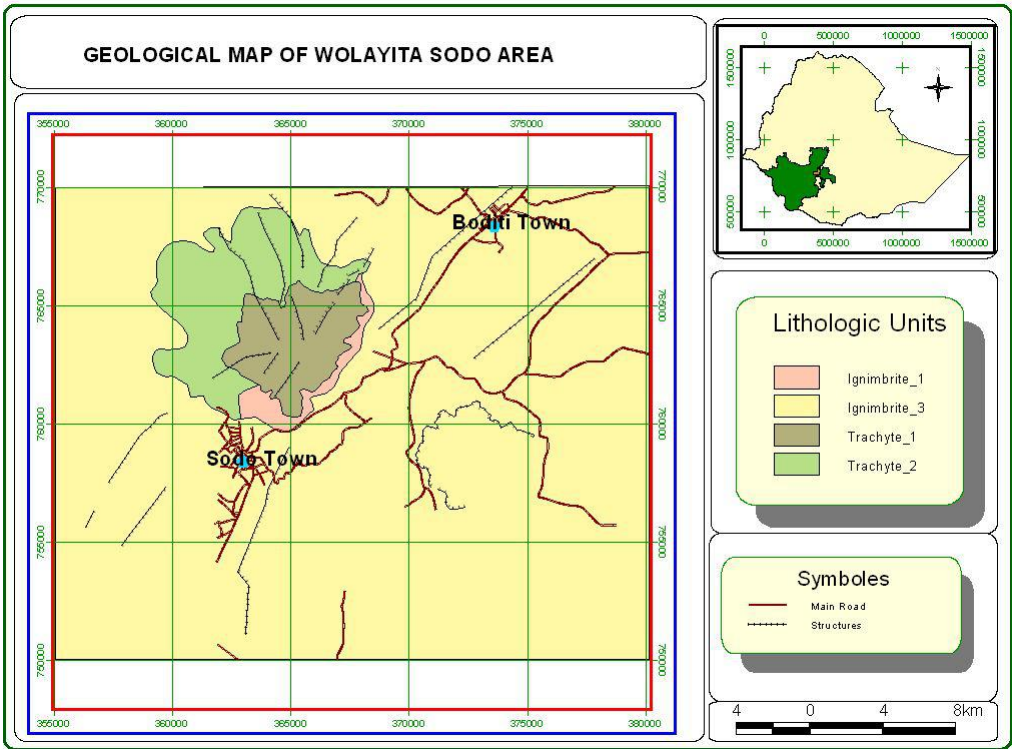

Figure 7.19 Geological map of Sodo-Shone area

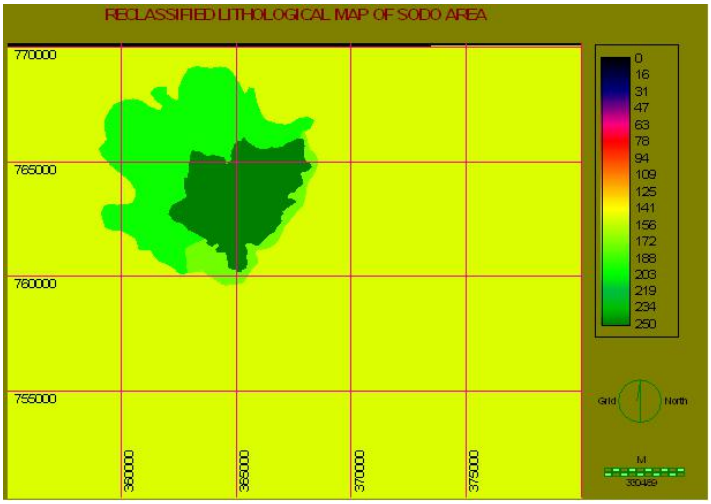

Figure 7.20 Reclassified Lithologic map of Mount Damot

The lithological map of the study area (Figure 7.19) is produced form visual interpretation of satellite images accompanied by detail field checking. Hard copy of Landsat ETM+ Color composite image produced from band 721 at RGB order was used to digitize the lithologic units. This lithologic map

is converted to raster format to integrate it with the other factor maps. An output scale of integer values ranging from 0 to 255 is assigned for the reclassified lithologic map (Figure 7.20). This scale represents the relative importance of the class in triggering the landslide hazard. A higher value is assigned to the trachytic units since they have a repetitive landslide occurrence record. These two trachyte units (trachyte-1 and trachyte-2) are given equal output scale of 255 since they are of the same type.

7.9.2 Pair-wise comparison using Analytical Hierarchy Process (AHP)

The weights developed to each factor are given based on the analytical hierarchy process proposed by Saaty (1997) by means of providing a series of pair-wise comparisons of the relative importance of factors. The rating assigned during the pair-wise comparison is a subjective term based on the knowledge of the problem with its causing factors obtained during the field. In each cell of the matrix the relative importance of the row variable to its corresponding column variable was considered and the appropriate rating was given (Table 7.3). All the diagonal cells in the matrix contain a 1 since it represents the comparison of each variable with itself. Only the lower-left triangular half will actually be evaluated since the upper right is symmetrically identical and values are equal to the reciprocal of the lower-left. The cells in the matrix will contain the evaluation for each possible pair of comparisons.

	Slope	**Aspect**	**Landuse**	**Drainage**	**Structure**	**Lithology**
Slope	1					
Aspect	1/3	1				
Landuse	1/5	1/3	1			
Drainage	1/6	1/4	1/2	1		
Structure	1/7	1/5	1/3	1/2	1	
Lithology	1/9	1/7	1/5	1/4	1/3	1

Table 7.3 Pair wise comparison matrix

7.9.3 Weighting

After the pair-wise comparison matrix is set, individual factor weights were calculated (Table 7.4.) using the WEIGHT module of IDRISI 32. The resulting consistency ratio of the above pair-wise comparison matrix (Table 7.3.) is 0.04 that indicate acceptable consistency range. This consistency

ratio value indicates the probability that the ratings were randomly assigned. The weights calculated indicate the relative significance of the factors in accomplishing the mass movement.

No.	Factors	Factor Weight
1	slope angle	0.4681
2	Slope aspect	0.2484
3	Landuse	0.1214
4	Drainage	0.0801
5	Structure	0.0536
6	Lithology	0.0284

Table 7.4. The eigenvector of weights

Slope angle correspond to gravity, the principal force acting to move surface materials such as soil and rock. Mass movement mainly resulted when the equilibrium condition (stability) of slope is disrupted by manmade and/or natural causes. It occurs when the restraining ability of that material is exceeded the weight of the surface material on the slope as a result of erosion, construction of road by excavating the foot of a slope, and loss of stabilizing roots through removal of vegetation. Based on this fact, slope factor has got the highest weight given that it is relatively the most significant factor in triggering the landslide and the rock fall of the study area. Next to the slope angle, slope aspect has been given the next highest weight as the landslide frequency is also highly controlled by the slope aspect. It mainly controls the ground temperature, amount of soil moisture, rainfall amount and thickness of the soil.

The landuse/land cover in the area has a great contribution in aggravating the mass movement and is weighted after the above two factors. Steep parts of Damot Mountain as a whole are intensively cultivated. These parts of the mountain are dominated by mixed annual and perennial landuse type. Perennial crops that are planted on slope sides such as "enset" (false banana) have an impact in aggravating landslide. Enset is a shallow rooted plant that is un-proportional to its weight above the ground. Therefore it may easily uprooted during intensive rainfall. It also can't hold the soil tightly due to its shallow roots. The seasonal nature of annual cropping has also an immense contribution in exposing the soil to erosion and consequently to mass movement.

Lithological units and structural setting of the area have reasonable contributions to the existing mass movements. The normal faults trending NNE-SSW found on Damot Mountain and the rift margin are significant in aggravating the landslide. The faults mainly dissect the mountain at NNE -SSW direction. These faults are significant factors in controlling the development of landslides and rock

fall. Generally, rock masses near the faults and fractures are highly weathered and severely fractured. Therefore, reasonable weight is assigned for the two factors.

7.9.4 Landslide hazard mapping using Multi-Criteria Evaluation (MCE)

According to Lulseged Ayalew and Hiromitsu Yamagishi (2004), the preparation of landslide susceptibility map is a major step forward in hazard management. Nowadays, such maps can be prepared by GIS-based qualitative and quantitative techniques.

Landslide hazard zonation is a process of marking different parts of an area according to the degree of actual or potential hazard from landslide (varnes, 1984). As discussed by Saha and Gupta (2002), mitigation of disasters caused by landslides can be taken up only when detailed knowledge about the expected frequency, character and magnitude of mass movements in an area is available. Landslide zonation is therefore important to take quick and safe mitigation measures and make strategic planning for the future

Amongst the commonly used techniques of landslide hazard mapping, MCE is one of the most appropriate techniques. It helps to handle the problem of integration of different data layers with heterogeneity and certain level of uncertainty.

After evaluating all six landslide suitability maps, appropriate weight is assigned and used as input for the MCE module. All the data layers used for this analysis were superimposed to a common geographic coordinate system (Figure 7.22). To combine the spatial layers to assess landslide hazard, algebraic combination techniques have been used (Wang and Unwin, 1992). The integration is done through the application of WLC procedure. Each factor was multiplied by its derived weight and then the results added using the formula:

$$S = w1\,X1 + w2\,X2 + w3\,X3 + w4\,X4 + w5\,X5 + w6\,X6 \quad (1)$$

Where: S = susceptibility coefficient

w1 . . . w6 = weights for each factor and

X1 . . . X6 = the six factors used in the analysis

For weights w1 . . . w6, the eigenvector of weight values that are obtained from the pair-wise comparison matrix were substituted (2) and they are the weights related to each X1…X6 factors.

$$S = 0.4681X1 + 0.2484X2 + 0.1214X3 + 0.0801X4 + 0.0536X5 + 0.0284X6 \quad (2)$$

Where X1 . . . X6 represent slope angle, slope aspect, landuse/landcover, drainage, structure and lithology factors, respectively.

Finally as a result of the integration analysis, susceptibility coefficient for each pixel is obtained that ranges from 0-255. These coefficients produce the susceptibility priority map of the area (Figure 7.23). In the susceptibility priority map, cell values that are 0 or close to zero indicates relatively secure area with flat or very gentle slope, areas found further away from structures and drainage, firm lithological units and areas covered by vegetation such as bush and shrub, plantation and grass. Whereas cell values that are 255 or close to 255 signify unstable areas with maximum slope angle, nearer to drainage and geological structures, with spars vegetation cover or shallow rooted plants. The histogram produced from the susceptibility map shows that large part of the study area falls between 100 to 150 susceptibility values whereas values greater than 200 covers a small portion of the area (Figure 7.21 & Annex 5).

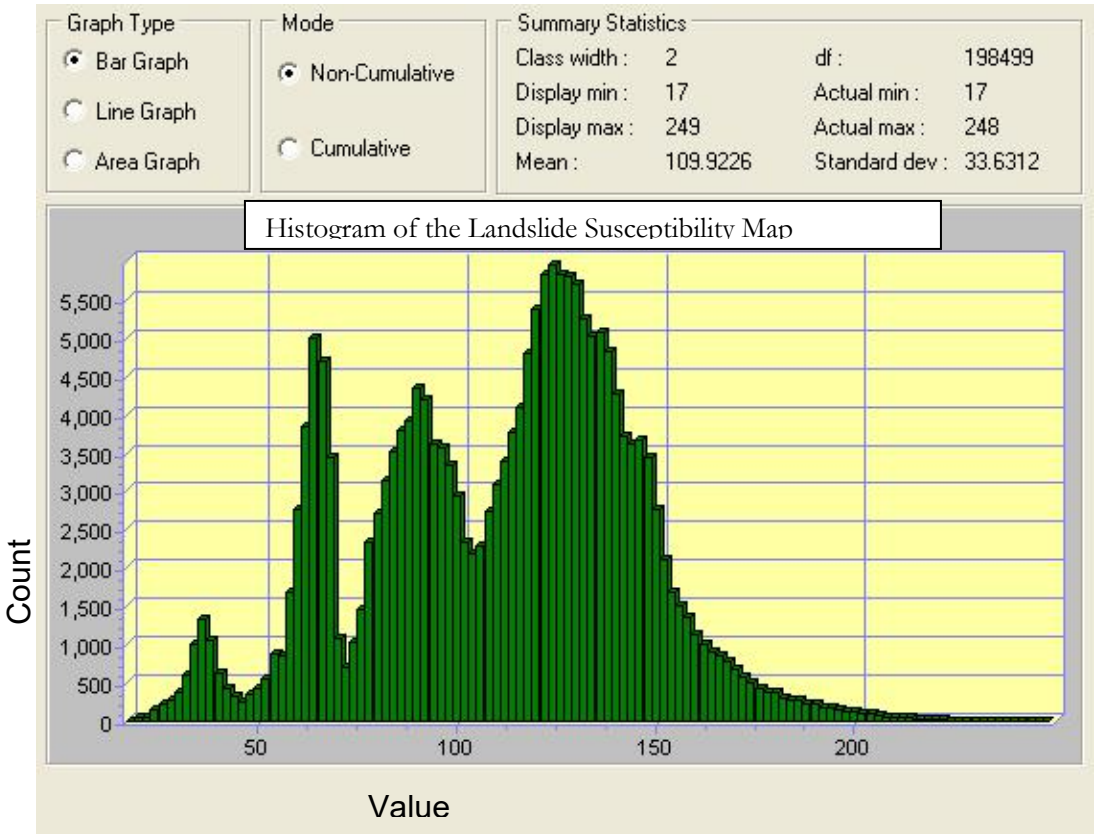

Figure 7.21 Histogram of the landslide susceptibility map around Wolayita Sodo area

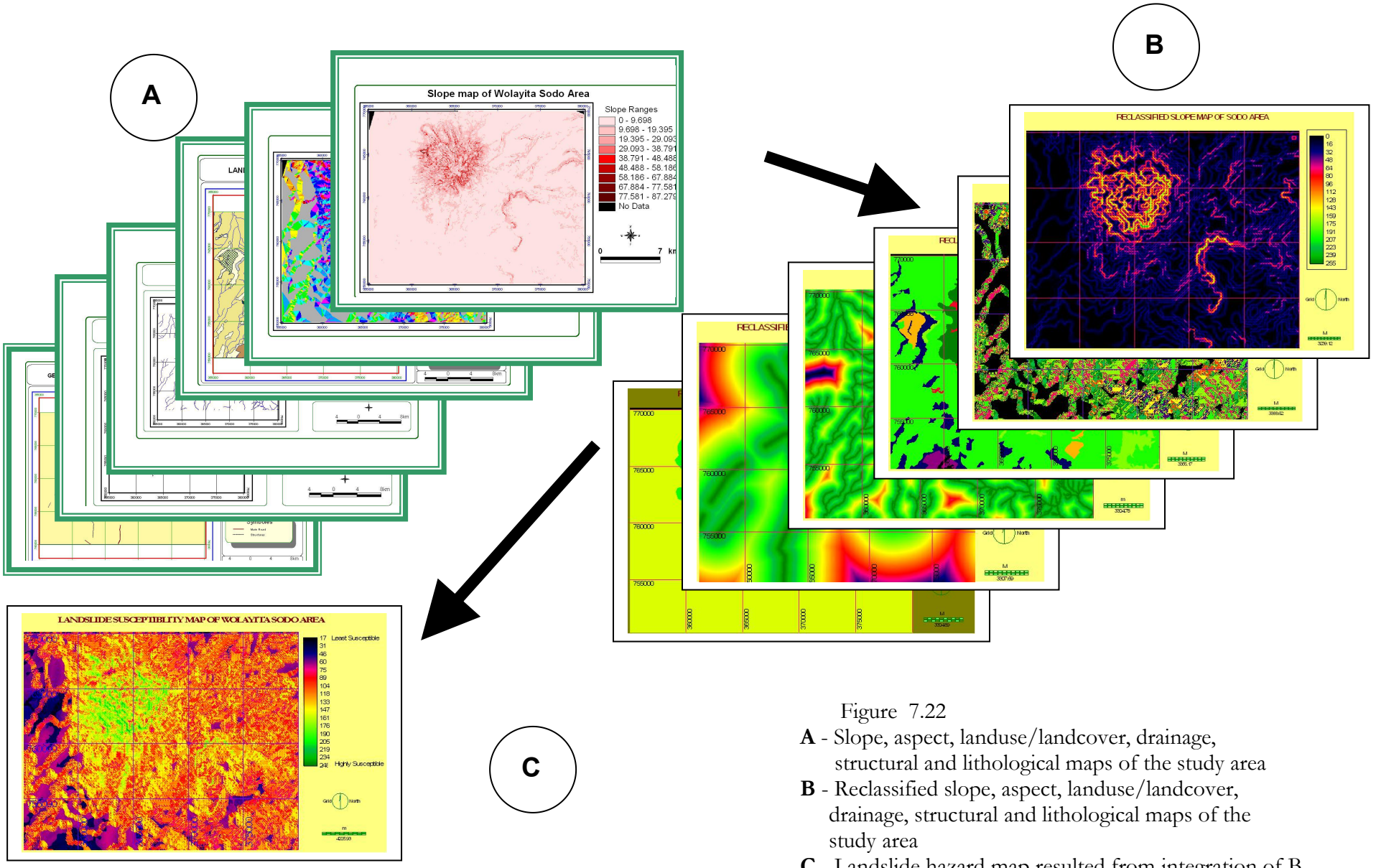

Figure 7.22

A - Slope, aspect, landuse/landcover, drainage, structural and lithological maps of the study area

B - Reclassified slope, aspect, landuse/landcover, drainage, structural and lithological maps of the study area

C - Landslide hazard map resulted from integration of B

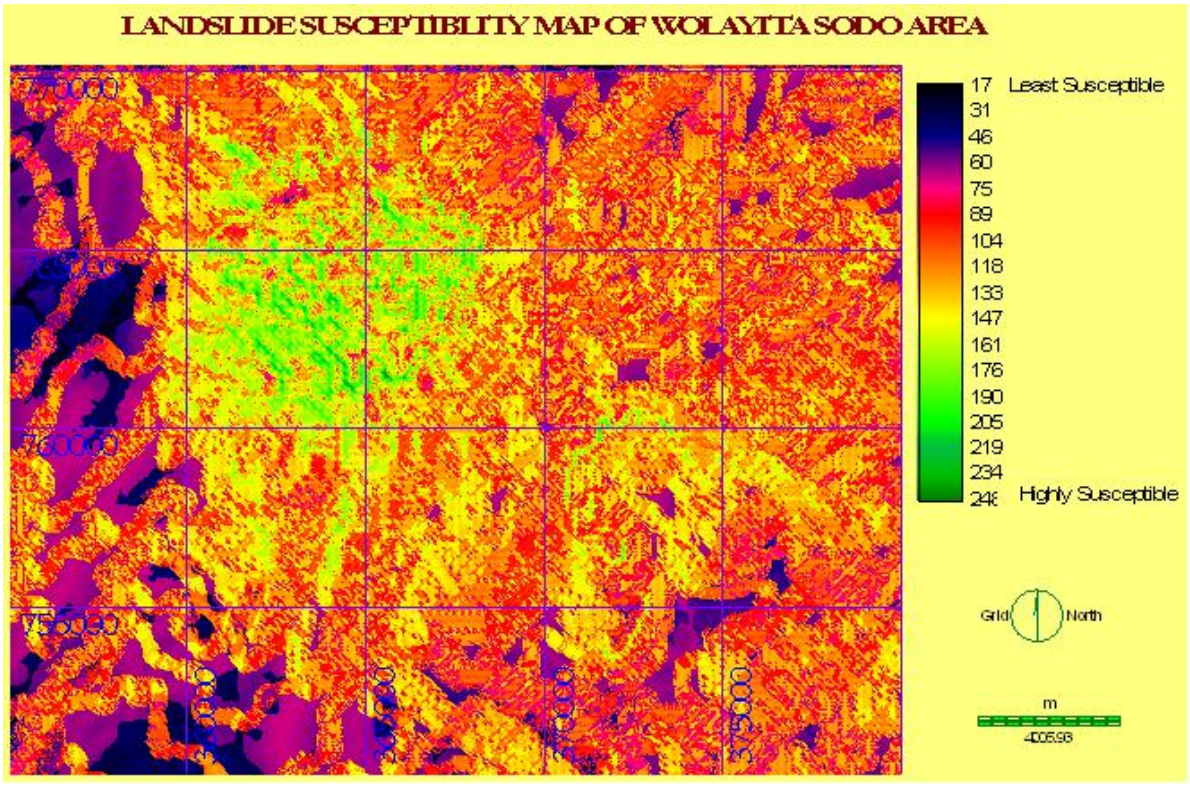

Figure 7.23 Landslide Hazard map

PART-IV

Recommendation, Summary and Conclusion

Chapter 8

Recommendation on Mitigation of Land Degradation and Landsliding

8.1 Controlling and rehabilitation strategy of land degradation based on GIS analysis

It is very difficult to reverse the effects of erosion considering the rate of soil formation. Areas which are changed into badlands have already lost their resilience and need a serious measure like closuring or conserving though it would be difficult with the ever increasing population number and strong demand for cultivation land. Avoiding overgrazing and the over-use of crop lands is crucial in order to sustain good environmental condition of the area. In addition, land degradation, particularly soil erosion from cultivated fields, is a threat to agricultural production, therefore, conservation measures and mitigation strategies are needed, including:

Bio-fertilizers: Land restoration often requires inputs such as bio-fertilizers which are probably the most environmental friendly in order to minimize the ongoing degradation. Bio-fertilizers such as plant residues and animal dung are cost-effective and most farmers can afford to use them as manure. Decaying plants and animal remains will enrich soil in humus; subsequently the organic matter will glue the soil particles together and may prevent erosion. Therefore, fertilizing is the best remedy against erosion and can be adopted by local communities since it helps in increasing fertility of the soil, soil aggregate stability, water infiltration capacity and soil water holding capacity.

Tree planting: particularly deep rooted trees provide protective cover on the land and prevent soil erosion. Plants will help to slow down running water as it flows on the surface. This in turn facilitates the infiltration of much of the water into the ground. Plant roots hold the soil in position and prevent it from being washed away. Moreover, plants minimize the impact of a raindrop before it hits the soil thus it will reduce its ability to erode.

Biological diversity: Encouraging biological diversity by planting several species of plants together will help to sustain the ecosystem in the area. Different species have different adaptation to the

deteriorating environmental condition. Moreover, the plant residues from various types of species will enrich the soil with enormous organic minerals and will facilitate favorable conditions for various types of micro-organisms to live. This may help to improve the fertility of the soil.

Retirement fencing: in most places, the highly degraded land which is becoming a badland should be retired (inclosured) from grazing and has to be fenced in order to avoid human and cattle encroachment. Preventing human exploitation of the land will allow regeneration of the more natural state as it was before the degradation and will encourage biodiversity. Reduction of animal density would also mitigate degradation by avoiding over-grazing. Crop lands that are susceptible should also be restricted or detached from cropping based on the intensity of the problem or they have to be prohibited from future agricultural expansion. But retirement fencing will remove land from production and as a consequence it will usually reduce the economic productivity of the land so alternative measures have to be taken to facilitate incentives for the farmers.

Avoiding burning of bush and grass: the farmers usually apply burning to clear land for cultivation and for charcoaling. Burning is destructive because it burns the seeds of plants and destroys the stem of trees and their barks. It can also burn the ecosystem of microorganisms and insects those produce humus from vegetal remains.

Stubble-mulching: is leaving stubble on the field. The use of crop residues had become of major importance as a means for erosion control and moisture conservation by reducing evaporation. It is also used to keep the soil covered so that rain drop impact is minimized.

Contour ploughing or contour farming: is one of the farming practices that apply plowing at right angles to the direction of the slope following its contours. Thus the resulting rows have the effect of slowing run-off during heavy rain so that the soil is not washed away. It also facilitates the water to percolate into the soil by lengthening the time that the water stays at a place.

Leaving unploughed grass strips between ploughed land; will help as a boundary between farms and at the same time it will help to reduce the amount of soil washed and transported from cultivated land. The grass strips will operate as filter to catch much of the soil that may run off the cultivated lands. They should be wide enough to mow across the hill easily as well as wide enough to effectively reduce the amount of soil washed by the run off.

Strip cropping; is practice of growing crops in narrow strips either at right angles to the direction of the prevailing wind, or following the natural contours of the terrain to prevent wind and water erosion. It is a systematic way to deal with long slopes. Strip cropping is an effective way of controlling transport of particles that detached from the surface. It does control by interrupting the flow of water. Sediment that is picked up by water in the row crop is almost immediately dropped when the water is slowed by the closer growing crop down slope. In the case of wind erosion it assists by disrupting wind currents. Typical strip cropping systems involve a rotation. Usually row crops alternate down slope with closer growing crops or forages. Forages are environmentally friendly in that they can reduce soil erosion and used as fertilizer. In addition, forages can increase soil structure and organic matter and will assist to enhance agricultural profitability. Generally, strip cropping can be quite effective in minimizing sediment loss from a field. Erosion may still occur but overall amount that might have been transported is at a greatly reduced rate.

Terracing: helps to catch runoff water from cultivated fields. It will facilitate the situation for water to soak into the ground and deliver the excess water that exceeds the infiltration capacity safely to the bottom of a hillside. It will also give soil particles that do erode a chance to settle out in the basin behind the terrace ridge. The stone ridges that are built around a hillside following contour line break up one long slope into a number of short ones. This may reduce the highly erosive force of water as it moves down slope. Terraces are often used in combination with other conservation practices to get more complete soil protection result.

Generally, terraces are very effective in controlling erosion by reducing both the amount and velocity of water moving across the soil surface which greatly decreases soil erosion. They intercept rainfall runoff as it starts down a slope thus they prevent a large accumulation of flow on the surface. This reduces the potential for sheet and rill erosion to occur.

Construction of water channels along road sides to prevent side washing of soil during rainy seasons. Constructing water ways will help to prevent road-side erosion. Covering the waterways with grass is cost effective and very effective protection. Making grassed waterways wide and shallow will help to slow the water down and to prevent it from rilling and gullying the waterway.

Allowing indigenous plants to grow: along the river banks instead of ploughing and planting crops right up to the water's edge. Plants and grasses on the banks of rivers are of particular

importance because they help to reduce the velocity of the water and their roots bind the soil. To grow several species of trees along the stream banks such as Bamboo (Bambusa vulgaris) have dual advantage. First, they will help to conserve the stream banks and provided sustainable protection to the land. Second, the farmers can use it as timber and firewood.

Grass cover: may help to protect soil from direct rain drop impact and prevent rill and sheet erosions. Grasses may have of great value for erosion control and forage, especially for converting abandoned cropland into useful and productive range.

Finally, lasting solutions to the problem of land degradation of the area should include easing population pressure from highly degraded areas, technological improvements in agriculture and development of the other sectors of the economy. Moreover, awareness has to be well created in the society regarding land degradations, its cause and the mitigation strategies. Involving the local people is essential in all initiatives of mitigation strategies since they are the direct beneficiaries and owner of the land.

8.2 Controlling and mitigation strategies of land slide based on GIS analysis

Mitigation of landslides includes any activities that prevent disaster, reduce the chance of an emergency happening, or lessen the damaging effects of disasters that can not be avoided, including:

- **Diverting water:** away from slip-prone areas by cutting channels is essential to improve slope stability. It minimizes over saturation of water in the soil as a result of water accumulation in one place for extended time. It also assists to reduce pore water pressure in order to keep the stability of a slope.

- **Fencing highly susceptible areas:** and control these areas in a different way from the rest of the farm. This may involve re-vegetation with trees such as planting deep-rooted trees, low growing trees, shrubs and grasses,...

- **Prevention is the best remedy than dealing with the damage.** So avoiding settlement on the sliding axis that has high potential for sliding is essential to reduce the damages.

- Mitigation of landslide risk can also be accomplished by **effective land use planning** to minimize development in slide-prone areas. Generally, land use planning needs to involve the

landslide hazard or susceptibility mapping so that high hazard areas can be demarcated in order to avoid from allocating them for expansion or other utilization.

- By construction of appropriate retaining walls or by other types of geotechnical remediation.

- Develop appropriate policies in consultation with the local people and encourage their participation is an alternative mitigation strategy.

- Moreover, it is important to provide training on landslide problems, cause and mitigation strategies for the community by preparing session like conferences, meetings, workshops, gatherings...

Chapter 9

Summery and Conclusions

9.1 Land degradation

Land degradation is a major environmental and economic problem in countries where the proper land use plan is not available and implanted. The Southern Ethiopian Rift valley segment that includes the study area is one of the locations where land degradation due to natural and anthropogenic driving forces is severe.

The area selected covers a surface area of 1750 sq.km, and an integrated GIS, remote sensing, laboratory analysis and field methods have been used. GIS is particularly used to derive quantitative values and integrate some variables based on MCE technique. The particular GIS method used in integrating and analysis of the data is authentic to this study. Because, it integrates a wide range of information layers in different formats, and does empirical analysis to derive spatial maps. The computations are based on raster data that allows pixel to pixel analysis increasing the accuracy of the method.

Evaluation of the existing land degradation, assessing the relative important factors and producing land degradation susceptibility mapping were accomplished using integrated GIS and remote sensing approach. This method was very helpful in prioritizing all the factors based on their suitability in triggering the land degradation presently occurring in the area. To understand the suitability of triggering factors, mechanism of occurrence and their priority will help to present ways to control and prevent it.

Various data layers including GIS layers, remotely sensed data, in-situ references and some auxiliary data layers were used during the progress of the study. Several softwares were also at great help starting from preliminary to final stage of this work. Different image processing techniques such as image registration, sub-setting, band ratioing, image enhancement, color composite, decorrelation stretching, linear filtering and edge enhancement were applied in order to prepare all the raster layers useful for further analysis. The GIS layers were digitized using the processed satellite images (ETM+ of 2001, Land sat TM of 1984 and 1995) and topographic map of the study area. Then all the thematic layers resulted from the digitization were finalized after performing detail field checking.

In this study the nature of the soil has its own great contribution for the problems which are the initiatives of the research. 5 samples were taken during the field survey and analyzed through laboratory work to get the necessary results. Classification for the analyzed samples was done using Unified Soil Classification System (USCS). According to this classification system soil of the area falls in to CL, MH, and CH group. The gradation test results of the samples ranges from silty clay to fine clay. In addition to gradation tests Atterberg limit test were conducted on the finer particles. Three samples (sample No 1, 2 and 3) have a liquid limit of less than 50% and their plasticity index ranges between 26.3-16.5, there for their typical class belongs to silty clays (CL). Whereas, sample No 4 and 5 have a liquid limit of 78.0 and 68.7 respectively. Their plasticity indexes are 69.1 and 9.84 respectively therefore they are classified as inorganic clays of high plasticity or fat clays. The test results show that most of the soil layers belong to silty clays. However the different soil layers show different liquid limits. The resistant layer shows a relatively high liquid limit of 78.0% while the friable and degraded layers show about 45% liquid limit on average. Similarly shrinkage limits are proportionally lower for resistant layer and higher for the highly eroded layers. These clearly indicated that the differential weathering is directly related to the differential properties of the soil layers. The layers with smaller shrinkage limit and higher liquid limit are very hard to firm soils with higher shear strength resistant against erosion. The soil layers underlying and overlaying these resistant layers are softer and are sensitive to change in moisture content which facilitates their erosion. These differential properties of the soil layers lead to differential weathering and erosion. Resulting is the degradation land for in the area together with the triggering factors.

One of the objectives of this study is to calculate the rate of degradation in the study area in areal base. Smaller representative site of about 640 square kilometer was selected based on the intensity of the problem. Then change in a time series of the degraded areas was produced using CROSSTAB module in IDRISI 32 for images of ETM+ (2001) and landsat TM (1984 and 1995). After performing the cross-classification between 1995 and 1984 images and 1995 and 2001 images, rate of change in degraded areas is calculated. The average rate of degradation from 1995 to 1984 is given as 1.8 sq. km/yr while the average rate of degradation between 2001 and 1995 is given as 3.1 sq. km/yr. These rates show degradation problem is becoming serious since recent times. If this rate continues with the same trend, in the last three years it has been added a roughly equal amount of degraded land between that of 1995 and 2001 (about 25 sq. km) to the already degraded land, resulting in a totally degraded zone of about 100 sq. km. (about 17% of the sample site) at this moment.

The amount of soil lost from the study area is estimated using cut and fill technique applied on 5 representative sites that are selected based on the intensity of the problem, their areal extent and accessibility to the main road. During the field survey, profiling was done using GPS reading taken at every 5-10m interval. All GPS reading were organized in a database. By considering relatively uneroded areas as a plane surface to represent the area before the degradation, volume loss is calculated by subtracting the plane surface from the presently existing degraded surface. As a result 2,485,818 m^3 amount of soil is lost from 291,241 m^2 area, there fore the net lose per area is about 8.53.

Several factors contributed to the exiting land degradation in the study area. The increasing rate of degradation and the loss of such amount of soil in the area are attributed to various factors such as structure, lithology, landuse, slope, soil, drainage, and climate factors. These factors can be reclassified into two major groups as back ground factors that are inherent to the geology of the area and triggering factors. Since several factors are involved in the process, integrated GIS analysis using IDRISI 32 was used to perform all the integration approach of MCE. During a Multi-Criteria Evaluation, an effort is made to combine all the factors as a set of criteria to accomplish a particular composite basis for a decision according to the specific objective which is to delineate land degradation prone areas. So criteria images such as land use type, type of lithology, angle of the slope, proximity to structures and drainages; were combined to form a single suitability map from which the final land degradation susceptible area was decided. All the factors used in this analysis are standardized by using a byte binary format with a standard scaling that range from 0-255. Once the standardized factor images have been created, a set of weights were developed that indicate the relative importance of each factor to the decision under consideration. Finally, each factor was multiplied by its factor weight and then added the results through the application of WLC procedure. The final land degradation susceptibility map which is resulted after many comparisons is highly related to the tangible reality observed during field survey.

This work demonstrates the advantage of applying an integrated GIS and remote sensing approach for environmental hazard assessment and risk mitigation planning. Given the time, the budget and data that were allocated and input to this work, the results are of higher calibers. This is in accordance with the advantages expected in using geoinformation to solve real problems in wider areas. The approach used is simple and requires multi spatial data. It can be applied for small or

wider areas with similar or related environmental hazard assessments (such as landslide hazard, draught prediction modeling and so on). Moreover, this work enhanced the extent of the problem in the study area which is extensive and affected the environment. The community of the area is affected either directly or indirectly from such environmental hazard. However the information and results obtained through this study will assist to raise the awareness and to emphasize the need for mitigation plans and strong agricultural policies.

Generally, the major results obtained from this study are: (1) Identification of the factors (structure, lithology, landuse/ landcover, slope, soil, drainage, and climate) that highly contribute to the land degradation and putting them in hierarchical order; (2) Calculation of the rate of land degradation which is logarithmically increasing in recent years. 2,485,818 m^3 amount of soil is lost from 291,241 m^2 area in less than 11 years. The net soil lose per area is about 8.53%; (3) Calculation of the total amount of area affected by land degradation, and (4) Proposing mitigation and controlling mechanisms. The computational results obtained at different levels in this research are closer to the reality, because, the assumptions that were taken in the processing and the analysis were insignificant. The errors introduced in data collection and interpretations were minimized by mathematical iterative process involved in Saaty matrix calculation.

The end users of the different results of this work are Regional Agriculture Bureaus Land Use Department, Crop and Range Land Management Department, Disaster Prediction, Preparedness and Control and Environmental authorities, NGOs, researchers and the local community.

9.2 Landslide

Landslide hazard is becoming a major issue since it causes a severe threat to human life and property. The study area that mainly encompasses Damot Mountain is controlled by tectonic structures given that it is situated in the western margin of the Ethiopian Main Rift System. It is affected by different geomorphic processes. It is mainly covered by thick soil cover of faty clays that swell up on wetting and crack upon drying. Water infiltrates through the cracks causing an increase in pore water pressure within the soil profile and may weaken inter-granular bonds. It also reduces the cohesive strength of the soil and ultimately the stability of the slope. Subsequently, the soil started to move downward as mud flow. As a result landslide occurred in the area frequently. The most common

mass movements in the study area are mud flow, rock fall and creeping. These mass movements are attributed to natural and manmade factors. Out of these factors rainfall is the main triggering one.
In order to examine threatening landslide hazards and predict future occurrence of landslides to reduce damage from such mass movement, attention should be given to understand landslide process, causing factors and mechanism of occurrence.

Landslide events on Damot Mountain are strongly correlated to many factors. Factor susceptive analysis relies on landslide inventory data mainly obtained from field investigation and aerial photograph interpretation. Landslide event mapping has done through the interpretation of aerial photograph and the available recent year ETM+ image of Landsat 7 that of 15m resolution for band8 using Photo geologic indicators. The quantitative relationship between affecting factors and landslides were achieved by applying MCE. To apply each factor in this analysis each factor was reclassified into several classes and assigned rating for each class based on their relative suitability to the same out put scaling of 0-255. Therefore the integration part is done through the application of WLC procedure. Each factor was multiplied by its derived weights and then added the results using empirical formula. . Finally as a result of the integration analysis, susceptibility coefficient for each pixel obtained that ranges from 0-255. These coefficients in general produce the susceptibility priority map of the area. In the susceptibility priority map, cell values that are 0 or close to zero indicates relatively secure area with flat or very gentle slope whereas, the indicators most sensitive to landslide in the study area are the result of: (1) steeper slopes; (2) slope facing W, NW and SW; (3) landuse type that dominates shallow rooted perennials and annual crops; (4) where drainage incised the foot of the mountain (5) near tectonic structure such as faults trending NNE-SSW; (6) the trachytic layer that is covered by thick clay soil.

In general, this study has an immense contribution in investigating and studying of landslides in the study area and to find ways to reduce and prevent their damages. This achievement is made possible through the application Integrated GIS and remote sensing approach. Particularly Amongst the commonly used techniques for landslide hazard mapping, MCE is one of the most appropriate techniques. It helps to handle the problem of integration of different data layers with heterogeneity and certain level of uncertainty. Thus, this methodology seems to be quite suitable for developing a landslide susceptibility mapping.

The major output of this study is the landslide susceptibility map that can assist to examine landslide prone areas. In addition all the factors that are responsible in triggering the landslides such as slope angle, aspect, landuse, drainage, structure, and slope are identified. The Landslide inventory data gathered from field investigation and aerial photograph interpretation and the recommendations that are suggested are also major outputs.

The primary beneficiaries of this study are the communities in the study area who are suffering from the damage. On the other hand the methods used, the available data, the result and the recommended technique will be valuable inputs for other researchers who are interested to work in this area and in other areas on similar topics or related one.

References

- A. K. SAHA, R. P. GUPTA, 2002. GIS-based Landslide Hazard Zonation in the Bhagirathi (Ganga) Vally, Himalayas, International Journal of Remote Sensing. vol.23, No. 2, pp. 357-369.

- Asfawossen Asrat et al., 1995. Land mass movment in northern Omo zone: The case of November 10, 1994 landslide in Goffa district, Southern Ethiopia. (Unpublished work).

- Berhanu Temesgen et al., 1999. Landslide hazard on the slope of Dabicho Ridge, Wondogenet area: The case of June 18, 1996 event. SINET: Ethiopia. J. Sci., 22(1):127-140,1999.

- Berhanu Temesgen et al., 2001. Natural hazard assessment using GIS and Remote Sensing methods, with particular reference to the landslides in the Wondogenet area, Ethiopia. phys. chem. Earth (C), vol. 26, No. 9, pp. 665-675,2001.

- Bezuayehu Tefera, Gezahegn Ayele, Yigezu Atnafe, Jabbar M.A. and Paulos Dubale. 2002. Nature and causes of land degradation in the Oromiya Region: A review. Socio-economics and Policy Research Working Paper 36. ILRI (International Livestock Research Institute), Nairobi, Kenya. 82 pp.

- Carrara A., 1983. Multivariate models for landslide hazard evaluation. Mathematical Geol., v. 15, 403-426.

- Carrara, A., and Guzzetti, F., eds., 1995, Geographical information systems in assessing natural hazards: Dordrecht, Netherlands, Kluwer, ??p.

- Carrara A, Cardinali M, Detti R, Guzzetti F, Pasqui V, Reichenbach P (1991). GIS techniques and statistical models in evaluating landslide hazard. Earth Surface Processes and Landforms. 16, 427-445.

- Chung C.F., A.G. Fabbri and C.J. van Westen, 1995. Multivariate Regression Analysis for Landslide Hazard Zonation, Geographical Information Systems in Assessing Natural Hazards (A. Carrara and F. Guzzetti, editors, Kluwer Academin Publishers, Dordrecht, The Netherlands, pp. 107-133.

- Chung, C.F., Fabbri, A.G., 2001. Prediction models for landslide hazard using fuzzy set approach. In: Marchetti, M., Rivas, V. (Eds.), Geomorphology and Environmental Impact Assessment. A.A. Balkema, Rotterdam, pp. 31–47.

- Chung, C.F., Fabbri, A.G., 1999. Probabilistic prediction models for landslide hazard mapping. Photogrammetric Engineering and Remote Sensing (PE&RS) 65 (12), 1388–1399.

- Christopher A. Legg, 1994. Remote Sensing And Geographic Information Systems: geological mapping, mineral exploration and mining. Ellis Horwood Library of Science And Space Technology: Series in remote sensing.

- D. G. A. Whitten with J. R. V. Brooks, 1972. The Penguin Dictionary of GEOLOGY.

- Di paola, G. M., 1972. Ethiopian Rift Valley (between 70 and 80 40' lat. North): Bulletin Volcanologique. v. 36. p. 517-560.

- EARTH MANUAL PART 1, 1998. Earth Sciences and Research Laboratory Geotechnical Research Technical Service Center Denver, Colorado 1998. Third Edition

- Fitsum Hagos, Pender J. and Nega Gebreselassie. 2002. Land degradation and strategies for sustainable land management in the Ethiopian highlands: Tigray Region. (Second edition). Socio-economics and Policy Research Working Paper 25. ILRI (International Livestock Research Institute), Nairobi, Kenya. 80 pp.

- FAO, 2001. LECTURE NOTES ON THE MAJOR SOILS OF THE WORLD. Edited by: Paul Driessen, Wageningen Agricultural University, International Institute for Aerospace Survey and Earth Sciences (ITC), Jozef Deckers, Catholic University of Leuven Otto Spaargaren, International Soil Reference and Information Centre Freddy Nachtergaele, FAO, 2001.

- Giday Woldegabriel, James L. Aronson, Robert C. Walter, 1990. Geology, geochronology, and rift basin development in the central sector of the Main Ethiopian Rift. Geological Sosity of America Bulletin, v. 102, p. 439-458.

- Gonghui WANG and Kyoji SASSA, Pore Pressure Generation and Motion of Rainfall-Induced Land-slides in Laboratory Flume Tests. Disaster Prevention Research Institute, Kyoto Univ., Kyoto, Japan Proceedings of International Symposium, Landslide Risk Mitigation and protection of Cultural and Natural Heritage 21 - 25 January 2002, Kyoto University, Kyoto, Japan.

- Guzzetti, A. Carrara., F, et al.,1999, Use of GIS technology in prediction and monitoring of landslide hazard, in Natural Hazards, p. 117-135.

- Guzzetti, F., Carrara, A., Cardinali, M., Reichenbach, P., 1999. Landslide evaluation: a review of current techniques and their application in a multi-scale study, Central Italy. Geomorphology 31, 181– 216.

- IDRISI, 1990-2000. "IDRISI for Windows Version 132.11", Decision Support in the IDRISI Guide to GIS and Image Processing Volume 2. Exercises 2-7 through 2-11.

- Jade S., and Sarkar, S, 1993, Statistical models for slope instability classification, Engineering Geology, v. 36, p. 91-98.

- Jan Nyssen, Jean poesen, Jan Moeyersons, Jozef Deckers, Mitiku Haile, Andreas Lang, 2003. Human impact on environment in the Ethiopian and Eritrean highlands-a state of the art. Earth-Science Reviews xx (2003) xxx-xxx.

- Lakew Desta, Menale Kassie, Benin S. and Pender J. 2000. Land degradation and strategies for sustainable development in the Ethiopian highlands: Amhara Region. Socio-economics and Policy Research Working Paper 32. ILRI (International Livestock Research Institute), Nairobi, Kenya. 122 pp.

- Leonard Berry, 2003. Land degradation in Ethiopia: Its extent and impact. Wiley InterScience. www.interscience.wilwy.com.

- Lillisand, Thomas M. and Ralph W.; Remote sensing and image interpretation, 4th ed. John wiley & sons 2000.

- Lulseged Ayalew, 1999. The effect of seasonal rainfall on landslides in the highlands of Ethiopia. Bull Eng Geology Env (1999) 58: 9-19.

- Lulseged Ayalew, (?). Cause and mechanisms of slope instablity in Dessie town, Ethiopia. Department of Engineering Geology, Technical University of Clausthal, Department of Engineering Geology, Clausthal-Zellerfeld, Germany.

- Lulseged Ayalew, (?). Factors affecting slope stability in the Blue Nile Basin. Research assistant, Technical University of Clausthal, Department of Engineering Geology, Clausthal-Zellerfeld, Germany.

- Massimo Dragan, Enrico Feoli, Michael Fernetti, Woldu Zerihun, 2003. Application of a spatial decision support system (SDSS) to reduce soil erosion in northern Ethiopia. Environmental modeling & Software 18 (2003) 861-868.

- P. L. ROSIN and J. HERVA´S, 2005. Remote sensing image thresholding methods for determining landslide activity. International Journal of Remote Sensing, Vol. 26, No. 6, 20 March 2005, 1075–1092.

- Peter V. Gorsevski, Paul Gessler and Randy B. Foltz, 2000. Spatial Prediction of Landslide Hazard Using Discriminant Analysis and GIS. GIS in the Rockies 2000 Conference and Workshop Applications for the 21st Century. Denver, Colorado. September 25 - 27, 2000.

- Schuster R. L, 1994, Socioeconomic significance of landslide. In: Turner A.K., and Schuster R. L, (Editors), Landslide, investigation and mitigation, Transport research Board Manual

- Saaty T.L., 1977. "A Scaling Method for Priorities in Hierarchical Structures", J. Math. Psychology, 15, 234-281.

- Solomon Abate. 1994. Land use dynamics, soil conservation and potential for use in Metu area, Illubabor Region, Ethiopia. African Studies Series A13. Berne: Geographica Bernensia.

- Sonneveled, B. G. J. S. & M, A. Keyzer, 2002. Land Under Pressure; Soil Conservations and Opportunities for Ethiopia in Land Degradation & Development. Wiley InterScience. www.interscience.wilwy.com.

- S. R. Templeton and S. J. Scherr, S. J. 1999. Effects of demographic and related microeconomic change on land quality in hils and mountains of developing countries. World Development, 27(6), 903-918.

- Tenalem Ayalew and Giulio Barbieri, 2004. Inventory of landslides and susceptibility mapping in the Dessie area, northern Ethiopia. SCIENCE@DIRECT, Engineering Geology 77 (2005) 1-15.

- Tesfaye Korme, 1999. Lithological And Structural Mapping Of The Northeast Lake Ziway Area, Ethiopian Rift, With The Help Of Landsat Tm Data. SENET: Ethiopia. J. Sci., 22(2) 151-174, 1999.

- Thomas M. Lillesand Ralph W. Kiefer, 2000. Remote Sensing and Image Interpretation, Fourth edition, John Wiley & Sons, Inc.

- Tor Bernhardsen, 1999. Geographic Information Systems: An introduction. Second Edition, John Wiley & Sons, Inc.

- Van Westen CJ, Rengers N, Terlien MTJ, Soeters R (1997). Prediction of the occurrence of slope instability phenomena through GIS-based hazard zonation. Geol Rundsch, 86, 404-414

- Van Westen, C.J. (1994) GIS in landslide hazard zonation : a review, with examples from the Andes of Colombia. In: Mountain environments & geographic information systems / ed. by M.F. Price and D.I. Heywood, 1994, pp. 135-166.

- VARNES D. J., 1984, Landslide Hazard Zonation: a Review of Principles and Practice (Paris: UNESCO), pp. 1-63.

- Wang, S.-Q., and Unwin, D.J. 1992. "Modelling landslide distribution on loess soils in China: an investigation", International Journal of Geographical Information Systems, 6, 391-405.

- W. Kenneth Hamblin, 1992. Earth Dynamic Systems. Sixth edition.

- Woody Biomass, 2001. A Strategic Plan For The Sustainable Development, Conservation, And Management of the Woody Biomass Resources, Final Draft Report.

- WoldeGabriel, G., and Aronsen, J. L., 1987. The Chow bahir Rift: A "failed" rift in southern Ethiopia: Geology, v. 15, p. 430-433.

- Zenettin, B., Nicoletti, M., and Petrucciani, C., 1978. The evolution of Chencha Escarpment and the Ganjuli Graben (Lake Abaya) in the southern Ethiopia Rift: Neues Jahrbuch fur Geologie und palaontologie. v. 8, p. 473-490.

Annex 1: Population size by sex, area, and density by region: July 2002

Region	male	female	total	Area in sq. km	density
Tigray Region	1,919,999	1,981,005	3,901,004	50,078.64	77.9
Afar Region	710,997	561,003	1,272,000	-	-
Amara Region	8,605,996	8,599,003	17,204,999	159,173.66	108.1
Oromia Region	11,829,993	11,873,997	23,703,990	353,006.81	67.1
Somalia Region	2,103,998	1,793,999	3,897,997	-	-
Benishangul-Gumuz Region	285,000	280,000	565,000	49,289.46	11.5
Southern Nations, Nationality & peoples' Region	6,606,005	6,687,005	13,293,010	112,343.19	118.3
Gambela Region	113,000	108,998	221,998	25,802.01	8.6
Harari Region	87,000	85,000	172,000	311.25	552.6
Addis Ababa	1,273,001	1,372,999	2,646,000	530.14	4,991.1
Dire Dawa prov/Adm.	172000	170000	342000	1,213.20	281.9

Table.1 Population size by sex, area, and density by region

Note: Areas of regions are calculated from maps drawn to assist in census work and are not from the Ethiopian Mapping Authority.

Annex 2: Soil data

Sample No	Location	Depth of sampling	Liquid limit (%)	Plastic limit (%)	Plastic index (%)	Shrinkage Limit (%)	Classification based on USCS	Grain size (%)
1	Cheleleki	20cm	32.2	15.7	16.5	12.1	CL	Sand: 36.40 Silt: 34.37 Clay: 29.23
2	Cheleleki	1m	48.7	27.3	21.4	21.9	CL	Sand: 26.50 Silt: 37.85 Clay: 35.65
3	Cheleleki	1.5m	45.4	19.0	26.3	15.8	CL	Sand: 23.20 Silt: 34.72 Clay: 42.08
4	Cheleleki	2.5m	78.0	8.9	69.1	9.84	CH	Sand: 23.20 Silt: 34.72 Clay: 42.08
5	Tejo	50cm	43.3	24.6	18.7	18.70	CL	Sand: 13.60 Silt: 34.68 Clay: 51.72
6	Gurmu Wayide	40cm	74.4	54	20.3	32.44	MH	Sand: 10.10 Silt: 52.00 Clay: 37.90
7	Gurmu Wayide	50cm	59.6	43.2	16.4	32.58	MH	Sand: 11.10 Silt: 49.39 Clay: 39.51
8	Adilo	30cm	68.7	26.3	42.4	9.84	CH	Sand: 13.10 Silt: 15.27 Clay:

								71.63
9	Adilo	35cm	-	-	-			Sand: 8.50 Silt: 68.05 Clay: 23.45

Annex-3

The Unified Soil Classification System

Major divisions			Group symbol	Typical names	Classification criteria for coarse-grained soils	
Coarse-grained soils (more than half of material is larger than No. 200)	Gravels (more than half of coarse fraction is larger than No. 4 sieve size)	Clean gravels (little or no fines)	GW	Well-graded gravels, gravel-sand mixtures, little or no fines	$C_U = D_{60}/D_{10} > 4$ $C_C = 1 < D^2_{30}/D_{10} \times D_{60} < 3$	
			GP	Poorly graded gravels, gravel-sand mixtures, little or no fines	Not meeting all gradation requirements for GW	
		Gravels with fines (appreciable amount of fines)	GM $\frac{d}{u}$	Silty gravels, gravel-sand-silt mixtures	Atterberg limits below A line or $I_p < 4$	Above A line with $4 < I_p < 7$ are borderline cases requiring use of dual symbols
			GC	Clayey gravels, gravel-sand-clay mixtures	Atterberg limits above A line with $I_p > 7$	
	Sands (more than half of course fraction is smaller than No. 4 sieve size)	Clean sands (little or no fines)	SW	Well-graded sands, gravelly sands, little or no fines	$C_U = D_{60}/D_{10} > 6$ $C_C = 1 < D^2_{30}/D_{10} \times D_{60} < 3$	
			SP	Poorly graded sands, gravelly sands, little or no fines	Not meeting all gradation requirements for SW	
		Sands with fines (appreciable amount of fines)	SM $\frac{d}{u}$	Silty sands, sand-silt mixtures	Atterberg limits below A line or $I_p < 4$	Limits plotting in hatched zone with $4 \leq I_p \leq 7$ are borderline cases requiring use of dual symbols
			SC	Clayey sands, sand-clay mixtures	Atterberg limits above A line with $I_p > 7$	
Fine-grained soils (more than half of material is smaller than No. 200)	Silts and clays (liquid limit < 50)		ML	Inorganic silts and very fine sands, rock flour, silty or clayey fine sands, or clayey silts with slight plasticity	1. Determine percentages of sand and gravel from grain-size curve. 2. Depending on percentages of fines (fraction smaller than 200 sieve size), coarse-grained soils are classified as follows: Less than 5%—GW, GP, SW, SP. More than 12%—GM, GC, SM, SC 5 to 12%—Borderline cases requiring dual symbols	
			CL	Inorganic clays of low to medium plasticity, gravelly clays, sandy clays, silty clays, lean clays		
			OL	Organic silts and organic silty clays of low plasticity	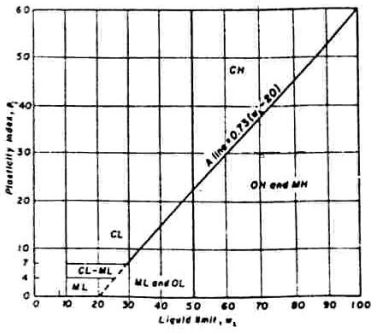	
	Silts and clays (liquid limit > 50)		MH	Inorganic silts, micaceous or diatomaceous fine sandy or silty soils, elastic silts		
			CH	Inorganic clays of high plasticity, fat clays		
			OH	Organic clays of medium to high plasticity, organic silts		
	Highly organic soils		Pt	Peat and other highly organic soils		

Annex 4

Profile data used fro cut and fill

Sample Site 1

ID	EAST	NORTH	ALTITUDE
1	381033	779119	1862
2	381035	779125	1865
3	381044	779141	1852
4	381051	779160	1851
5	381063	779182	1849
6	381075	779193	1843
7	381088	779206	1842
8	381100	779222	1850
9	381118	779238	1849
10	381144	779260	1844
11	381128	779270	1845
12	381118	779257	1847
13	381104	779246	1849
14	381092	779234	1850
15	381079	779225	1852
16	381072	779218	1857
17	381068	779212	1857
18	381054	779197	1855
19	381046	779182	1854
20	381033	779162	1854
21	381026	779148	1855
22	381023	779137	1855
23	381015	779125	1856
24	381013	779119	1860
25	380997	779113	1860
26	380996	779122	1856
27	381003	779134	1859
28	381013	779152	1855
29	381023	779170	1857
30	381034	779183	1856
31	381040	779188	1857
32	381039	779188	1860
33	381042	779193	1855
34	381048	779206	1856
35	381051	779208	1861
36	381053	779216	1860
37	381058	779224	1855
38	381073	779235	1854
39	381089	779247	1856
40	381099	779259	1846
41	381093	779267	1846
42	381105	779277	1845
43	381107	779268	1844
44	381120	779267	1843

45	381129	779298	1844
46	381140	779318	1843
47	381118	779305	1846
48	381104	779292	1849
49	381088	779279	1849
50	381076	779265	1851
51	381064	779254	1851
52	381053	779241	1854
53	381038	779226	1856
54	381028	779212	1854
55	381019	779196	1856
56	381013	779186	1860
57	381007	779170	1865
58	381001	779164	1870
59	381004	779158	1864
60	380994	779139	1862
61	380985	779128	1864
62	380977	779114	1865
63	380973	779092	1867
64	380968	779074	1870
65	380960	779070	1871
66	380944	779061	1872
67	380937	779053	1868
68	380942	779080	1864
69	380951	779096	1863
70	380956	779112	1867
71	380965	779128	1864
72	380970	779134	1864
73	380974	779136	1865
74	380973	779142	1863
75	380981	779149	1866
76	380980	779164	1861
77	380987	779181	1860
78	380989	779200	1870
79	380985	779205	1870
80	380996	779207	1862
81	381004	779213	1864
82	380995	779207	1864
83	381009	779207	1864
84	381014	779229	1856
85	381026	779246	1854
86	381032	779263	1852
87	381039	779277	1850
88	381042	779297	1856
89	381044	779325	1852
90	381023	779317	1849
91	381021	779364	1849
92	381016	779286	1853
93	380999	779291	1852
94	380989	779296	1853

95	380993	779287	1853
96	381006	779277	1853
97	381016	779268	1858
98	381005	779256	1853
99	380998	779250	1857
100	380994	779236	1851
101	380988	779220	1855
102	380974	779224	1852
103	380974	779237	1856
104	380968	779212	1857
105	380965	779200	1854
106	380962	779196	1861
107	380959	779188	1859
108	380947	779170	1855
109	380941	779150	1854
110	380953	779129	1860
111	380934	779134	1863
112	380936	779124	1867
113	380916	779113	1875
114	380928	779103	1871
115	380921	779085	1865
116	380922	779073	1862
117	380918	779054	1862
118	380918	779045	1858
119	380902	779037	1865
120	380904	779020	1876
121	380889	779021	1871
122	380877	779019	1871
123	380870	779020	1874
124	380864	779027	1871
125	380874	779046	1871
126	380853	779037	1870
127	380849	779048	1868
128	380865	779073	1867
129	380891	779016	1869
130	380887	779090	1863
131	380873	779096	1864
132	380872	779102	1864
133	380877	779101	1865
134	380893	779126	1860
135	380873	779132	1865
136	380882	779133	1864
137	380889	779138	1866
138	380891	779145	1864
139	380900	779156	1862
140	380907	779175	1867
141	380909	779185	1860
142	380911	779195	1861
143	380917	779207	1857
144	380922	779222	1859

145	380925	779231	1860
146	380931	779246	1855
147	380944	779266	1854
148	380954	779279	1853
149	380932	779281	1855
150	380924	779275	1850
151	380906	779284	1856
152	380905	779263	1856
153	380896	779257	1858
154	380968	779244	1857
155	380919	779243	1858
156	380904	779225	1857
157	380876	779232	1859
158	380886	779232	1861
159	380877	779212	1859
160	380889	779193	1856
161	380890	779175	1855
162	380820	779168	1858
163	380863	779170	1866
164	380857	779180	1864
165	380877	779154	1866
166	380871	779149	1863
167	380876	779142	1860
168	380855	779141	1866
169	380837	779120	1861
170	380850	779109	1861
171	380849	779092	1862
172	380824	779096	1866
173	380828	779084	1868
174	380835	779092	1865
175	380804	779080	1854
176	380805	779071	1863
177	380820	779059	1864
178	380834	779067	1858
179	380847	779062	1861
180	380854	779082	1860
181	381006	779139	1858
182	380981	779147	1856
183	380975	779165	1853
184	380960	779195	1856
185	380927	779222	1855
186	380902	779233	1851
187	380914	779260	1851
188	380935	779239	1858
189	380931	779161	1859
190	380958	779136	1854
191	380967	779131	1858
192	380972	779124	1860
193	380990	779112	1862
194	381020	779116	1869

195	380984	779094	1869
196	380919	779040	1872
197	380837	779028	1879
198	380801	779090	1878
199	380833	779181	1875
200	380868	779246	1872
201	380926	779296	1862
202	381013	779272	1864
203	381117	779257	1858
204	381131	779189	1860
205	381063	779140	1870

Sample Site 2

ID	EASTING	NORTHING	ALTITUDE
1	382543	788440	1930
2	382521	788426	1933
3	382501	788404	1937
4	382488	788378	1937
5	382493	788356	1938
6	382500	788339	1936
7	382491	788310	1938
8	382499	788294	1937
9	382485	788264	1938
10	382471	788246	1938
11	382466	788228	1937
12	382444	788197	1938
13	382422	788174	1938
14	382404	788161	1938
15	382401	788147	1937
16	382412	788118	1938
17	382442	788095	1934
18	382477	788079	1935
19	382494	788070	1935
20	382554	788022	1930
21	382567	788043	1929
22	382593	788078	1932
23	382601	788091	1933
24	382599	788119	1932
25	382590	788155	1932
26	382587	788181	1934
27	382584	788211	1931
28	382595	788247	1933
29	382611	788269	1935
30	382617	788298	1936
31	382625	788330	1937
32	382650	788343	1937
33	382651	788366	1936
34	382630	788382	1933
35	382621	788390	1930
36	382614	788393	1931

37	382599	788403	1928
38	382597	788412	1929
39	382587	788413	1933
40	382575	788419	1932
41	382555	788429	1934
42	382548	788429	1935
43	382543	788435	1939
44	382535	788421	1938
45	382538	788420	1936
46	382549	788410	1937
47	382566	788399	1934
48	382588	788390	1929
49	382604	788382	1931
50	382610	788373	1932
51	382627	788365	1933
52	382624	788347	1935
53	382614	788352	1931
54	382604	788358	1933
55	382592	788365	1928
56	382587	788372	1929
57	382581	788378	1933
58	382576	788392	1932
59	382561	788389	1934
60	382537	788396	1935
61	382525	788407	1935
62	382518	788414	1938
63	382510	788402	1939
64	382518	788394	1935
65	382535	788378	1932
66	382540	788364	1934
67	382562	788353	1935
68	382574	788347	1933
69	382581	788340	1931
70	382585	788330	1933
71	382595	788321	1928
72	382602	788301	1932
73	382614	788295	1934
74	382609	788284	1935
75	382597	788288	1931
76	382584	788298	1928
77	382570	788303	1928
78	382560	788323	1931
79	382543	788335	1932
80	382529	788351	1935
81	382509	788359	1936
82	382497	788359	1938
83	382501	788345	1937
84	382513	788345	1934
85	382517	788341	1935
86	382525	788331	1933

87	382543	788314	1930
88	382555	788296	1933
89	382569	788281	1930
90	382582	788274	1928
91	382593	788270	1930
92	382598	788266	1933
93	382598	788249	1933
94	382585	788250	1931
95	382576	788257	1930
96	382576	788262	1927
97	382558	788270	1927
98	382546	788285	1931
99	382534	788296	1933
100	382523	788302	1930
101	382507	788308	1934
102	382505	788295	1937
103	382514	788285	1930
104	382529	788277	1931
105	382542	788264	1930
106	382564	788253	1928
107	382572	788243	1930
108	382561	788230	1930
109	382552	788236	1927
110	382543	788245	1930
111	382534	788252	1928
112	382520	788262	1930
113	382510	788264	1931
114	382505	788269	1935
115	382492	788262	1937
116	382500	788253	1932
117	382511	788244	1930
118	382529	788237	1929
119	382541	788229	1930
120	382545	788226	1927
121	382556	788218	1926
122	382562	788215	1930
123	382556	788206	1932
124	382549	788212	1929
125	382532	788220	1927
126	382528	788225	1930
127	382512	788236	1930
128	382500	788247	1933
129	382489	788260	1937
130	382475	788246	1936
131	382490	788240	1933
132	382492	788236	1934
133	382507	788226	1932
134	382520	788216	1933
135	382533	788210	1929
136	382541	788204	1926

137	382546	788199	1930
138	382545	788189	1931
139	382538	788192	1926
140	382526	788197	1926
141	382510	788202	1932
142	382494	788212	1933
143	382483	788217	1935
144	382469	788228	1938
145	382458	788217	1939
146	382468	788208	1936
147	382481	788199	1934
148	382508	788184	1932
149	382519	788178	1932
150	382526	788178	1929
151	382540	788184	1927
152	382545	788179	1931
153	382552	788168	1932
154	382539	788164	1929
155	382536	788164	1928
156	382528	788173	1929
157	382519	788170	1934
158	382482	788185	1935
159	382462	788198	1934
160	382454	788204	1939
161	382448	788191	1939
162	382461	788180	1937
163	382483	788169	1937
164	382505	788159	1933
165	382527	788150	1932
166	382535	788150	1925
167	382540	788145	1927
168	382553	788140	1931
169	382566	788139	1935
170	382580	788132	1934
171	382573	788121	1933
172	382564	788122	1931
173	382552	788122	1930
174	382540	788131	1927
175	382529	788129	1930
176	382512	788139	1932
177	382497	788142	1933
178	382475	788151	1935
179	382451	788166	1937
180	382435	788177	1939
181	382425	788174	1939
182	382438	788159	1937
183	382457	788145	1936
184	382484	788128	1935
185	382498	788118	1932
186	382503	788116	1932

187	382536	788103	1930
188	382540	788102	1927
189	382543	788099	1927
190	382578	788096	1933
191	382583	788102	1933
192	382597	788090	1935
193	382567	788085	1932
194	382541	788085	1929
195	382537	788084	1927
196	382529	788088	1930
197	382511	788095	1931
198	382479	788104	1934
199	382465	788109	1933
200	382567	788085	1932
201	382541	788085	1929
202	382537	788084	1927
203	382529	788088	1930
204	382511	788095	1931
205	382497	788093	1934
206	382479	788104	1934
207	382465	788109	1933
208	382448	788113	1935
209	382437	788130	1936
210	382423	788139	1938
211	382416	788148	1939
212	382426	788130	1936
213	382445	788154	1936
214	382472	788190	1936
215	382504	788228	1937
216	382523	788248	1933
217	382537	788273	1934
218	382541	788284	1936
219	382551	788297	1934
220	382559	788304	1936
221	382574	788309	1934
222	382585	788319	1932
223	382590	788329	1934
224	382599	788341	1937
225	382612	788361	1936
226	382621	788386	1935
227	382628	788380	1936
228	382614	788350	1936
229	382604	788329	1934
230	382592	788310	1938
231	382572	788282	1935
232	382552	788256	1935
233	382544	788245	1936
234	382539	788233	1936
235	382538	788225	1931
236	382529	788199	1932

237	382525	788176	1933
238	382526	788163	1935
239	382524	788144	1932
240	382512	788125	1930
241	382508	788109	1931
242	382503	788095	1934
243	382496	788092	1935

Sample site 3

ID	EASTING	NORTHING	ALTITUDE
1	386576	796510	1937
2	386597	796516	1937
3	386628	796528	1936
4	386651	796536	1935
5	386674	796546	1936
6	386692	796554	1936
7	386716	796562	1937
8	386736	796570	1939
9	386745	796574	1939
10	386746	796582	1938
11	386733	796580	1930
12	386722	796578	1931
13	386710	796576	1929
14	386700	796576	1926
15	386693	796574	1926
16	386684	796571	1927
17	386679	796568	1929
18	386669	796567	1926
19	386653	796566	1925
20	386652	796562	1927
21	386644	796560	1923
22	386631	796565	1922
23	386633	796557	1917
24	386618	796550	1917
25	386606	796567	1918
26	386611	796589	1918
27	386603	796606	1920
28	386608	796620	1919
29	386594	796634	1917
30	386600	796656	1916
31	386613	796664	1915
32	386587	796683	1920
33	386558	796702	1920
34	386543	796713	1918
35	386531	796716	1920
36	386509	796725	1921
37	386492	796746	1919
38	386489	796756	1920
39	386488	796767	1919

46	386498	796750	1929
47	386502	796761	1940
48	386505	796762	1940
49	386514	796764	1940
50	386530	796762	1940
51	386545	796766	1944
52	386551	796762	1944
53	386544	796758	1941
54	386540	796751	1940
55	386538	796750	1946
56	386534	796753	1939
57	386530	796749	1935
58	386523	796748	1935
59	386504	796742	1932
60	386515	796729	1930
61	386516	796732	1932
62	386520	796741	1933
63	386529	796742	1930
64	386524	796725	1930
65	386529	796722	1930
66	386533	796720	1929
67	386533	796723	1933
68	386527	796727	1933
69	386523	796725	1933
70	386531	796734	1932
71	386537	796730	1933
72	386540	796735	1934
73	386546	796744	1940
74	386549	796739	1940
75	386550	796760	1942
76	386554	796748	1941
77	386568	796761	1945
78	386566	796753	1942
79	386564	796750	1941
80	386580	796754	1943
81	386586	796748	1945
82	386593	796745	1945
83	386606	796755	1947
84	386594	796755	1949
85	386616	796752	1947
86	386626	796742	1942
87	386621	796735	1939
88	386610	796736	1937
89	386613	796726	1935
90	386609	796724	1938
91	386592	796726	1933
92	386592	796732	1937
93	386588	796736	1936
94	386583	796739	1936
95	386579	796743	1935

96	386575	796732	1931
97	386564	796735	1933
98	386558	796729	1931
99	386545	796725	1934
100	386543	796719	1931
101	386543	796717	1928
102	386554	796711	1932
103	386559	796713	1928
104	386555	796711	1925
105	386560	796707	1929
106	386567	796701	1927
107	386574	796713	1928
108	386569	796720	1933
109	386566	796720	1936
110	386574	796697	1928
111	386581	796708	1936
112	386589	796712	1928
113	386595	796717	1936
114	386599	796719	1930
115	386602	796714	1936
116	386621	796711	1935
117	386628	796706	1935
118	386622	796700	1935
119	386618	796703	1932
120	386616	796704	1935
121	386612	796698	1930
122	386614	796686	1928
123	386607	796683	1926
124	386591	796684	1927
125	386609	796676	1924
126	386614	796686	1928
127	386622	796690	1929
128	386628	796695	1930
129	386633	796697	1933
130	386641	796702	1934
131	386641	796700	1937
132	386639	796696	1935
133	386637	796692	1935
134	386630	796689	1939
135	386624	796684	1934
136	386623	796678	1929
137	386618	796674	1929
138	386621	796661	1924
139	386614	796652	1927
140	386604	796653	1929
141	386600	796644	1929
142	386600	796639	1931
143	386605	796636	1932
144	386616	796634	1931
145	386621	796642	1930

146	386628	796646	1931
147	386631	796648	1925
148	386634	796650	1929
149	386643	796660	1931
150	386652	796663	1935
151	386646	796667	1939
152	386649	796669	1933
153	386647	796682	1934
154	386650	796676	1938
155	386651	796682	1938
156	386653	796682	1937
157	386649	796686	1936
158	386649	796692	1939
159	386645	796697	1940
160	386655	796707	1944
161	386640	796716	1943
162	386630	796707	1938
163	386627	796717	1941
164	386673	796696	1943
165	386667	796685	1945
166	386666	796675	1940
167	386664	796666	1939
168	386662	796664	1936
169	386657	796663	1938
170	386668	796676	1937
171	386671	796683	1940
172	386673	796689	1940
173	386677	796696	1942
174	386672	796684	1945
175	386675	796682	1942
176	386675	796673	1941
177	386675	796669	1939
178	386669	796660	1938
179	386667	796654	1936
180	386675	796657	1938
181	386689	796658	1944
182	386695	796652	1943
183	386708	796649	1944
184	386726	796651	1944
185	386661	796659	1933
186	386666	796664	1931
187	386661	796654	1930
188	386656	796652	1933
189	386650	796653	1930
190	386611	796628	1928
191	386609	796616	1929
192	386614	796615	1929
193	386620	796622	1930
194	386630	796636	1930
195	386636	796644	1930

196	386646	796646	1931
197	386653	796640	1931
198	386660	796632	1931
199	386661	796647	1935
200	386666	796645	1937
201	386667	796643	1933
202	386658	796635	1935
203	386659	796636	1932
204	386648	796640	1934
205	386640	796629	1930
206	386625	796612	1928
207	386632	796605	1929
208	386637	796597	1929
209	386641	796610	1933
210	386640	796614	1930
211	386647	796606	1931
212	386647	796603	1934
213	386646	796607	1932
214	386650	796608	1934
215	386657	796614	1933
216	386659	796619	1934
217	386665	796622	1932
218	386674	796615	1934
219	386668	796616	1936
220	386680	796613	1936
221	386683	796622	1940
222	386685	796631	1941
223	386692	796638	1940
224	386704	796642	1940
225	386712	796640	1938
226	386724	796639	1941
227	386723	796629	1940
228	386723	796619	1941
229	386712	796617	1938
230	386712	796628	1939
231	386698	796622	1938
232	386695	796609	1936
233	386684	796603	1936
234	386672	796598	1933
235	386660	796595	1930
236	386647	796588	1929
237	386613	796598	1924
238	386609	796604	1924
239	386617	796607	1926
240	386619	796604	1927
241	386624	796605	1928
242	386628	796600	1924
243	386634	796594	1926
244	386630	796594	1928
245	386635	796587	1925

246	386648	796581	1927
247	386648	796560	1933
248	386640	796572	1933
249	386629	796588	1934
250	386626	796584	1933
251	386621	796577	1935
252	386627	796571	1932
253	386618	796572	1929
254	386615	796579	1928
255	386611	796563	1927
256	386618	796561	1926
257	386625	796566	1925
258	386552	796541	1940
259	386538	796560	1939
260	386533	796583	1942
261	386515	796582	1942
262	386503	796581	1945
263	386507	796570	1943
264	386499	796574	1941
265	386482	796554	1943
266	386489	796567	1946
267	386476	796566	1949
268	386546	796591	1933
269	386461	796589	1948
270	386457	796608	1948
271	386445	796621	1949
272	386442	796634	1950
273	386447	796639	1949
274	386431	796635	1950
275	386420	796641	1949
276	386419	796652	1951
277	386425	796660	1946
278	386435	796664	1946
279	386441	796654	1946
280	386441	796645	1946
281	386432	796642	1946
282	386439	796674	1944
283	386453	796674	1942
284	386461	796664	1943
285	386450	796656	1945
286	386468	796650	1944
287	386453	796643	1945
288	386453	796643	1945
289	386455	796625	1944
290	386462	796629	1944
291	386468	796640	1943
292	386479	796645	1942
293	386475	796631	1944
294	386486	796638	1943
295	386496	796628	1944

296	386484	796628	1944
297	386489	796612	1945
298	386476	796610	1948
299	386466	796618	1949
300	386465	796633	1947
301	386477	796599	1947
302	386479	796593	1947
303	386497	796598	1944
304	386487	796591	1945
305	386478	796587	1944
306	386475	796578	1944
307	386485	796584	1943
308	386500	796592	1944
309	386503	796589	1944
310	386510	796594	1942
311	386520	796598	1941
312	386527	796600	1940
313	386533	796598	1943
314	386521	796686	1940
315	386510	796627	1940
316	386505	796636	1941
317	386502	796640	1940
318	386502	796647	1942
319	386493	796657	1943
320	386484	796667	1943
321	386473	796679	1943
322	386465	796689	1942
323	386475	796700	1941
324	386485	796686	1943
325	386496	796666	1942
326	386505	796656	1943
327	386512	796646	1946
328	386514	796642	1939
329	386514	796640	1938
330	386519	796636	1939
331	386523	796632	1939
332	386529	796623	1938
333	386536	796616	1936
334	386542	796610	1937
335	386550	796622	1937
336	386539	796631	1937
337	386535	796633	1940
338	386536	796635	1939
339	386538	796640	1937
340	386529	796651	1939
341	386524	796652	1943
342	386526	796665	1946
343	386509	796679	1944
344	386499	796690	1943
345	386482	796709	1942

346	386494	796708	1944
347	386501	796702	1945
348	386507	796695	1946
349	386508	796689	1944
350	386518	796689	1948
351	386522	796696	1945
352	386519	796676	1946
353	386530	796680	1944
354	386545	796684	1943
355	386544	796676	1941
356	386540	796670	1938
357	386536	796663	1940
358	386535	796660	1942
359	386538	796655	1942
360	386545	796650	1939
361	386500	796711	1943
362	386501	796719	1942
363	386508	796715	1942
364	386512	796716	1941
365	386519	796710	1942
365	386509	796704	1947
366	386509	796704	1944
367	386514	796700	1944
368	386526	796707	1939
369	386526	796702	1936
370	386539	796706	1936
371	386551	796701	1935
372	386556	796691	1940
373	386550	796682	1940
374	386556	796693	1935
375	386553	796686	1937
376	386562	796684	1937
377	386564	796688	1934
378	386572	796681	1934
379	386587	796674	1936
380	386584	796671	1933
381	386604	796661	1933
382	386592	796650	1932
383	386587	796638	1932
384	386576	796648	1932
385	386570	796652	1932
386	386571	796664	1933
387	386558	796664	1935
388	386554	796663	1940
389	386548	796662	1937
390	386547	796659	1939
391	386552	796667	1934
392	386551	796666	1941
393	386561	796674	1941
394	386552	796674	1936

395	386547	796660	1937
396	386542	796654	1939
397	386542	796650	1937
398	386540	796650	1939
399	386542	796651	1938
400	386546	796649	1938
401	386557	796653	1938
402	386565	796660	1941
403	386545	796645	1933
404	386554	796649	1933
405	386558	796642	1932
406	386571	796634	1931
407	386563	796630	1936
408	386556	796627	1937
409	386549	796624	1937
410	386547	796633	1937
411	386543	796641	1937
412	386580	796638	1925
413	386586	796631	1936
414	386589	796623	1935
415	386584	796625	1930
416	386573	796611	1929
417	386565	796613	1934
418	386557	796617	1935
419	386551	796607	1937
420	386547	796597	1939
421	386547	796585	1940
422	386555	796590	1939
423	386561	796583	1942
424	386566	796593	1941
425	386566	796581	1940
426	386574	796590	1937
427	386574	796586	1935
428	386578	796579	1934
429	386578	796573	1935
430	386574	796568	1938
431	386569	796575	1939
432	386565	796603	1937
433	386568	796605	1939
434	386569	796609	1940
435	386564	796597	1936
436	386568	796600	1931
437	386569	796594	1931
438	386574	796598	1933
439	386584	796603	1932
440	386594	796601	1930
441	386587	796586	1931
442	386579	796587	1932
443	386585	796578	1933
444	386581	796571	1931

445	386585	796564	1933
446	386593	796564	1934
447	386595	796572	1931
448	386596	796579	1933
449	386598	796584	1932
450	386600	796587	1932
451	386599	796593	1929
452	386595	796594	1932
453	386583	796569	1932
454	386592	796554	1935
455	386607	796546	1937
456	386618	796540	1938
457	386628	796540	1936
458	386635	796540	1934
459	386606	796534	1936
460	386593	796534	1935
461	386587	796532	1934
462	386582	796534	1937
463	386575	796536	1938
464	386579	796548	1934
465	386583	796556	1932
466	386576	796559	1933
467	386569	796554	1935
468	386567	796553	1933
469	386560	796553	1937
470	386559	796556	1938
471	386554	796545	1938
472	386561	796535	1941
473	386567	796525	1941
474	386751	796602	1938
475	386732	796599	1936
476	386719	796597	1936
477	386707	796597	1933
478	386701	796594	1933
479	386694	796593	1932
480	386682	796590	1933
481	386676	796586	1932
482	386669	796587	1930
483	386660	796585	1931
484	386647	796583	1929

Sample site 4

ID	EASTING	NORTHING	ALTITUDE
1	389038	797677	1921
2	389023	797680	1919
3	389018	797676	1919
4	389017	797667	1918
5	389009	797673	1916
6	388986	797687	1916

7	388992	797702	1914
8	389003	797715	1913
9	389013	797703	1914
10	389006	797692	1915
11	389017	797681	1916
12	389026	797687	1915
13	389036	797685	1916
14	389041	797672	1919
15	389047	797659	1921
16	389049	797648	1920
17	389055	797641	1922
18	389061	797648	1923
19	389072	797657	1924
20	389086	797666	1922
21	389093	797691	1921
22	389115	797704	1921
23	389126	797720	1920
24	389130	797737	1917
25	389131	797750	1918
26	389125	797744	1916
27	389117	797729	1912
28	389117	797754	1909
29	389112	797753	1912
30	389107	797745	1913
31	389112	797736	1911
32	389103	797738	1909
33	389100	797748	1908
38	389102	797758	1907
39	389095	797747	1913
40	389094	797757	1913
41	389095	797737	1914
42	389096	797728	1915
43	389103	797724	1916
44	389112	797725	1918
45	389113	797716	1917
46	389106	797706	1915
47	389098	797701	1915
48	389092	797714	1915
49	389088	797719	1916
50	389086	797728	1916
51	389090	797731	1914
52	389091	797735	1912
53	389087	797739	1909
54	389086	797732	1909
55	389084	797726	1907
56	389081	797721	1911
57	389082	797739	1912
58	389079	797713	1915
59	389074	797715	1915
60	389066	797719	1915

61	389072	797707	1915
62	389089	797697	1916
63	389085	797686	1915
64	389075	797695	1914
65	389064	797706	1914
66	389054	797715	1913
67	389044	797725	1913
68	389039	797732	1912
69	389035	797739	1906
70	389031	797739	1904
71	389026	797728	1903
72	389020	797718	1904
73	389016	797713	1905
74	389014	797709	1909
75	389009	797711	1913
76	389014	797717	1914
77	389020	797728	1914
78	389011	797727	1911
79	388999	797724	1912
34	388986	797725	1913
35	388994	797717	1911
80	388989	797715	1909
81	388982	797709	1915
82	388989	797708	1913
83	388986	797703	1912
84	389021	797697	1916
85	389034	797702	1915
86	389043	797696	1915
87	389052	797690	1915
88	389067	797692	1918
89	389070	797685	1917
90	389078	797676	1916
91	389072	797670	1915
92	389069	797664	1915
93	389054	797659	1916
94	389056	797646	1917
95	389050	797671	1916
96	389058	797673	1917
97	389058	797726	1915
98	389048	797736	1915
99	389059	797742	1914
100	389065	797756	1915
101	389068	797744	1910
102	389071	797753	1910
103	389065	797751	1912
104	389068	797754	1913
105	389065	797768	1913
106	389061	797775	1912
107	389054	797776	1911
108	389045	797776	1911

109	389035	797780	1910
110	389032	797776	1909
111	389030	797768	1910
112	389040	797767	1911
113	389052	797763	1912
114	389051	797754	1911
115	389041	797756	1909
116	389035	797756	1908
117	389031	797752	1907
118	389036	797746	1908
119	389035	797748	1906
120	389031	797749	1909
121	389027	797745	1907
122	389035	797740	1907
123	389023	797738	1910
127	389025	797741	1910
128	389044	797745	1911
129	389065	797727	1910
130	389071	797727	1910
131	389074	797724	1908
132	389075	797733	1909
133	389075	797739	1908
134	389072	797738	1911
135	389081	797740	1910
136	389081	797745	1913
137	389077	797746	1912
138	389072	797745	1908
139	389082	797754	1911
140	389079	797764	1912
141	389081	797768	1914
142	389079	797773	1914
143	389069	797773	1909
144	389071	797762	1909
145	389067	797780	1910
146	389073	797782	1913
147	389080	797787	1914
148	389087	797794	1912
149	389072	797793	1913
150	389080	797797	1910
151	389078	797811	1910
152	389089	797813	1911
153	389087	797807	1912
154	389068	797803	1911
155	389064	797793	1909
156	389060	797788	1909
157	389059	797778	1911
158	389051	797781	1911
159	389047	797789	1910
160	389051	797799	1909
161	389057	797795	1909

162	389059	797786	1913
163	389054	797790	1913
164	389039	797786	1908
165	389032	797778	1910
166	389036	797787	1916
167	389049	797798	1914
168	389048	797804	1913
169	389041	797800	1914
170	389034	797784	1916
171	389055	797811	1910
172	389053	797819	1905
173	389058	797826	1906
174	389062	797831	1907
175	389055	797814	1909
176	389062	797821	1909
177	389066	797825	1909
36	389064	797814	1910
37	389072	797812	1910
124	389072	797812	1910
125	389079	797821	1910
178	389074	797826	1910
179	389067	797830	1911
180	389072	797838	1911
181	389075	797842	1912
182	389079	797844	1912
183	389084	797851	1908
184	389081	797854	1906
185	389086	797850	1906
186	389086	797857	1906
187	389090	797862	1907
188	389084	797862	1907
189	389083	797864	1909
190	389081	797872	1909
191	389092	797873	1909
192	389095	797874	1909
193	389100	797871	1910
194	389082	797882	1904
195	389079	797885	1903
196	389073	797878	1902
197	389077	797871	1904
198	389079	797863	1902
199	389083	797891	1902
200	389089	797894	1901
201	389087	797897	1901
202	389090	797887	1907
203	389097	797887	1907
204	389096	797879	1907
205	389103	797893	1904
206	389112	797903	1900
207	389118	797907	1903

208	389119	797896	1901
209	389109	797894	1903
210	389112	797883	1902
211	389121	797883	1904
212	389122	797875	1906
213	389115	797872	1905
214	389111	797871	1907
215	389106	797670	1908
216	389115	797866	1906
217	389127	797865	1906
218	389127	797855	1907
219	389115	797855	1908
220	389089	797894	1901
221	389087	797897	1901
222	389090	797887	1907
223	389089	797868	1905
224	389093	797859	1906
225	389095	797854	1907
226	389093	797851	1908
227	389094	797852	1907
228	389094	797852	1906
229	389087	797850	1906
230	389082	797841	1906
231	389076	797833	1907
232	389083	797827	1908
233	389089	797821	1907
234	389095	797819	1910
235	389096	797826	1909
236	389093	797832	1908
237	389090	797836	1909
238	389093	797838	1910
239	389096	797842	1912
240	389099	797848	1912
241	389101	797846	1905
242	389114	797846	1907
243	389122	797845	1905
244	389127	797838	1908
245	389122	797836	1910
246	389106	797833	1908
247	389102	797824	1909
248	389114	797825	1912
249	389123	797824	1910
250	389136	797826	1911
251	389137	797822	1913
255	389133	797822	1911
256	389140	797813	1910
257	389125	797815	1910
258	389118	797818	1910
259	389114	797822	1911
260	389102	797820	1909

261	389099	797807	1909
262	389114	797806	1913
263	389125	797806	1912
264	389138	797804	1911
265	389138	797793	1912
266	389125	797795	1915
267	389111	797796	1913
268	389098	797799	1912
269	389106	797785	1909
270	389093	797790	1911
271	389103	797790	1913
272	389111	797790	1910
273	389111	797788	1915
274	389122	797791	1911
275	389139	797791	1910
276	389095	797784	1910
277	389088	797786	1910
278	389087	797787	1909
279	389091	797777	1913
280	389086	797771	1910
281	389084	797768	1911
282	389085	797761	1910
283	389086	797756	1910
284	389088	797749	1908
285	389089	797743	1909
286	389088	797739	1909
287	389098	797764	1910
288	389099	797772	1910
289	389105	797771	1915
290	389110	797774	1909
291	389115	797766	1910
292	389112	797764	1912
293	389114	797757	1910
294	389117	797759	1910
295	389116	797751	1911
296	389119	797751	1912
297	389123	797759	1912
298	389131	797759	1911
299	389131	797770	1910
300	389120	797770	1911
301	389119	797769	1908
302	389117	797776	1908
303	389120	797780	1910
126	389124	797778	1909
304	389128	797785	1914
305	389132	797780	1914
306	389137	797771	1914
307	389140	797769	1914
308	389150	797772	1913
309	389142	797773	1911

310	389141	797782	1907
311	389135	797792	1907
312	389145	797793	1907
313	389153	797784	1906
314	389151	797777	1908
315	389162	797780	1912
316	389164	797786	1910
317	389167	797777	1909
318	389163	797769	1910
319	389154	797767	1911
320	389147	797768	1911
321	389145	797764	1912
322	389149	797759	1912
323	389151	797752	1914
324	389153	797749	1914
325	389158	797755	1913
326	389157	797751	1909
327	389158	797750	1912
328	389163	797751	1911
329	389165	797760	1909
330	389172	797754	1913
331	389173	797764	1913
332	389180	797762	1913
333	389182	797770	1912
334	389176	797775	1912
335	389190	797775	1914
336	389183	797760	1914
337	389173	797745	1917
338	389164	797739	1917
339	389148	797748	1916
340	389139	797757	1916
341	389197	797775	1917
342	389207	797769	1919
343	389211	797768	1917
344	389172	797787	1912
345	389187	797791	1909
346	389197	797792	1908
347	389201	797786	1908
348	389206	797788	1912
349	389211	797791	1913
350	389209	797795	1913
351	389210	797801	1911
352	389216	797796	1907
353	389225	797813	1907
354	389225	797813	1907
355	389224	797814	1909
356	389212	797815	1910
357	389197	797816	1912
358	389183	797813	1913
359	389170	797812	1913

360	389155	797812	1913
361	389150	797826	1910
362	389169	797827	1910
363	389178	797826	1912
364	389208	797822	1911
365	389213	797820	1913
366	389220	797818	1910
367	389235	797832	1907
368	389219	797836	1909
369	389207	797839	1908
370	389205	797839	1912
371	389200	797847	1912
372	389193	797843	1911
373	389179	797845	1912
374	389160	797841	1912
375	389152	797840	1911
376	389145	797850	1909
377	389151	797852	1909
378	389155	797854	1914
379	389165	797855	1912
380	389182	797852	1910
381	389199	797852	1911
382	389208	797850	1909
383	389219	797846	1908
384	389233	797843	1909
385	389236	797852	1908
386	389240	797861	1907
387	389233	797860	1909
388	389215	797867	1909
389	389197	797866	1910
390	389181	797866	1912
391	389166	797868	1908
392	389147	797867	1909
393	389140	797868	1910
394	389135	797868	1908
395	389131	797880	1905
396	389131	797897	1904
397	389131	797909	1903
398	389131	797919	1901
399	389139	797925	1900
400	389147	797925	1899
401	389149	797911	1901
402	389144	797909	1903
403	389144	797906	1903
404	389154	797903	1904
405	389155	797896	1906
406	389149	797895	1907
407	389140	797893	1906
408	389141	797884	1906
409	389172	797883	1910

410	389173	797902	1910
411	389173	797904	1905
412	389169	797915	1904
413	389169	797921	1903
414	389167	797923	1905
415	389168	797937	1901
416	389174	797939	1899
417	389175	797931	1901
418	389177	797924	1902
419	389186	797919	1901
420	389180	797935	1902
421	389188	797939	1903
422	389194	797943	1901
423	389196	797932	1901
424	389192	797919	1903
425	389200	797913	1904
426	389208	797914	1902
427	389209	797930	1903
428	389209	797942	1900
429	389211	797951	1903
430	389218	797946	1904
431	389217	797951	1904
432	389239	797948	1902
433	389237	797943	1901
434	389225	797929	1900
435	389218	797918	1901
436	389213	797907	1902
437	389212	797897	1903
438	389212	797891	1904
439	389207	797880	1907
440	389193	797880	1908
441	389193	797895	1907
442	389195	797909	1907
443	389203	797903	1906
444	389226	797881	1905
445	389247	797875	1905
446	389253	797889	1905
447	389259	797895	1904
448	389247	797899	1905
449	389236	797898	1906
450	389226	797907	1905
451	389245	797906	1905
452	389265	797919	1904
453	389266	797924	1904
454	389254	797918	1905
455	389258	797922	1903
456	389258	797925	1902
457	389261	797937	1900
458	389255	797940	1900
459	389245	797939	1900

460	389249	797937	1903
461	389243	797924	1902
462	389240	797915	1900
463	389225	797911	1902
464	389231	797924	1901
465	389270	797925	1900
466	389276	797916	1900
467	389262	797903	1902
468	389256	797903	1902
469	389157	797883	1906

Sample site 4

ID	EASTING	NORTHING	ALTITUDE
1	388183	786874	1895
2	388180	786864	1894
3	388178	786871	1888
4	388169	786874	1886
5	388162	786869	1888
6	388157	786866	1890
7	388151	786868	1892
8	388151	786868	1892
9	388159	786879	1892
10	388164	786881	1888
11	388169	786882	1889
12	388169	786883	1888
13	388172	786883	1889
14	388179	786882	1889
15	388183	786882	1890
16	388180	786890	1890
17	388181	786896	1890
18	388174	786894	1889
19	388170	786892	1890
20	388163	786888	1892
21	388161	786886	1888
22	388159	786892	1885
23	388159	786886	1895
24	388153	786884	1895
25	388148	786884	1897
26	388142	786880	1893
27	388141	786891	1895
28	388150	786891	1893
29	388148	786897	1894
30	388142	786903	1892
31	388137	786908	1895
32	388138	786914	1893
33	388141	786911	1892
34	388148	786908	1892
35	388155	786898	1891
36	388154	786912	1891

37	388151	786917	1892
38	388148	786916	1893
39	388150	786924	1894
40	388145	786927	1896
41	388140	786928	1895
42	388142	786935	1894
43	388144	786939	1889
44	388145	786936	1884
45	388173	786933	1887
46	388162	786926	1885
47	388160	786910	1885
48	388156	786903	1887
49	388159	786892	1887
50	388162	786895	1892
51	388120	786899	1888
52	388178	786902	1889
53	388187	786901	1889
54	388189	786909	1888
55	388191	786912	1888
56	388196	786914	1889
57	388203	786916	1890
58	388207	786916	1891
59	388204	786911	1893
60	388213	786917	1890
61	388217	786914	1892
62	388220	786917	1893
63	388218	786925	1893
64	388211	786932	1895
65	388219	786936	1895
66	388221	786932	1894
67	388225	786927	1892
68	388231	786920	1894
69	388223	786922	1896
70	388229	786943	1897
71	388213	786938	1896
72	388204	786947	1899
73	388215	786954	1899
74	388218	786964	1898
75	388207	786963	1897
76	388185	786973	1899
77	388200	786983	1900
78	388209	786983	1902
79	388213	786982	1903
80	388217	786982	1899
81	388227	786975	1900
82	388226	786978	1903
83	388224	786986	1903
84	388226	786995	1901
85	388236	786997	1901
86	388236	786997	1901

87	388228	787002	1901
88	388223	787007	1901
89	388218	787010	1899
90	388211	787011	1899
91	388216	786998	1897
92	388219	786990	1900
93	388208	786994	1899
94	388204	786989	1900
95	388202	786999	1900
96	388207	787005	1901
97	388202	787012	1902
98	388210	787030	1901
99	388202	787044	1900
100	388193	787036	1899
101	388181	787052	1901
102	388189	787053	1901
103	388168	787028	1898
104	388175	787016	1899
105	388181	787005	1901
106	388172	786993	1895
107	388190	786990	1896
108	388190	786996	1898
109	388195	786986	1899
110	388178	786987	1897
111	388180	786974	1896
112	388168	786974	1895
113	388169	786977	1896
114	388160	786987	1897
115	388152	786978	1894
116	388153	786967	1894
117	388152	786961	1896
118	388163	786961	1896
119	388175	786964	1896
120	388185	786961	1894
121	388170	786951	1893
122	388170	786947	1895
123	388174	786937	1892
124	388180	786939	1892
125	388192	786943	1893
126	388200	786939	1892
127	388198	786935	1895
128	388205	786928	1894
129	388208	786930	1891
130	388208	786927	1892
131	388196	786920	1893
132	388191	786930	1894
133	388181	786930	1890
134	388186	786917	1891
135	388182	786917	1890
136	388179	786912	1890

137	388173	786908	1892
138	388169	786905	1889
139	388169	786901	1890
140	388163	786902	1888
141	388159	786914	1889
142	388157	786920	1891
143	388167	786916	1891
144	388178	786921	1891
145	388177	786932	1891
146	388169	786934	1889
147	388165	786929	1889
148	388162	786928	1893
149	388158	786928	1889
150	388155	786925	1891
151	388158	786928	1890
152	388151	786932	1893
153	388149	786937	1890
154	388160	786940	1890
155	388156	786935	1892
156	388150	786941	1889
157	388150	786942	1891
158	388150	786946	1889
159	388156	786949	1892
160	388157	786952	1891
161	388155	786952	1889
162	388151	786956	1892
163	388155	786959	1892
164	388145	786960	1891
165	388140	786916	1891
166	388142	786968	1892
167	388149	786972	1891
168	388142	786977	1891
169	388146	786985	1892
170	388150	786983	1893
171	388151	786985	1894
172	388155	786987	1895
173	388157	786990	1896
174	388154	786994	1897
175	388152	787002	1897
176	388163	787000	1898
177	388169	787003	1898
178	388173	787011	1899
179	388169	787012	1899
180	388168	787020	1902
181	388163	787021	1902
182	388161	787021	1899
183	388165	787013	1900
184	388149	787011	1897
185	388149	787016	1895
186	388146	787026	1896

187	388145	787032	1896
188	388148	787032	1898
189	388153	787031	1897
190	388157	787029	1898
191	388163	787033	1897
192	388154	787040	1897
193	388159	787047	1898
194	388166	787045	1901
195	388156	787044	1900
196	388153	787042	1899
197	388163	787058	1900
198	388160	787065	1903
199	388157	787068	1902
200	388153	787070	1902
201	388148	787062	1903
202	388124	787041	1899
203	388124	787041	1899
204	388117	787037	1899
205	388119	787055	1901
206	388130	787056	1902
207	388144	787063	1901
208	388136	787063	1901
209	388131	787065	1900
210	388139	787078	1900
211	388150	787079	1900
212	388146	787082	1899
213	388132	787062	1902
214	388125	787058	1902
215	388120	787063	1903
216	388118	787068	1905
217	388111	787074	1903
218	388115	787069	1904
219	388113	787059	1903
220	388101	787056	1903
221	388103	787045	1905
222	388116	787046	1903
223	388118	787033	1902
224	388108	787028	1902
225	388097	787032	1903
226	388070	787020	1902
227	388080	787017	1902
228	388088	787000	1900
229	388098	787003	1903
230	388088	786989	1902
231	388098	786984	1902
232	388089	786988	1904
233	388092	786991	1900
234	388097	786992	1899
235	388104	786990	1898
236	388114	786984	1898

237	388117	786979	1899
238	388117	786987	1896
239	388127	786980	1895
240	388135	786986	1897
241	388134	786983	1897
242	388135	786975	1898
243	388132	786970	1898
244	388134	786966	1898
245	388127	786961	1898
246	388121	786965	1899
247	388115	786968	1898
248	388113	786963	1897
249	388105	786962	1901
250	388093	786953	1900
251	388108	786952	1898
252	388111	786952	1897
253	388120	786957	1897
254	388127	786957	1897
255	388127	786952	1896
256	388124	786948	1891
257	388129	786943	1892
258	388137	786944	1890
259	388143	786949	1892
260	388130	786953	1891
261	388136	786959	1890
262	388137	786967	1891
263	388139	786977	1891
264	388137	786976	1895
265	388136	786982	1895
266	388146	786989	1898
267	388145	786995	1896
268	388144	786998	1896
269	388138	787000	1896
270	388137	786994	1896
271	388135	786990	1895
272	388130	786986	1897
273	388126	786991	1898
274	388126	786999	1898
275	388133	787004	1898
276	388134	787006	1900
277	388142	787003	1901
278	388143	787006	1900
279	388137	787012	1900
280	388141	787012	1899
281	388139	787012	1898
282	388143	787017	1898
283	388148	787026	1898
284	388144	787028	1897
285	388136	787017	1898
286	388139	787020	1899

287	388139	787023	1899
288	388138	787029	1902
289	388140	787032	1901
290	388133	787025	1900
291	388124	787029	1900
292	388119	787026	1899
293	388114	787031	1899
294	388109	787023	1901
295	388103	787029	1900
296	388089	787027	1901
297	388091	787021	1902
298	388103	787018	1901
299	388109	787011	1901
300	388102	787010	1900
301	388096	787010	1899
302	388102	787004	1899
303	388098	786999	1896
304	388102	786996	1896
305	388107	787000	1897
306	388109	787004	1900
307	388113	786996	1898
308	388109	786991	1900
309	388120	786986	1897
310	388120	786993	1896
311	388126	787018	1899
312	388126	787010	1901
313	388123	787020	1901
314	388120	787021	1905
315	388118	787013	1907
316	388114	787016	1905
317	388117	787008	1904
318	388127	787008	1905
319	388123	787000	1908
320	388118	786998	1906
321	388119	787003	1905
322	388117	787007	1903
323	388144	786992	1890
324	388140	786982	1891
325	388141	786977	1892
326	388138	786968	1891
327	388138	786961	1891
328	388143	786951	1891
329	388141	786944	1892
330	388144	786940	1890
331	388141	786935	1891
332	388121	786946	1900
333	388137	786937	1899
334	388130	786918	1900
335	388132	786898	1900
336	388145	786880	1900

337	388153	786866	1896
338	388163	786858	1897
339	388107	786939	1901
340	388081	786949	1904
341	388085	786972	1907
342	388025	786992	1909
343	388062	787009	1910
344	388052	787027	1911
345	388081	787042	1911
346	388088	787067	1913
347	388093	787090	1913
348	388100	787082	1911
349	388100	787071	1910
350	388106	787075	1912
351	388119	787089	1911
352	388125	787096	1912
353	388136	787107	1911
354	388129	787093	1907
355	388138	787083	1907
356	388147	787101	1906
357	388142	787107	1904
358	388159	787118	1906
359	388165	787113	1905
360	388169	787107	1907
361	388179	787103	1905
362	388177	787096	1906
363	388158	787092	1903
364	388153	787086	1902
365	388151	787023	1903
366	388165	787075	1905
367	388175	787062	1903
368	388182	787067	1904
369	388177	787077	1903
370	388173	787080	1903
371	388188	787094	1905
372	388198	787070	1907
373	388204	787054	1908
374	388216	787039	1909
375	388224	787021	1908
376	388235	787008	1908
377	388243	787094	1907
378	388239	787075	1905
379	388232	787051	1904
380	388235	787037	1905
381	388237	786909	1905
382	388219	786906	1902
383	388199	786902	1901
384	388186	786887	1897
385	388182	786825	1898
386	388182	786859	1897

387	388144	786932	1885
388	388111	787042	1901
389	388100	787041	1902
390	388083	787030	1903
391	388091	786979	1899
392	388101	786965	1900
393	388108	786975	1899

Annex 5

Histogram of the landslide hazard zones

Class	Lower Limit	Upper Limit	Frequency	Prop.	Cum. Freq.	Cum. Prop.
0	17.0000	18.9999	12	0.0001	12	0.0001
1	19.0000	20.9999	54	0.0003	66	0.0003
2	21.0000	22.9999	55	0.0003	121	0.0006
3	23.0000	24.9999	160	0.0008	281	0.0014
4	25.0000	26.9999	229	0.0012	510	0.0026
5	27.0000	28.9999	275	0.0014	785	0.0040
6	29.0000	30.9999	373	0.0019	1158	0.0058
7	31.0000	32.9999	611	0.0031	1769	0.0089
8	33.0000	34.9999	997	0.0050	2766	0.0139
9	35.0000	36.9999	1336	0.0067	4102	0.0207
10	37.0000	38.9999	1043	0.0053	5145	0.0259
11	39.0000	40.9999	624	0.0031	5769	0.0291
12	41.0000	42.9999	438	0.0022	6207	0.0313
13	43.0000	44.9999	322	0.0016	6529	0.0329
14	45.0000	46.9999	253	0.0013	6782	0.0342
15	47.0000	48.9999	344	0.0017	7126	0.0359
16	49.0000	50.9999	427	0.0022	7553	0.0381
17	51.0000	52.9999	550	0.0028	8103	0.0408
18	53.0000	54.9999	889	0.0045	8992	0.0453
19	55.0000	56.9999	859	0.0043	9851	0.0496
20	57.0000	58.9999	1674	0.0084	11525	0.0581
21	59.0000	60.9999	2750	0.0139	14275	0.0719
22	61.0000	62.9999	3838	0.0193	18113	0.0912
23	63.0000	64.9999	4983	0.0251	23096	0.1164
24	65.0000	66.9999	4701	0.0237	27797	0.1400
25	67.0000	68.9999	3433	0.0173	31230	0.1573
26	69.0000	70.9999	1076	0.0054	32306	0.1628
27	71.0000	72.9999	694	0.0035	33000	0.1662
28	73.0000	74.9999	1038	0.0052	34038	0.1715
29	75.0000	76.9999	1463	0.0074	35501	0.1788
30	77.0000	78.9999	2333	0.0118	37834	0.1906
31	79.0000	80.9999	2717	0.0137	40551	0.2043
32	81.0000	82.9999	3142	0.0158	43693	0.2201
33	83.0000	84.9999	3522	0.0177	47215	0.2379
34	85.0000	86.9999	3790	0.0191	51005	0.2570
35	87.0000	88.9999	3910	0.0197	54915	0.2766
36	89.0000	90.9999	4331	0.0218	59246	0.2985
37	91.0000	92.9999	4197	0.0211	63443	0.3196
38	93.0000	94.9999	3603	0.0182	67046	0.3378
39	95.0000	96.9999	3564	0.0180	70610	0.3557
40	97.0000	98.9999	3337	0.0168	73947	0.3725
41	99.0000	100.9999	2927	0.0147	76874	0.3873
42	101.0000	102.9999	2338	0.0118	79212	0.3991
43	103.0000	104.9999	2177	0.0110	81389	0.4100
44	105.0000	106.9999	2290	0.0115	83679	0.4216
45	107.0000	108.9999	2727	0.0137	86406	0.4353
46	109.0000	110.9999	3088	0.0156	89494	0.4509
47	111.0000	112.9999	3388	0.0171	92882	0.4679
48	113.0000	114.9999	3757	0.0189	96639	0.4868
49	115.0000	116.9999	4088	0.0206	100727	0.5074
50	117.0000	118.9999	4801	0.0242	105528	0.5316
51	119.0000	120.9999	5370	0.0271	110898	0.5587
52	121.0000	122.9999	5822	0.0293	116720	0.5880
53	123.0000	124.9999	5940	0.0299	122660	0.6179
54	125.0000	126.9999	5813	0.0293	128473	0.6472
55	127.0000	128.9999	5797	0.0292	134270	0.6764
56	129.0000	130.9999	5695	0.0287	139965	0.7051
57	131.0000	132.9999	5248	0.0264	145213	0.7316
58	133.0000	134.9999	5022	0.0253	150235	0.7569
59	135.0000	136.9999	5061	0.0255	155296	0.7823
60	137.0000	138.9999	4820	0.0243	160116	0.8066

61	139.0000	140.9999	4268	0.0215	164384	0.8281
62	141.0000	142.9999	3727	0.0188	168111	0.8469
63	143.0000	144.9999	3608	0.0182	171719	0.8651
64	145.0000	146.9999	3667	0.0185	175386	0.8836
65	147.0000	148.9999	3449	0.0174	178835	0.9009
66	149.0000	150.9999	2763	0.0139	181598	0.9149
67	151.0000	152.9999	2113	0.0106	183711	0.9255
68	153.0000	154.9999	1679	0.0085	185390	0.9340
69	155.0000	156.9999	1504	0.0076	186894	0.9415
70	157.0000	158.9999	1355	0.0068	188249	0.9484
71	159.0000	160.9999	1137	0.0057	189386	0.9541
72	161.0000	162.9999	1010	0.0051	190396	0.9592
73	163.0000	164.9999	897	0.0045	191293	0.9637
74	165.0000	166.9999	847	0.0043	192140	0.9680
75	167.0000	168.9999	773	0.0039	192913	0.9719
76	169.0000	170.9999	672	0.0034	193585	0.9752
77	171.0000	172.9999	569	0.0029	194154	0.9781
78	173.0000	174.9999	492	0.0025	194646	0.9806
79	175.0000	176.9999	435	0.0022	195081	0.9828
80	177.0000	178.9999	378	0.0019	195459	0.9847
81	179.0000	180.9999	371	0.0019	195830	0.9865
82	181.0000	182.9999	307	0.0015	196137	0.9881
83	183.0000	184.9999	278	0.0014	196415	0.9895
84	185.0000	186.9999	287	0.0014	196702	0.9909
85	187.0000	188.9999	236	0.0012	196938	0.9921
86	189.0000	190.9999	228	0.0011	197166	0.9933
87	191.0000	192.9999	180	0.0009	197346	0.9942
88	193.0000	194.9999	172	0.0009	197518	0.9951
89	195.0000	196.9999	156	0.0008	197674	0.9958
90	197.0000	198.9999	115	0.0006	197789	0.9964
91	199.0000	200.9999	129	0.0006	197918	0.9971
92	201.0000	202.9999	98	0.0005	198016	0.9976
93	203.0000	204.9999	91	0.0005	198107	0.9980
94	205.0000	206.9999	76	0.0004	198183	0.9984
95	207.0000	208.9999	55	0.0003	198238	0.9987
96	209.0000	210.9999	47	0.0002	198285	0.9989
97	211.0000	212.9999	52	0.0003	198337	0.9992
98	213.0000	214.9999	47	0.0002	198384	0.9994
99	215.0000	216.9999	17	0.0001	198401	0.9995
100	217.0000	218.9999	32	0.0002	198433	0.9997
101	219.0000	220.9999	17	0.0001	198450	0.9997
102	221.0000	222.9999	21	0.0001	198471	0.9999
103	223.0000	224.9999	11	0.0001	198482	0.9999
104	225.0000	226.9999	4	0.0000	198486	0.9999
105	227.0000	228.9999	1	0.0000	198487	0.9999
106	229.0000	230.9999	1	0.0000	198488	0.9999
107	231.0000	232.9999	2	0.0000	198490	0.9999
108	233.0000	234.9999	0	0.0000	198490	0.9999
109	235.0000	236.9999	1	0.0000	198491	1.0000
110	237.0000	238.9999	4	0.0000	198495	1.0000
111	239.0000	240.9999	1	0.0000	198496	1.0000
112	241.0000	242.9999	1	0.0000	198497	1.0000
113	243.0000	244.9999	2	0.0000	198499	1.0000
114	245.0000	246.9999	0	0.0000	198499	1.0000
115	247.0000	248.9999	1	0.0000	198500	1.0000

```
Class width      =       2.0000
Display minimum  =      17.0000
Display maximum  =     249.0000
Actual minimum   =      17.0000
Actual maximum   =     248.0000
Mean             =     109.9226
Stand. Deviation =      33.6312
df               =       198499
```